

TALLINN UNIVERSITY OF TECHNOLOGY
DOCTORAL THESIS
48/2018

Evaluation of Haar Wavelet Method for Analysis of Functionally Graded and Nanostructures

MAARJUS KIRS



TALLINN UNIVERSITY OF TECHNOLOGY

School of Engineering

Department of Mechanical and Industrial Engineering

This dissertation was accepted for the defence of the degree 05/07/2018

Supervisor:

Lead Research Scientist, Jüri Majak
School of Engineering
Tallinn University of Technology
Tallinn, Estonia

Co-supervisor:

Associate Professor, Kristo Karjust
School of Engineering
Tallinn University of Technology
Tallinn, Estonia

Opponents:

Senior Research Scientist, Janis Sliseris
Institute of Building and Reconstruction
Riga Technical University
Riga, Latvia

Associate Professor, Helle Hein
Institute of Computer Science
Tartu University
Tartu, Estonia

Defence of the thesis: 29/08/2018, Tallinn

Declaration:

Hereby I declare that this doctoral thesis, my original investigation and achievement, submitted for the doctoral degree at Tallinn University of Technology, has not been previously submitted for doctoral or equivalent academic degree.

Maarjus Kirs

signature



Copyright: Maarjus Kirs, 2018

ISSN 2585-6898 (publication)

ISBN 978-9949-83-306-1 (publication)

ISSN 2585-6901 (PDF)

ISBN 978-9949-83-307-8 (PDF)

TALLINNA TEHNIKAÜLIKOO
DOKTORITÖÖ
48/2018

**Haari lainikute meetodi hindamine
funktsionaalgradient- ja nanostruktuuride
analüüsiks**

MAARJUS KIRS

Contents

List of Publications	6
Author's Contribution to the Publications	7
Introduction	8
Abbreviations	10
Symbols	11
1 Theoretical background	13
1.1 Haar wavelet method (HWM)	16
1.2 Reference methods	19
1.2.1 Differential quadrature method (DQM)	19
1.2.2 Finite difference method (FDM)	20
1.2.3 Finite element method (FEM)	22
1.3 Evaluation criteria	25
1.3.1 Accuracy	25
1.3.2 Convergence	27
1.4 Improved Haar Wavelet Method (HOHWM)	28
1.5 Objectives of the research	29
2 Evaluation of Haar wavelet method – case studies	31
2.1 Functionally Graded Structures	31
2.1.1 Description of functionally graded materials	31
2.1.2 Modelling properties of the FG material	32
2.1.3 Free vibration analysis of FGM beam	34
2.2 Nanostructures	45
2.2.1 Nonlocal elasticity model	45
2.2.2 Free Vibration analysis of nanobeams	46
3 Conclusions	51
The scientific novelty	52
References	53
Acknowledgements	60
Abstract	61
Lühikokkuvõte	63
Appendix	65
Curriculum vitae	103
Elulookirjeldus	104

List of Publications

List of author's publications on the basis of which the thesis has been prepared:

- I Kirs, M., Karjust, K., Aziz, I., Õunapuu, E., Tungel, E. (2018). Free vibration analysis of a functionally graded material beam: evaluation of the Haar wavelet method. *Proceedings of the Estonian Academy of Sciences*, 67 (1), 1–9.
- II Kirs, M., Mikola, M., Haavajõe, A., Õunapuu, E., Shvartsman, B., Majak, J. (2016). Haar wavelet method for vibration analysis of nanobeams. *Waves Wavelets and Fractals Advanced Analysis*, 2, 20–28.
- III Majak, J., Shvartsman, B., Kirs, M., Pohlak, M., Herranen, H. (2015). Convergence theorem for the Haar wavelet based discretization method. *Composite Structures*, 126, 227–232.
- IV Kirs, M., Tungel, E. (2018). Evaluation of Haar wavelet method in engineering applications. *International Conference of Numerical Analysis and Applied Mathematics (ICNAAM 2018), Greece, AIP Conference Proceedings*.

Author's Contribution to the Publications

The author has contributed to the papers in this thesis as follows:

- I Theoretical and numerical analysis, comparison and analysis of results. Evaluation of the Haar wavelet method. Finite element model development for a functionally graded beam.
- II Theoretical and numerical analysis, comparison and analysis of results. Evaluation of the Haar wavelet method.
- III Computing and estimating the rates of convergence, comparison with theoretical results.
- IV Theoretical and numerical analysis, comparison and analysis of results. Evaluation of the Haar wavelet method.

Introduction

Nanomaterials (NM) and functionally graded materials (FGM) are becoming increasingly popular, allowing marked improvement of the efficiency of different types of structures and products. Nanomaterials and nanotechnologies are advancing continually in various research areas from mechanics, physics, chemistry to biology and medicine. Adding nanoparticles or graphene in the matrix of a composite is one of the simplest and most widely used techniques for producing materials with improved properties such as stiffness, strength, thermal and electrical conductivity, wear resistance, etc. (Ekrem et al., 2016). Nanocomposites are most commonly produced from polymer, ceramics or metal by applying various techniques like vapour phase processing, powder metallurgy and solidification processing, etc. In practice, FG materials are utilized most commonly as interfaces between two different materials. For example, the metal-ceramic interface allows excellent strength and thermal properties of the material simultaneously as well as avoiding stress concentrations caused by sharp changes in material properties. Both FG and nanomaterials have found application in the automotive and aerospace industry (reinforcement, thermal protection), energy industry (batteries, solar cells, fuel cells), electronics (sensors, actuators), medicine (a nanoparticle can pass through the lining of the intestines into the bloodstream).

Current study addresses numerical modelling of the stress-strain behaviour of FGM and NM. A number of numerical methods are available in the literature for the analysis of solid structures. The choice of the numerical method for solving a particular problem is rather complicated due to the presence of a huge number of techniques. The selection of a numerical method depends mainly on the nature of the problem, also on the commercial software available. However, problems related to advanced material models and constitutive laws are much less covered by existing numerical techniques and commercial software. Obviously, the material models for FGM and NM belong to the latter class of problems and the numerical techniques available for the analysis of FG and nanomaterials are still limited in comparison with traditional solid mechanics. Based on the literature review, the author has observed that the finite difference method (FDM), differential quadrature method (DQM) and finite element method (FEM) are most frequently used for the analysis of FG and nanostructures. These methods can be classified as most widely used in engineering design. From most recent methods, the Haar wavelet method (HWM) has been pointed out as a simple and effective method for solving a wide class of differential and integral equations covering FG materials (Lepik et al., 2014; Hariharan et al., 2014; Feklistova et al., 2015). However, most commonly, these evaluations are based on its simplicity of implementation and reasonable absolute error against other simple and strong formulation based methods like the Semi-orthogonal B-spline wavelet method, Legendre polynomials and block-

pulse functions approach, triangular functions method (Islam et al., 2013a), and quantic spline-based approach (Majak et al., 2009a).

Thus, in the early stage of the current study:

- on the one hand, HWM was considered as a perspective method (simple and effective);
- on the other hand, the author was unable to find from the literature comparisons of HWM with mainstream methods in engineering design like FDM and DQM, neither any proved convergence results for HWM.

Motivation of the current study is based on the latter two facts. Detailed analysis and evaluation of the HWM was planned.

Main goal of the current study is to evaluate HWM for the analysis of FG and nanostructures based on the comparison with widely used methods in engineering design. The accuracy of the numerical results and simplicity of the implementation, also complexity of the solution, are the topics of interest. The following activities have been performed in order to achieve the posed goal.

Activity 1:

- Implementation of the Haar wavelet method for the analysis of the FGM and nanostructures

Activity 2:

- Comparison of the accuracy of HWM, FDM and DQM based on the case studies covering FGM and nanostructures (absolute error)
- Analysis and comparison of numerical convergence rates

Activity 3:

- Evaluation of improved HWM, comparison with widely used HWM (absolute error, convergence rate)
- Complexity analysis

The novelties of the current study can be outlined as follows:

- The comparison of HWM with widely used methods in engineering design leads to a principally new understanding – the Chen and Hsiao approach based HWM needs improvement in order to compete with mainstream methods in engineering design. The conclusion made formed a basis for the development of a higher order Haar wavelet method (HOHWM).
- Testing of HOHWM produced unexpectedly accurate results. However, these results need validation for the particular problems considered.

The main results of the study have been published in peer-reviewed journal papers and presented at a number of conferences.

Abbreviations

AbsErr	Absolute Error
APDL	Ansys Parametric Design Language
DQM	Differential Quadrature Method
FDM	Finite Difference Method
FEM	Finite Element Method
FG	Functionally Graded
FGM	Functionally Graded Materials
GDQM	Generalized Differential Quadrature Method
HOHWM	Higher Order Haar Wavelet Method
HWM	Haar Wavelet Method
NM	Nanomaterials
ODE	Ordinary Differential Equation
PDE	Partially Differential Equation
RConv	Rate of Convergence

Symbols

Greek

β	value of the exponent parameter
$\varepsilon_{abs_xi_N}$	absolute error at fixed point $x=x_i$ and mesh size N
$\varepsilon_{abs_freq_N}$	absolute error of i-th eigenfrequency with mesh size N
$\varepsilon_{max_abs_N}$	maximum absolute error with mesh size N
$\varepsilon_{rel_xi_N_proc}$	relative error at fixed point $x=x_i$ and mesh size N in percentages
$\varepsilon_1(i)$	initial point of the i-th wavelet
$\varepsilon_2(i)$	midpoint of the i-th wavelet
$\varepsilon_3(i)$	endpoint of the i-th wavelet
η	upper bound for derivative
Δh	step size of the grid
$\Delta(N)$	relative increase of the area underneath the curve $ u^N(x) , x \in [0,1]$ for one iteration step
Δx	length of subinterval
π	product - product of all values in range of series
ρ	density
$\rho A(0)$	reference value of distributed mass per unit length of the beam at $x=0$
$\rho A(x)$	distributed mass per unit length
Σ	summation
Ω	frequency parameter
$\Omega_{i,ex}$	exact value of the i-th eigenfrequency
$\Omega_{i,N}$	numerical value of i-th eigenfrequency with mesh size N
ω	eigenfrequency of the beam

Latin

A	cross-section of the beam
$[A, B]$	closed interval $\{x A \leq x \leq B\}$
$A_{i,j}^{(m)}$	weighting coefficient for the m-th order derivative
a_i	coefficient of i-th Haar wavelet
$DV(0)$	differential equation at point $x=0$
E	Young's modulus
$EI(0)$	reference value of bending stiffness of the beam at $x=0$

$EI(x)$	bending stiffness
$\ E_M\ _2$	L ² norm of error function
$G(x, u, u', u'', \dots, u^{(n-1)}, u^{(n)}) = 0,$	general form of ODE
$G(z)$	effective local shear modulus
$h_i(x)$	i-th Haar wavelet
I	area moment of inertia of the beam cross-section about the axis of interest
J	maximum value of dilatation parameter
j	dilatation parameter
k	translation parameter
k^A	numerical rate of convergence when exact solution is unknown
k^E	numerical rate of convergence when exact solution is known
$K(z)$	effective local bulk modulus
L	length of the beam
M	maximum level of resolution
m	level of the wavelet
N	number of collocation points (mesh size)
P_A	value of the effective property of material A
P_C	value of the effective property of ceramic
P_B	value of the effective property of material B
P_m	value of the effective property of metal
$p_{n,i}(x)$	n-th order integral of Haar function
$P(z)$	effective material property according to z coordinate
$q(x)$	load of the beam
$S_{BT}(x)$	boundary term
$S(N)$	area underneath the curve $ u^N(x) $ in interval [0,1]
z	coordinate in thickness direction
t_l	l-th uniform grid point for discretization
$V_A(z)$	volume fraction function of the material A according to z coordinate
$v(x)$	trial function
W	corresponding amplitude function
$w(x)$	transverse deflection of the beam at position x
X	non-dimensional coordinate
x	variable, unknown value to find

1 Theoretical background

The Haar wavelet method was introduced by Chen and Hsiao (Chen et al., 1997) to solve differential equations. According to this approach, the highest order derivative included in the differential equation is expanded into the series of Haar functions. Most commonly, approximations are proposed to solve the differential equation. However, the Haar functions are not differentiable due to their piece-wise constant character. Thus, expanding the solution of the differential equation into Haar wavelets causes problems in the evaluation of the derivatives included in the differential equation. For that reason, an approach proposed by Chen and Hsiao has been used during two decades as mainstream in the Haar wavelet method for solving a wide class of ordinary (Hsiao, 1997; Lepik, 2005; Majak et al., 2009a, Xie et al., 2013, 2014a, 2014b, 2014c; Lepik, 2009; Paper II) and partial (Lepik, 2007a, 2007b; 2011; Jiwari, 2012; Islam et al., 2013a; Arbabi et al., 2017) differential equations. In (Hsiao, 1997) the state analysis of the linear time delayed systems is reported. In (Lepik, 2005) the segmentation method is proposed, according to which the interval of integration is divided into segments (reduced Haar transform). Both ordinary and partial differential equations are covered. The vibration analysis of the rectangular tapered composite plates, cylindrical shells and composite laminated cylindrical shells is reported in (Majak et al., 2009a), (Xie et al., 2013; 2014), respectively. In these studies, first, the partial differential governing equations are converted to an ordinary differential equation (ODE) by changing of variables and then the HWM is applied to ODE. In (Paper II) HWM is applied to the vibration analysis of nanobeams. The two-dimensional Haar wavelet method was developed in (Lepik, 2011) and applied for the solution of diffusion and Poisson as well as evolution equations. In (Jiwari, 2012) the HWM is adapted for solving Burgers' equation. The parabolic partial differential equations (PDE) are explored in (Islam et al., 2013a) by implementing the Haar and Legendre wavelet methods. Solution of systems of PDE by applying HWM is studied in (Arbabi et al., 2017). In all of these papers, the strong formulation based approach has been applied, i.e. the wavelet expansions for solution and its derivatives are inserted to original differential equations. The weak formulation based HWM approach is developed in (Majak, 2009b) and applied for solving the nonlinear Burgers equation. Despite weak formulation, the Chen and Hsiao approach has been applied in this study. An alternative approach how to overcome non-smooth properties of Haar wavelets is proposed in (Cattani, 2005; Castro et al., 2010), where the regularization of quadratic waves has been performed (for example, smoothing with interpolating splines). In the latter case, the solution of the differential equation can be expanded into Haar wavelets (regularized) and all necessary derivatives computed. However, such regularization is an additional task and the simplicity of the method is blemished. For that reason, the latter approach is not widely applied.

The HWM proposed by Chen and Hsiao for the solution of differential equations has been extended to solve integro-differential (Lepik, 2006; Islam et al., 2013, 2014; Babaaghaie et al., 2017; Kumar et al., 2018) and integral equations (Lepik 2008; Aziz et al., 2013, 2014). In (Lepik, 2006) the Haar wavelet method is developed for nonlinear Volterra integral equations and integro-differential equations. The Newton method is applied for handling nonlinearity. Modified HWM approach for solving integral and integro-differential equations is proposed in (Islam et al., 2013, 2014; Aziz 2013; Singh et al., 2016). According to this approach, the Kernel function is expanded into wavelets (also, the highest order derivative if it exists in an integro-differential equation). In earlier studies, the Kernel function was expanded into 2D Haar wavelets (Islam et al., 2013; Aziz 2013). Later in (Islam et al., 2014), the Kernel function is expanded into 1D wavelets, which allows reduction of the computational cost of the algorithm. In recent studies (Babaaghaie et al., 2017; Kumar et al., 2018), HWM is applied for solving nonlinear two-dimensional partial integro-differential equations. Lepik (Lepik, 2008) adapted HWM for solving integral equations. In (Lepik, 2008) HWM for non-uniform grid was developed. In (Aziz et al., 2014) HWM based solution procedure is developed for nonlinear Volterra and Fredholm integral equations. Nonlinear Volterra integral equations of the first kind were explored by applying HWM in (Singh et al., 2016).

New methods are often used to solve problems covering advanced material and constitutive models for which commercial software and solution methods are not yet available. One emerging research area is the solution of fractional differential and integral equations (Lepik, 2009; Ray et al., 2014; Ray, 2012; Saeed et al., 2013, 2014, 2015; Li et al., 2014; Wang et al., 2014; Yi et al., 2014; Majak et al., 2016). Fractional derivatives allow us to describe more accurately real world materials and processes (e.g. viscoelastic materials). One of the pioneering studies here was conducted by Lepik. In (Lepik, 2009) an HWM based solution procedure was developed for fractional linear Volterra and Fredholm integral equations. In (Ray et al., 2014) the HWM is adapted for solving the fractional order stationary neutron transport equation. Fractional differential equations were solved first by applying HWM in (Lepik, 2009), where the differential equation of fractional harmonic vibration was converted into the Volterra integral equation and then solved numerically. Li and Zhao (Li et al., 2010) and Ray (Ray, 2012) introduced the Haar wavelet operational matrix method for the numerical solution of the fractional Bagley Torvik equation. The solution obtained by Ray (Ray, 2012) validated the results against an analytical solution given in (Podlubny, 1999). The Haar wavelet operational matrix method has been employed by Yi and Huang (Yi et al., 2014) for solving fractional differential equations with variable coefficients and by Li et al. (Li et al., 2014) for solving the Riccati differential equation. By applying the quasilinearization technique, the HWM is adapted for solving fractional nonlinear differential equations in (Saeed et al., 2013, 2014, 2015). In (Wang et al., 2014) a truncated Haar wavelet series together with the wavelet operational matrix are used to reduce the fractional partial differential equations to Sylvester equations. In (Majak et al., 2016) it is reported that in the case of fractional ODE, the order of convergence

of the Haar wavelet method is equal to two if a higher order derivative α in the fractional differential equation exceeds one ($\alpha > 1$). However, in the case of $0 < \alpha < 1$, the order of convergence of the Haar wavelet method tends to the value $1 + \alpha$.

From the point of view of the current thesis research, the studies addressing composite and nanostructures are most interesting. The composite structures were explored by HWM in (Chun et al., 2007; Majak et al., 2009a; Hein et al., 2011; Jin et al., 2013, 2014; Xie et al., 2014a, 2014b, 2014c; Paper I). In (Majak, 2009a) the free vibration analysis of the multilayer composite plate is performed and possibilities for higher order wavelet expansion are discussed. In (Hein et al., 2011) delamination of the composite beam is studied. In (Xie et al., 2014b, 2014c; Jin et al., 2014) the HWM is adapted for the vibration analysis of conical and cylindrical shells and a general approach for handling boundary conditions is introduced. Functionally graded (FG) structures were studied by applying HWM in (Chun et al., 2007; Jin et al., 2014; Xie et al., 2014a; Paper I, IV). In (Chun et al., 2007) the HWM is employed for the stress-strain analysis of 3D functionally graded plate. First, the trigonometric expansion is utilized and the governing differential equations are converted to ordinary differential equations (ODE). Next, the HWM is implemented for solving a system of ODE. Free vibration analysis of FG conical and cylindrical shells is covered in (Jin et al., 2014; Xie et al., 2014a). In (Paper I, IV) main attention is paid to the comparison of HWM with widely used numerical methods in engineering (finite difference method-FDM, differential quadrature method-DQM, finite element method-FEM), also to the accuracy analysis. The author has not found studies addressing the structural analysis of nanostructures by employing HWM. In (Paper II) an attempt is made to adapt HWM for the vibration analysis of nanobeams using the Eringen's nonlocal elasticity model. In (Majak et al., 2013) the design of graphene laminate is optimized considering orientations of layers as design variables and maximal fundamental frequency as an objective.

The HWM has been successfully applied in all abovementioned studies. Furthermore, this method was considered commonly as simple and effective; later it was confirmed also in a review paper (Hariharan et al., 2014) and a monograph (Lepik et al., 2014). However, as pointed out above, the HWM is a simple rather than a powerful and widely used numerical method for structural analysis like FDM, DQM and FEM. Also, in the early phase of the current study, the theoretical convergence results for the Chen and Hsiao approach based HWM were not yet available.

In the current study, an attempt is made to cover at least partially the abovementioned white spaces, i.e. to evaluate HWM for the analysis of FGM and nanostructures based on their comparison with widely used numerical methods in engineering design. Planned study includes detailed analysis and comparison of the accuracy and numerical convergence rates.

1.1 Haar wavelet method (HWM)

The Haar wavelet is a sequence of rescaled "square-shaped" functions which together form a wavelet family or a basis (see Figure 1.1). It was proposed in 1909 by Alfred Haar to give an orthonormal system for the space of square-integrable functions on the unit interval $[0, 1]$.

The i -th Haar wavelet is defined as (Lepik, 2014):

$$h_i(x) = \begin{cases} 1 & \text{for } x \in [\varepsilon_1(i), \varepsilon_2(i)), \\ -1 & \text{for } x \in [\varepsilon_2(i), \varepsilon_3(i)), \\ 0 & \text{elsewhere,} \end{cases} \quad (1.1)$$

where

$$\begin{aligned} \varepsilon_1(i) &= A + 2k\mu\Delta x, & \varepsilon_2(i) &= A + (2k + 1)\mu\Delta x, \\ \varepsilon_3(i) &= A + 2(k + 1)\mu\Delta x, & \mu &= M/m. \end{aligned} \quad (1.2)$$

Haar wavelets are defined in the interval $x \in [A, B]$, where A and B are given constants. The interval $[A, B]$ is divided into $2M$ subintervals of equal length, where the length of each subinterval $\Delta x = (B - A)/(2M)$. The integer $m = 2^j$ ($j = 0, 1, \dots, J$) indicates the level of the wavelet and j is called the dilatation parameter (when we increase the value of j , then the wavelet narrows down). Maximum level of the resolution is denoted by $M = 2^J$. The parameter $k = 0, 1, \dots, m - 1$ is the translation parameter; it indicates the location of the particular square wave (Figure 1.1).

The index i is calculated according to the formula $i = m + k + 1$; at minimal values, $j = 0, m = 1, k = 0$ and it implies that $i = 2$, at maximum values, $i = 2M = 2^{J+1}$. It is assumed that the value $i = 1$ corresponds to the scaling function for which $h_1 \equiv 1$ in the whole interval $[0, 1]$ and vanishes elsewhere.

The n -th order integrals of the Haar function (1.1) can be computed as:

$$p_{n,i}(x) = \begin{cases} 0 & \text{for } x \in [A, \xi_1(i)) \\ \frac{(x - \xi_1(i))^n}{n!} & \text{for } x \in [\xi_1(i), \xi_2(i)) \\ \frac{(x - \xi_1(i))^n - 2(x - \xi_2(i))^n}{n!} & \text{for } x \in [\xi_2(i), \xi_3(i)) \\ \frac{(x - \xi_1(i))^n - 2(x - \xi_2(i))^n + (x - \xi_3(i))^n}{n!} & \text{for } x \in [\xi_3(i), B) \end{cases} \quad (1.3)$$

Any integrable and finite function in the interval $[A, B]$ can be expanded into Haar wavelets as:

$$f(x) = \sum_{i=1}^{\infty} a_i h_i(x). \quad (1.4)$$

However, in the numerical calculation, the sum (1.4) is limited to the finite number of the terms

$$f_M(x) = \sum_{i=0}^{2M} a_i h_i(x). \quad (1.5)$$

Let us consider the Euler-Bernoulli beam equation as a simple sample

$$EI \frac{\partial^4 w(x)}{\partial x^4} = q(x), \quad (1.6)$$

where $w(x)$ is the deflection of the beam, EI and q stand for the flexural rigidity and load terms, respectively. According to the approach proposed by Chen and Hsiao (Chen et al., 1997), the higher order derivative included in the differential equation is expanded into the Haar wavelet, i.e.

$$f(x) = \frac{d^4 u(x)}{dx^4} = \sum_{i=1}^{\infty} a_i h_i(x). \quad (1.7)$$

The solution of the differential Eq. (1.6) $u(x)$ can be obtained by integrating the relation (1.7) n times

$$u(x) = \frac{a_1 x^4}{4!} + \sum_{j=0}^{\infty} \sum_{k=0}^{2^j-1} a_{2^j+k+1} p_{4,2^j+k+1}(x) + S_{BT}(x). \quad (1.8)$$

In (1.8) $S_{BT}(x)$ stand for the boundary term and $p_{4,2^j+k+1}(x)$ is computed according to relations (1.3).

Substituting the solution (1.8) and all its derivatives in the differential equation (1.6) (in the considered simple sample only fourth order derivative is present in (1.6)), satisfying boundary conditions and taking into account the finite number of terms, one obtains a linear algebraic system with respect to coefficients a_i (uniform grid points $t_l = (2l-1)/(2N)$, $l = 1, \dots, N$ are used for discretization). After determining the coefficients a_i , the value of the solution $u(x)$ can be computed in any point in the interval $[A, B]$ by use of the formula (1.8). Obviously, the HWM introduced above can be applied for solving a wide class of ordinary and partial differential equations.

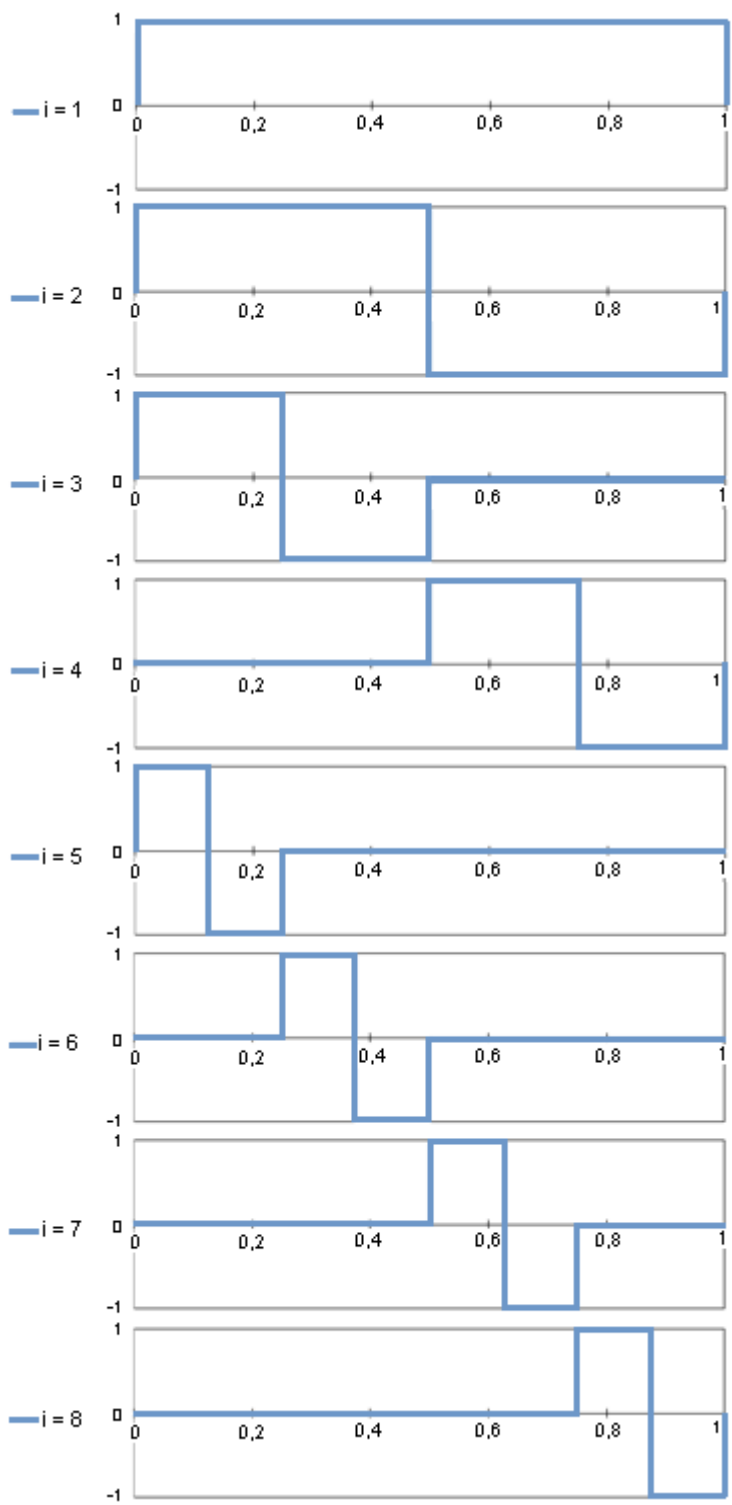


Figure 1.1 Eight first Haar wavelets

1.2 Reference methods

Two strong formulation based numerical methods FDM and DQM used widely in engineering design are considered as reference methods for the evaluation of the Haar wavelet method. The FEM as a more complex weak formulation based method is used for general validation/comparison. In the following, a short description of the reference methods and FEM is given to review basic working principles and formulas.

1.2.1 Differential quadrature method (DQM)

The differential quadrature method is a numerical solution technique developed by Richard Bellman in the early 1970s for initial and/or boundary problems. The idea of the DQM is that the solution domain is discretized into N sampling points and the derivatives at any point are approximated by a weighted sum of function values at discrete points in the variable domain.

$$\left. \frac{d^{(m)}f(x)}{d^m x} \right|_{x=x_i} \cong \sum_{j=1}^N A_{i,j}^{(m)} * f(x_j), \quad \text{for } i = 1, 2, \dots, N \text{ and } m = 1, 2, \dots, M. \quad (1.9)$$

In (1.9) the m -th derivative of a function $f(x)$ with respect to x at point $x = x_i$ is approximated by the sum over the product of weighting coefficients $A_{i,j}^m$ and the values of the function at $x = x_j$. Here, N and M stand for the number of the grid points and the order of the highest derivative in the differential equation.

In (Bellman et al., 1972) two different approaches for determining the weighting coefficients are introduced:

- In the first approach, such simple functions as test functions were utilized, but when the sampling points are relatively large, the coefficient matrix becomes ill conditioned;
- In the second approach, similarly, simple functions are used as test functions, but the grid points are chosen as the roots of shifted Legendre polynomial.

To overcome the abovementioned shortcomings, the DQM was generalized in (Shu et al., 1990; 1992; Shu, 1991, 2000). In the latter studies, the Lagrange interpolating polynomials were employed as the set of tests functions. The advantages of the generalized differential quadrature method (GDQM) can be outlined as:

- The weighting coefficients of the first and higher order derivatives can be computed by a simple algebraic formula and a recurrence relationship, respectively;
- There are no restrictions on the distribution of discrete grid points.

Applying the Lagrangian interpolation formula, the weighting coefficients for the first order derivative can be computed as (Shu, 1991):

$$A_{i,j}^{(1)} = \frac{M(x_i)}{(x_i - x_j) * M(x_j)} \quad i = 1, 2, \dots, N, \quad j = 1, 2, \dots, N, \quad i \neq j, \quad (1.10)$$

$$A_{i,i}^{(1)} = -\sum_{j=1, j \neq i}^N A_{i,j}^{(1)} \quad i = 1, 2, \dots, N. \quad (1.11)$$

where

$$M(x_i) = \prod_{k=1, k \neq i}^N (x_i - x_k), \quad i = 1, 2, \dots, N. \quad (1.12)$$

Similarly, the weighting coefficients for the higher order derivative can be determined by using such recurrence relationship as (Shu, 1991):

$$A_{i,j}^{(m)} = m \left[A_{i,j}^{(1)} A_{i,i}^{(m-1)} - \frac{A_{i,j}^{(m-1)}}{(x_i - x_j)} \right] \quad i = 1, 2, \dots, N, \quad j = 1, 2, \dots, N, \quad i \neq j, \quad m = 2, 3, \dots \quad (1.13)$$

$$A_{i,i}^{(m)} = -\sum_{j=1, j \neq i}^N A_{i,j}^{(m)} \quad i = 1, 2, \dots, N. \quad (1.14)$$

For the discretization points, the normalized Gauss-Chebyshev – Lobatto distribution is a frequently used method

$$x_i = \frac{1}{2} \left[1 - \cos \left(\frac{(i-1)\pi}{N-1} \right) \right], \quad i = 1, 2, \dots, N. \quad (1.15)$$

In the current study, the GDQM has been used for the comparison of the results.

1.2.2 Finite difference method (FDM)

The finite difference approximation to solve differential equations has been known already from the 18th century for a one-dimension space and was extended for a two-dimension space at the beginning of the 20th century.

The principle of finite difference methods is to approximate the differential operator by replacing the derivatives in the equation using differential quotients. The domain is partitioned in space and in time and approximations of the solution are computed at the space or time points.

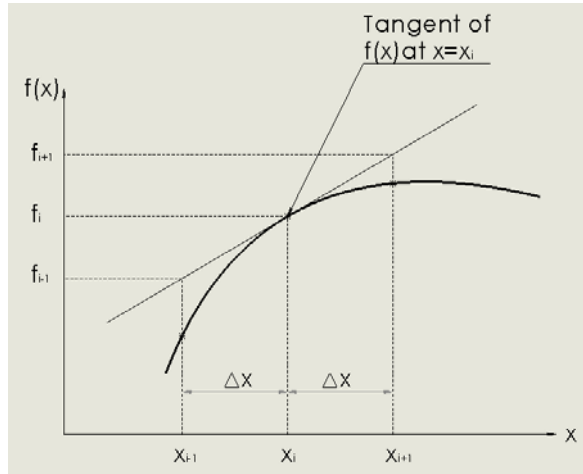


Figure 1.2 Geometric interpretation of the finite difference method

By definition of the derivative

$$\frac{df(x)}{dx} = \lim_{\Delta x \rightarrow 0} \frac{f_{i+1} - f_i}{\Delta x} \approx \frac{\Delta f}{\Delta x}, \quad \text{where } x_{i+1} = x + \Delta x, \quad f_{i+1} = f(x_{i+1}). \quad (1.16)$$

It can be seen from the graph (Figure 1.2) and from the formula (1.16) that the more Δx tends to 0, the closer the values between the differential and difference of the rate change of the function.

The simplest finite difference schemes for the approximation of the first derivative can be outlined as (LeVeque, 2005):

$$\text{Forward difference scheme: } \left. \frac{df(x)}{dx} \right|_{x=x_i} = \frac{f_{i+1} - f_i}{\Delta x}, \quad (1.17)$$

$$\text{Backward difference scheme: } \left. \frac{df(x)}{dx} \right|_{x=x_i} = \frac{f_i - f_{i-1}}{\Delta x}, \quad (1.18)$$

$$\text{Central difference scheme: } \left. \frac{df(x)}{dx} \right|_{x=x_i} = \frac{f_{i+1} - f_{i-1}}{2\Delta x}. \quad (1.19)$$

Note that the central difference scheme is a second order scheme (error $O(h^2)$), and the remaining two schemes are first order schemes. The accuracy of the forward and backward schemes (also central scheme) can be improved by including new terms. For example, the second order forward difference scheme can be introduced as (LeVeque, 2005):

$$\left. \frac{df(x)}{dx} \right|_{x=x_i} = \frac{-f_{i+2} + 4f_{i+1} - 3f_i}{2\Delta x}. \quad (1.20)$$

The simplest second order scheme, i.e. the central difference scheme, is computationally the cheapest and most widely used approach. This approach is also used in the current study. The higher order derivatives included in the governing

equations of the FG and nanostructures considered can be approximated by the second order central difference scheme as (LeVeque, 2005):

$$\left. \frac{d^2 f(x)}{dx^2} \right|_{x=x_i} = \frac{f_{i+1} - 2f_i + f_{i-1}}{\Delta x^2}, \quad (1.21)$$

$$\left. \frac{d^3 f(x)}{dx^3} \right|_{x=x_i} = \frac{f_{i+2} - 2f_{i+1} + 2f_{i-1} - f_{i-2}}{2\Delta x^3}, \quad (1.22)$$

$$\left. \frac{d^4 f(x)}{dx^4} \right|_{x=x_i} = \frac{f_{i+2} - 4f_{i+1} + 6f_{i-1} - 4f_{i-2} + f_{i-3}}{\Delta x^4}. \quad (1.23)$$

Substituting the approximations of the derivatives (1.19), (1.21)-(1.23) in the governing differential equations (e.g. in (1.6)), we obtain the system of algebraic equations with respect to the values of the function f_i in node points x_i . Thus, solution of the latter algebraic system results in the solution of the governing differential equation(s) in node points x_i .

1.2.3 Finite element method (FEM)

Finite element method (FEM) is a numerical method that grew out of aerospace and civil engineering for solving problems with complicated geometries, loadings and material properties. Nowadays, FEM is obviously the most widely used mathematical method in engineering design and it is difficult to underestimate the role of FEM.

In FEM, the physical structure (one-, two- or three-dimensional solid) is divided hypothetically into an assembly of small parts called finite elements (Zienkiewicz, 1977). The finite elements are interconnected at points common to two or more elements and boundary lines/surfaces. The connection points of the two or more elements are called nodes. There is no overlapping, neither are there any cracks or surfaces between the elements. The complete set of elements is known as a mesh.

In the finite element analysis, the accuracy of the solution is judged by "mesh" convergence, checking difference of various solutions of the same problem. H-refinement and p-refinement are two main methods of mesh refinement, to find out the size of the elements where the results are not affected by changing the size of the mesh. In the h-refinement method, using the same element type, the existing elements are divided into two or more elements. In the p-refinement method, the number of elements is not changed, but the degree of the polynomial within an element is increased (Moaveni, 2007).

Benefits of the FEM:

- Well-developed theory - close relationship between the numerical formulation and weak formulation of the PDE problem;
- A number of powerful software packages that provide selection of materials, constitutive laws, pre-processing and post processing tools are available;
- It offers great freedom in the selection of discretization, both in the elements that may be used to discretize space and the basic functions.

Some limitations of the FEM:

- As a rule, in the FEM, software packages/tools are used where the newest material models, constitutive laws, etc. are not covered (or covered poorly);
- Using software packages/tools sets certain limitations for implementing features of the particular problems, also user defined material models, etc.

FEM in its widely used “classical” form is a weak formulation based method, the working principle of which is explained on the sample of a simple second order ordinary differential equation (ODE) given as (Zienkiewicz, 1977; Mohsen, 1982):

$$y''(x) = f(x). \quad (1.24)$$

First, the differential equation (1.24) is multiplied by a trial function $v(x)$ and integrated with the interval $[0, 1]$.

$$\int_0^1 y''(x)v(x)dx = \int_0^1 f(x)v(x)dx. \quad (1.25)$$

Next, the left hand side of (1.25) is integrated by parts

$$y'(x)v(x)|_0^1 - \int_0^1 y'(x)v'(x)dx = \int_0^1 f(x)v(x)dx. \quad (1.26)$$

Note that the obtained integral equation includes the derivatives of order one (integration by parts reduce the order of the derivative). As a result, the solution of (1.26) is less restrictive than that of (1.24). The solution $y(x)$ of (1.24) is required to be differentiable, but not twice differentiable.

Basic steps of the FEM are depicted in Figure 1.3. As a rule, generating mesh and the whole second group of activities are performed in most cases by software tools (if not own coded method).

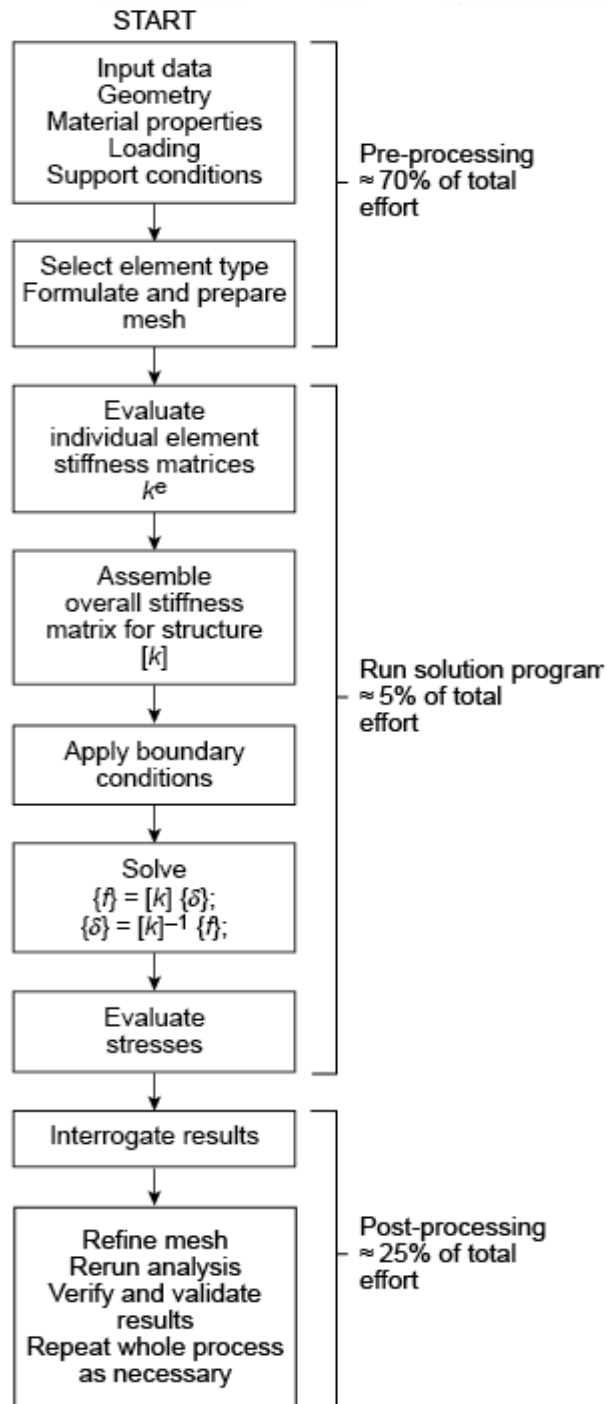


Figure 1.3 Basic steps of the FEM (<http://www.open.edu/openlearn/science-maths-technology/introduction-finite-element-analysis/content-section-1.6>)

Since FEM is a powerful but also a more complicated weak formulation based method, it is used in the current study for general validation of the FG structures only (not for direct comparison).

1.3 Evaluation criteria

The evaluation of the Haar Wavelet method is the main aim of the current study. The reference methods were introduced above. However, to analyse and compare the methods, certain criteria are needed. A number of criteria characterizing numerical methods can be outlined:

- Consistency - discretization of a PDE should become exact as the mesh size tends to zero (truncation error should vanish);
- Stability - numerical errors which are generated during the solution of discretized equations should not be magnified;
- Convergence - the numerical solution should approach the exact solution of the ODE or PDE and converge to it as the mesh size tends to zero (measure – rate of convergence);
- Conservation - underlying conservation laws should be respected at the discrete level (artificial sources/sinks are to be avoided);
- Boundedness - quantities like densities, temperatures, concentrations etc. should remain nonnegative and free of spurious wiggles;
- Accuracy – deviation from exact value (absolute or relative error of the particular parameter, absolute or relative error at fixed point, maximum error, average error, truncation error etc.);
- Complexity – number of basic operations needed to perform may be given as a complexity class by use of O notation.

In the studies addressing Haar wavelets, most attention is paid to the accuracy, convergence and simplicity/complexity of the implementation. Furthermore, similar to the well-known traditional methods considered (FD and DQM), the Haar wavelet method is characterized as a strong formulation based method with simple implementation (Lepik, 2005; Lepik et al., 2014; Hariharan et al., 2014; Majak et al. 2015a, 2015b; Xie 2014a, 2014b, 2014c; Islam et al., 2014). For that reason, in the following, two evaluation criteria - the accuracy and the rate of convergence are considered. Obviously, these two criteria are critical for any numerical method.

1.3.1 Accuracy

As was pointed out above, a number of characteristics can be used to describe the accuracy of the numerical method like HWM, FDM and DQM. Note that in the following, different error measures will be introduced for an 1D problem (can be extended for 2D and 3D). One of the simplest and most widely used characteristics is the absolute error $\varepsilon_{abs_xi_N}$ at fixed point $x = x_i$ and mesh size $N = 2M$.

$$\varepsilon_{abs_xi_N} = |u_N(x_i) - u_{ex}(x_i)|. \quad (1.27)$$

In (1.27) $u_{ex}(x_i)$ and $u_N(x_i)$ stand for the values of the exact and obtained numerical solutions at point $x = x_i$, respectively ($N = 2M$). In practice, the absolute error is most commonly used, but in cases where the error limit is defined in terms of percentages of the quantity, it is reasonable to use the relative error $\varepsilon_{rel_xi_N_proc}$ in the following form:

$$\varepsilon_{rel_xi_N_proc} = \left| \frac{u_N(x_i) - u_{ex}(x_i)}{u_{ex}(x_i)} \right| \times 100\%. \quad (1.28)$$

In practice, it is often important to find out a worse situation, i.e. maximum absolute error in the whole domain D (in the case of 1D problems, most commonly unit interval $[0, 1]$). In the latter case, the error $\varepsilon_{max_abs_N}$ can be expressed as:

$$\varepsilon_{max_abs_N} = \max_{x \in D} |u_N(x) - u_{ex}(x)|. \quad (1.29)$$

The problems considered may include other key parameters among numerical solutions of the differential equations $u_N(x)$. In the case of free vibration analysis, problems of the FG material and nanostructure parameters are the values of eigenfrequencies.

$$\varepsilon_{abs_freq_N} = |\Omega_{i,N} - \Omega_{i,ex}|. \quad (1.30)$$

In (1.30) Ω_i and $\Omega_{i,ex}$ stand for the obtained numerical and exact values of the i -th eigenfrequencies, respectively. From a practical point of view, the first frequency or fundamental frequency is most important. Thus, the two solutions can be compared by comparing two scalars (the values of fundamental frequencies), only. For that reason, the vibration problems are often selected for the validation of new numerical methods in the area of engineering design.

The error estimates (1.27)-(1.30) are based on the comparison of a numerical solution with an exact one, i.e. it assumes that the exact solution is known. However, the exact solution is known in the case of simple test problems only. In the case of most problems, the exact solution is unknown and the following integral criteria can be employed for estimating the accuracy (Lepik, 2006):

$$\Delta(N) = \left| \frac{S(2N)}{S(N)} - 1 \right|, \quad (1.31)$$

where

$$S(N) = \Delta x^{(N)} \sum_{r=1}^{2M} |u_N(x_r)|. \quad (1.32)$$

In (1.32) the notation introduced in section (1.1) is used. Here $N = 2M$, $\Delta x^{(N)} = (B - A)/N$,

$x_r = \frac{(2r-1)\Delta x^{(N)}}{2}$, $r = 1, \dots, N$ and $S(N)$ stands for the area which lies underneath the curve $|u_N(x)|$ in the integration domain, respectively.

1.3.2 Convergence

Convergence is one of the main characteristics of the numerical methods. Most commonly and also herein, the convergence in regard to the mesh is considered (in the case of nonlinear problems, convergence to the solution with a fixed mesh can be studied additionally). Thus, in the following, the convergence means that at $\Delta h \rightarrow 0$ (here Δh stands for the step size of the grid), the numerical solution collapses onto the exact solution and the error vanishes. However, in practice not only the fact of convergence is extremely important, but also how fast the convergence process is, i.e. the value of the rate of convergence.

The numerical rate of convergence can be estimated through the ratio of absolute errors computed for two sequential values of the step size Δh . In the Haar wavelet method, it is common to reduce the step size of the grid twice in each iteration, i.e. $h_i = h_{i-1}/2$ and the numerical rate of convergence k^E is given as (Paper III):

$$k^E = \log\left(\left|\frac{\Omega_{i,N/2} - \Omega_{i,ex}}{\Omega_{i,N} - \Omega_{i,ex}}\right|\right) / \log(2). \quad (1.33)$$

Obviously, the formula (1.33) can be used only in cases when the exact solution is known. When the exact solution is unknown, the numerical rate of convergence can be computed using three values of the eigenfrequencies $\Omega_{i,N/4}$, $\Omega_{i,N/2}$ and $\Omega_{i,N}$, corresponding to the three sequential values of the mesh $N/4$, $N/2$ and N , respectively

$$k^A = \log\left(\left|\frac{\Omega_{i,N/4} - \Omega_{i,N/2}}{\Omega_{i,N/2} - \Omega_{i,N}}\right|\right) / \log(2). \quad (1.34)$$

Similarly, formulas (1.33)-(1.34) can be implemented for the function $u(x)$.

Although the Haar wavelet method was introduced already in 1997 (Chen and Hsiao, 1997), the theoretical convergence results were open when the current PHD study was started. The convergence theorem has been proved in (Paper III) for the n -th order ODE ($n \geq 2$).

THEOREM: Let us assume that $f(x) = \frac{d^n u(x)}{dx^n} \in L^2(R)$ is a continuous function on

$$[0,1] \text{ and its first derivative is bounded } \forall x \in [0,1] \quad \exists \eta : \left| \frac{df(x)}{dx} \right| \leq \eta. \quad (1.35)$$

Then the Haar wavelet method based on the approach (Chen et al., 1997) will be convergent, i.e. absolute error $|E_M|$ vanishes as the number of collocation points N goes to infinity.

The convergence is of order two

$$\|E_M\|_2 = O\left[\left(\frac{1}{N}\right)^2\right]. \quad (1.36)$$

Thus, based on the above theorem, the values of the numerical rate of convergence computed using (1.33) or (1.34) should tend to two (with growing mesh).

The theoretical convergence results and evaluation results of the HWM obtained in (Paper I, IV) lead to unequivocal corollary - in order to compete with mainstream numerical methods in engineering (like FDM, DQM, FEM), the HWM needs further improvement.

1.4 Improved Haar Wavelet Method (HOHWM)

Recently, a new higher order Haar wavelet method approach has been introduced (Majak et al., 2018). This approach is based on:

- higher order wavelet expansion,
- algorithms for determining integration constants.

The higher order wavelet expansion is introduced as:

$$f(x) = \frac{d^{n+2s}u(x)}{dx^{n+2s}} = \sum_{i=1}^{\infty} a_i h_i(x), \quad s = 1, 2, \dots \quad (1.37)$$

where n stands for the order of highest derivative included in the differential equation. In comparison with the Chen and Hsiao approach, the order of expansion is increased by $2s$. However, it has been confirmed that the higher order expansion itself may not provide higher convergence rate and accuracy if the integration constants are not determined appropriately. Note that the number of boundary conditions is equal to n and there is a need for additional conditions for determining $2s$ integration constants. In (Majak et al., 2018) two algorithms are proposed based on the use of

- selected uniform grid points,
- selected Chebyshev-Gauss-Lobatto grid points.

In the case of $s = 1$, these two algorithms coincide, the selected additional points where the differential equation will be satisfied are the boundary points. On the one side, the obtained results confirm that the new approach allows principal improvement of the accuracy and the rate of convergence (from two to four) even with $s = 1$. On the other side, the double precision computing used (MATLAB) seems not good enough for computing at higher values of s ($s > 1$). For that reason, in the current study, the

higher order Haar wavelet expansion (1.37) with $s = 1$ is employed and the differential given in the general form

$$G(x, u, u', u'', \dots, u^{(n-1)}, u^{(n)}) = 0, \quad (1.38)$$

is completed by the following two supplemental conditions (in addition to the boundary conditions)

$$DV(0) = G(0, u(0), u'(0), u''(0), \dots, u^{(n-1)}(0), u^{(n)}(0)) = 0, \quad (1.39)$$

$$DV(1) = G(1, u(1), u'(1), u''(1), \dots, u^{(n-1)}(1), u^{(n)}(1)) = 0. \quad (1.40)$$

According to (1.37), in the case of $s = 1$, there are $n + 2$ integration constants from which n can be determined from the boundary conditions and two from the conditions (1.39)-(1.40). Note that the collocation points used in the widely used HWM (Chen and Hsiao approach) are internal points. Thus, there is no conflict with existing and added discretization points.

Similar to the HWM discussed in detail in section 1.1, the coefficients a_i can be determined from the linear system obtained by substituting the expansion (1.37) in governing differential equations and performing discretization in uniform grid points ($t_l = (2l - 1)/(2N)$, $l = 1, \dots, N$).

1.5 Objectives of the research

Objective and activities:

The main objective of the current study is to evaluate the Haar wavelet method for the analysis of FG structures and nanostructures. The following activities (sub-objectives) can be performed to achieve the posed goal.

Activity 1:

Implementation of the Haar wavelet method for the analysis of the FG structures and nanostructures.

Activity 2:

Comparison of the accuracy of HWM, FDM and DQM based on the case studies covering FG structures and nanostructures (absolute error). Analysis and comparison of numerical convergence rates.

Activity 3:

Evaluation of improved HWM, comparison with the widely used HWM (absolute error, convergence rate). Complexity analysis.

Main hypothesis of the thesis research:

The main hypotheses of the study can be outlined as:

- H1: HWM is known by its simple implementation, which can be confirmed also in the case of structural analysis of FG structures and nanostructures.
- H2: The accuracy of the HWM and FDM is in the same range. The convergence rate is equal to two in the case of both methods. The absolute error of the HWM outperforms that of the FDM (observed in the case of considered problems, exceptions area available).
- H3: The accuracy of the HWM is lower than that of DQM (exceptions may occur at high resolution where DQM has certain limitations). Although simple in implementation, HWM based on the Chen and Hsiao approach needs improvement.
- H4: The accuracy of the HWM can be improved substantially. The order of convergence can be improved to four and the absolute error can be reduced several orders magnitude depending on the mesh level used. The increase of complexity can be kept minimal for the problems considered.
- H5: Simplicity of the HWM forms a basis for further applications for new materials, constitutive models not yet well covered by traditional numerical techniques (including nanomaterials, fractional calculus, etc.).

2 Evaluation of Haar wavelet method – case studies

In the following, the HWM has been applied for the analysis of the following two kinds of advanced structures:

- functionally graded structures
- nanostructures.

The FG materials have a key role in applications such as interface layers, providing a smoother change of material properties and avoiding stress concentrations, cracks, spalling, etc. Use of FG material allows often provision of multiple properties/functionalities like high strength and thermal resistance (e.g., metal ceramic FG materials). Nanomaterials/nanostructures allow the small scale effect to be considered.

2.1 Functionally Graded Structures

This section gives an overview of FG materials and their advantages, widely used models for describing FG material properties and presents a case study to evaluate a wide HWM and compare it with improved HOHWM.

2.1.1 Description of functionally graded materials

Materials in which the composition, microstructure or porosity are changing across the volume in arbitrary direction are called functionally graded materials (FGM). There are three main types of FGMs: porosity and pore size gradient-structured FGMs, chemical gradient-structured FGMs, and microstructural gradient-structured FGMs (Mahamood et al., 2017). The idea of functionally graded materials is to combine two distinct material phases smoothly and continuously to avoid abrupt changes in the stress and displacement distributions (Moita et al., 2016) (Figure 2.1). That kind of composition constitutes a new material which includes desirable properties of used materials.

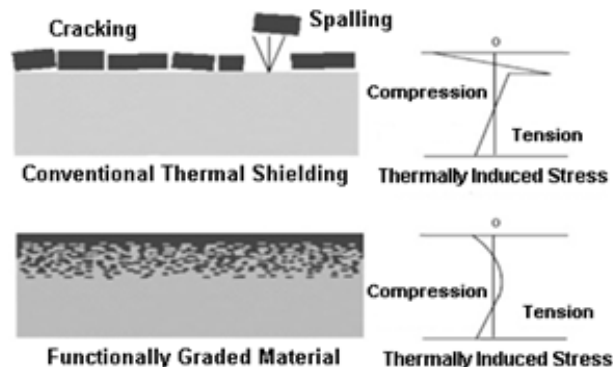


Figure 2.1 Example of stress distributions in Conventional Thermal Shielding and FGM [Gupta A., Talha M. (2015)]

The principle of FGM is used in sandwich-structured composites, where the inner lightweight and thicker core is covered with thick and stiffer skin layers, to obtain a strong and lightweight structure. There are two main types of functionally graded sandwich-structures: in the first case, the core is functionally graded, in the second case, the skins are functionally graded (Figure 2.2).

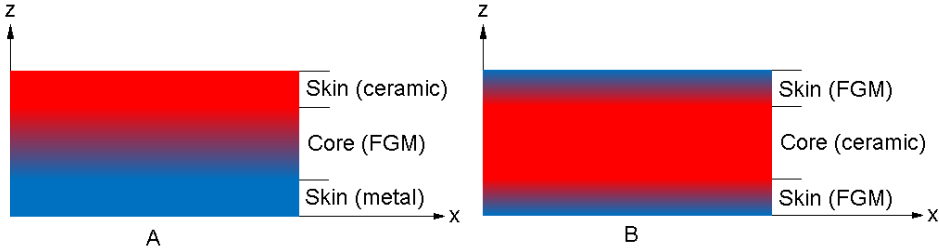


Figure 2.2 Types of functionally graded sandwich-structure composites

The structure of FGMs may be graded continuously or step-wise (Figure 2.3). At step-wise graduation, the multi-layered structure is generated with interfaces existing between discrete layers (Miyamoto et al., 1999).



Figure 2.3 Types of graded structures: a) continuously graded structure, b) step-wise graded structure

The shape of this material gradient is an important factor in determining the properties of an FGM structure (Sayyad et al., 2018). Obviously, structures can be graded axially, through thickness or even in multiple directions simultaneously.

2.1.2 Modelling properties of the FG material

In the numerical analysis, the FGM properties of the structure are commonly implemented through variation of the elasticity properties, density, volume fraction, etc. In the following, four widely used functions for describing the variation of FG materials are introduced, where graduation is assumed in the thickness direction.

The power-law gradient function

Let us assume that the structure is made of two materials with properties P_A and P_B and the properties vary through the thickness. The effective material properties of the FG structure can be evaluated by applying the rule of mixtures (Chi et al., 2006; Bhandari et al., 2015; Sayyad et al., 2018)

$$P(z) = P_B + (P_A - P_B)V_A(z), \quad (2.1)$$

where V_A is the volume fraction function of the material A given as:

$$V_A(z) = \left(\frac{1}{2} + \frac{z}{h}\right)^p \quad \text{for } z \in [-h/2, h/2], \quad (0 \leq p \leq \infty). \quad (2.2)$$

In (2.1)-(2.2) h is a thickness of the structure, z - a coordinate in thickness direction, P_A and P_B stand for the values of the effective properties of the materials A and B , respectively. The material variation is described by the non-negative power law exponent parameter p .

The exponential-law gradient function

The function $P(z)$ describing material distribution through thickness can be presented as (Chi et al., 2006; Bhandari et al., 2015; Sayyad et al., 2018):

$$P(z) = P_B \exp\left[\left(\frac{1}{2} + \frac{z}{h}\right) \ln\left(\frac{P_A}{P_B}\right)\right] \quad \text{for } z \in [0, L]. \quad (2.3)$$

The notation introduced for the power law function is utilized. This function is often used especially in the fracture mechanics analyses of functionally graded materials.

The sigmoid-law gradient function

If a single power-law function is utilized in the multi-layered composite, the stress concentrations appear on one of the interfaces where the material is continuous but changes rapidly. Therefore, to provide more smooth distribution of stresses among all the interfaces, the two power-law functions can be introduced as in (Chung et al., 2001):

- Anti-symmetric power law function

$$P(z) = P_m + (P_c - P_m) \left[1 + \left(\frac{z}{h} - \frac{1}{2}\right)^p\right] \quad \text{for } z \in \left[-\frac{h}{2}, 0\right], \quad (2.4)$$

$$P(z) = P_m + (P_c - P_m) \left(\frac{z}{h} + \frac{1}{2}\right)^p \quad \text{for } z \in \left[0, \frac{h}{2}\right]. \quad (2.5)$$

- Symmetric power law function

$$P(z) = P_c + (P_m - P_c) \left(\frac{-2z}{h}\right)^p \quad \text{for } z \in \left[-\frac{h}{2}, 0\right], \quad (2.6)$$

$$P(z) = P_c + (P_m - P_c) \left(\frac{2z}{h}\right)^p \quad \text{for } z \in \left[0, \frac{h}{2}\right]. \quad (2.7)$$

The combination of the two power-law functions is used in the case of bi-sectioned (bi-layered) structural elements, laminates, etc.

The Mori-Tanaka's gradient function

The micromechanics based approach proposed by (Mori et al., 1973) accounts the effect of elastic fields among neighbouring inclusion and its interactions with the constituents. It is assumed that the matrix phase is reinforced by spherical particles of a

particulate phase. The estimated effective local bulk modulus $K(z)$ and shear modulus $G(z)$ read (Sayyad et al., 2018; Ke et al., 2012)

$$\frac{K(z)-K_A}{K_B-K_A} = \frac{V_B(z)}{1+(1-V_B(z))\left(\frac{K_B-K_A}{K_A+\frac{4}{3}G_A}\right)}, \quad \frac{G(z)-G_A}{G_B-G_A} = \frac{V_B(z)}{1+(1-V_B(z))\left(\frac{G_B-G_A}{G_A+f_A}\right)}, \quad (2.8)$$

where

$$f_A = \frac{G_A(9K_A+8G_A)}{6(K_A+2G_A)}.$$

The effective Young's modulus and Poisson's ratio can be derived in terms of $K(z)$ and $G(z)$ as (Sayyad et al., 2018; Ke et al., 2012; Ebrahimi et al., 2014)

$$E(z) = \frac{9K(z)G(z)}{3K(z)+G(z)}, \quad \nu(z) = \frac{3K(z)-2G(z)}{6K(z)+2G(z)}. \quad (2.9)$$

Note that in the Mori-Tanaka model, it is commonly assumed that the volume fraction follows a simple power law (2.2).

2.1.3 Free vibration analysis of FGM beam

The case study comprises the formulation of the problem, the user defined procedure for modelling the FGM beam (FG beam) using ANSYS and the numerical results.

Problem formulation

The free vibration analysis of the FGM beam is considered as one of the two case studies for the evaluation of the HWM. On the one hand, it provides exact analytical solutions with a better possibility for error estimation and convergence analysis. On the other hand, due to varying material properties, the FG structures cover a much wider class of problems than isotropic or even orthotropic materials/structures.

The free vibration analysis of the axially graded FGM Euler-Bernoulli beam of length L is considered in Figure 2.4.

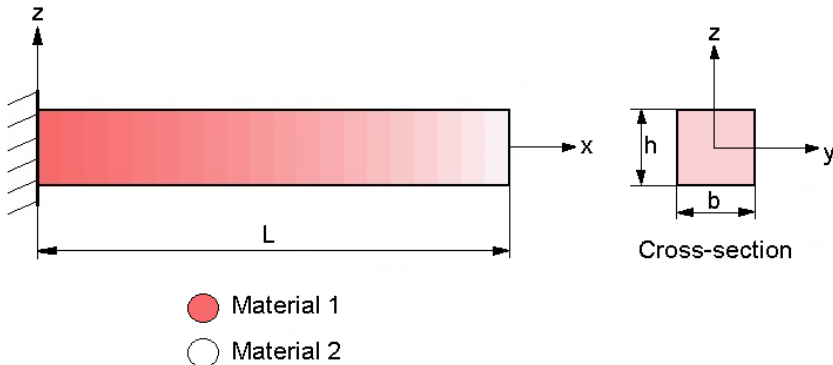


Figure 2.4 Beam graded functionally along the x-axis

The boundary conditions utilized are depicted in Figure 2.5.

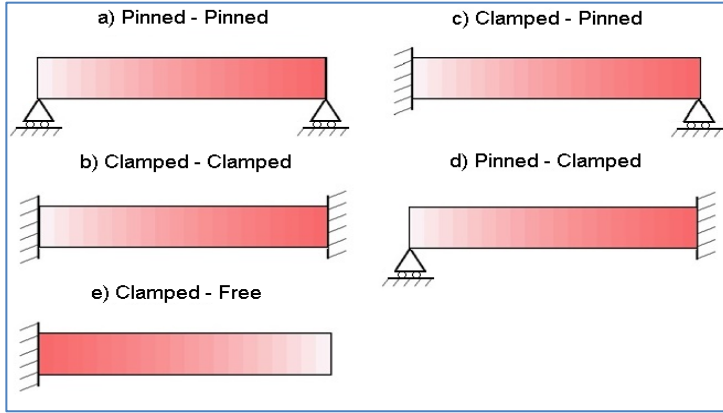


Figure 2.5 Boundary conditions for the FGM beam

In the following, two of the above described widely known gradient functions are implemented: the exponential and power law functions. However, due to the radial graduation direction, the graduation laws differ from (2.2) and (2.4). Radial graduation functions applied for the bending stiffness $EI(x)$ and the distributed mass per unit length $\rho A(x)$ are given for the exponential law function as (Li et al., 2013; Lu et al., 2017; Paper I, IV):

$$EI(x) = EI(0)e^{2\beta x/L}, \rho A(x) = \rho A(0)e^{2\beta x/L}, \quad (2.10)$$

and for the power law function as:

$$EI(x) = (EI_L - EI_R) \left(1 - \frac{x}{L}\right)^k + EI_R, \quad \rho A(x) = (\rho A_L - \rho A_R) \left(1 - \frac{x}{L}\right)^k + \rho A_R. \quad (2.11)$$

In (2.10) $EI(0)$ and $\rho A(0)$ stand for the reference values of the bending stiffness and distributed mass per unit length at the left end of the beam ($x = 0$). The indexes L and R in (2.10)-(2.11) refer to the left and right end of the beam, respectively. Note that the power law function (2.11) is more flexible than (2.10), allowing provision of different material distributions depending on the values assigned to the power law exponent k . At the exponential law function (2.10), the value of the exponent parameter β is determined by the value of the bending stiffness or distributed mass per unit length at the right end of the beam ($\beta = \frac{1}{2} \ln\left(\frac{EI(L)}{EI(0)}\right)$).

At harmonic vibrations, the governing differential equation of the FG beam corresponding to the exponential law function (2.10) can be derived in the non-dimensional form as (Lu et al., 2017; Paper I, IV):

$$\frac{d^2}{dx^2} \left(e^{2\beta x} \frac{d^2 W}{dx^2} \right) - \Omega^2 e^{2\beta x} W = 0, \quad (2.12)$$

where the non-dimensional coordinate X and the frequency parameter Ω are given as:

$$X = \frac{x}{L}, \Omega = \omega L^2 \sqrt{\frac{\rho A(0)}{EI(0)}}. \quad (2.13)$$

Similarly, more comprehensive expressions for the power law function are omitted herein for the sake of conciseness.

The implementation of the HWM, reference methods (FDM and DQM) and also improved HOHWM in the case of the particular differential equation considered is described in Chapter 1. However, the implementation of the FEM using the software package ANSYS is quite different. The standard steps of the ANSYS model development are well-known and are omitted herein. However, to model a functionally graded beam, the user coded procedure has been developed by the author of the thesis.

Modelling of FGM beam in ANSYS APDL

In the FEM analysis, it is assumed that the length of the FGM beam $L = 1m$ is divided into N_L parts, the cross-section of the beam is square, where the height and the width of the cross-section are equal to $b = 0.01m$ and are divided respectively into N_W and N_H parts.

The elements considered were cubic 3D 8-Node Homogeneous Structural Elements SOLID185, which have plasticity, hyperelasticity, stress stiffening, creep, large deflection, and large strain capabilities. The FGM beam with two different material compositions has been analysed for two symmetric and three non-symmetric boundary conditions and for four different finite elements partitions $N_W \times N_H \times N_L$ respectively $3 \times 3 \times 300$, $4 \times 4 \times 400$, $5 \times 5 \times 500$ and $10 \times 10 \times 1000$ (see Figure 2.6).

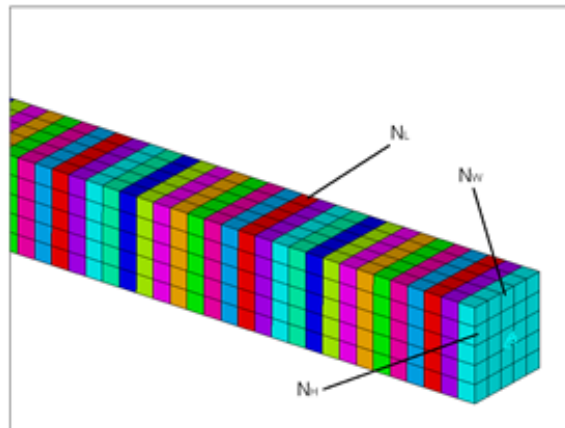


Figure 2.6 Zoomed right end of the FGM beam with finite elements

The basic steps of the user coded procedure are shown in Fig. 2.7.

In (Paper I) commercial analysis software Mechanical APDL 16.0 a 3D finite element model was created to model the free vibration analysis problem of an axial functionally graded beam. The APDL code was generated for the modelling of the FGM beam that is portioned through the length of the beam into a number of strips with constant properties. In the code, the varying properties of the bending stiffness $EI(x)$ and the distributed mass per unit length $\rho A(x)$ were described for different FG beam material compositions.

Figure 2.7 below shows the scheme describing the user-defined code for adding material properties to the finite elements of the functionally graded beam. The describable code assumes that the certain FG beam is already divided into cubic shaped finite elements and the distribution function is the exponential-law gradient function:

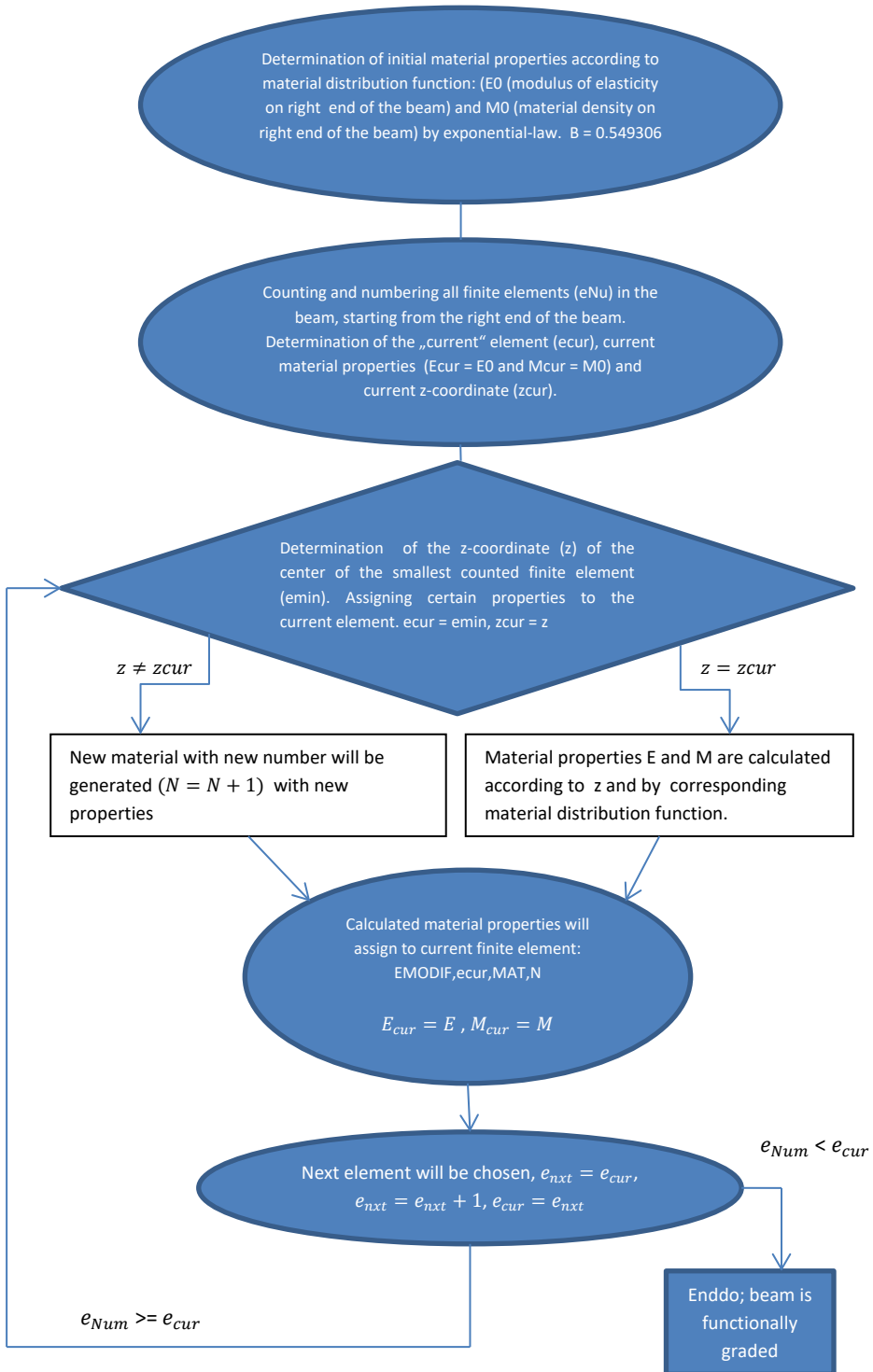


Figure 2.7 Scheme of code for the Finite Element Model

Numerical results

The numerical results were obtained for five boundary conditions depicted in Figure 2.5. In Tables 2.1-2.10, the results obtained by applying the widely used HWM (based on Chen and Hsiao approach), FDM and DQM are compared at five different boundary conditions.

Table 2.1 Fundamental frequency parameter Ω_1 values for a clamped-clamped beam ($\beta=2$, exact solution 24.78955023)

N	HWM			FDM			DQM		
	Ω_1	AbsErr	RConv	Ω_1	AbsErr	RConv	Ω_1	AbsErr	RConv
4	21.24272	3.5468		21.21278	3.5768				
8	24.01679	0.7728	2.1984	23.51733	1.2722	1.4913	24.2427724	5.47E-01	5.50
16	24.60232	0.1872	2.0452	24.43203	0.3575	1.8313	24.7895491	1.08E-06	18.95
32	24.74310	0.0464	2.0111	24.69728	0.0923	1.9542	24.7895502	5.48E-11	14.27
64	24.77796	0.0116	2.0028	24.76629	0.0233	1.9883	24.7895502	2.77E-09	-5.66
128	24.78665	0.0029	2.0007	24.78372	0.0058	1.9971	24.7895501	1.00E-07	-5.18
256	24.78882	0.0007	2.0002	24.78809	0.0015	1.9993	24.7895509	6.85E-07	-2.77
Exact: 24.789550	FEM analysis results - 100000 elem. (10x10x1000)						24.8074		

Table 2.2 Fundamental frequency parameter Ω_2 values for a clamped-clamped beam ($\beta=2$, exact solution 64.70943426)

N	HWM			FDM			DQM		
	Ω_2	AbsErr	RConv	Ω_2	AbsErr	RConv	Ω_2	AbsErr	RConv
4	57.20269	7.5067							
8	62.96688	1.7425	2.1070	57.405312	7.3041		65.2103257	5.01E-01	
16	64.28732	0.4221	2.0455	62.612504	2.0969	1.8004	64.7094620	2.78E-05	14.14
32	64.60487	0.1046	2.0133	64.163748	0.5457	1.9421	64.7094342	5.13E-11	19.05
64	64.68335	0.0261	2.0034	64.571582	0.1379	1.9849	64.7094342	2.56E-09	-5.64
128	64.70291	0.0065	2.0009	64.674880	0.0346	1.9962	64.7094343	7.55E-08	-4.88
256	64.70780	0.0016	2.0002	64.700790	0.0086	1.9990	64.7094380	3.77E-06	-5.64
Exact: 64.709434	FEM analysis results - 100000 elem. (10x10x1000)						64.7032		

Table 2.3 Fundamental frequency parameter Ω_1 values for a pinned-pinned beam ($\beta=2$, exact solution 8.41047573)

N	HWM			FDM			DQM		
	Ω_1	AbsErr	RConv	Ω_1	AbsErr	RConv	Ω_1	AbsErr	RConv
4	7.23557	1.1749		8.157141	0.2533				
8	8.11895	0.2915	2.0108	8.332735	0.0777	1.7043	8.4082266	2.25E-03	
16	8.33794	0.0725	2.0069	8.390010	0.0205	1.9255	8.4104757	9.02E-12	27.89
32	8.39236	0.0181	2.0018	8.405292	0.0052	1.9813	8.4104757	1.55E-10	-4.10
64	8.40595	0.0045	2.0005	8.409176	0.0013	1.9953	8.4104757	5.78E-08	-8.54
128	8.40934	0.0011	2.0001	8.410150	0.0003	1.9988	8.4104771	1.37E-06	-4.57
256	8.41019	0.0003	2.0000	8.410394	0.0001	1.9997	8.4104751	5.93E-07	1.21
Exact: 8.410475	FEM analysis results - 100000 elem. (10x10x1000)						8.4136		

Table 2.4 Fundamental frequency parameter Ω_2 values for a pinned-pinned beam ($\beta=2$, exact solution 41.07055822)

N	HWM			FDM			DQM			
	Ω_2	AbsErr	RConv	Ω_2	AbsErr	RConv	Ω_2	AbsErr	RConv	
4	36.59523	4.4753		34.453858	6.6167					
8	39.99909	1.0715	2.0624	39.252370	1.8182	1.8636	41.0759676	5.41E-03		
16	40.80503	0.2655	2.0127	40.603112	0.4674	1.9596	41.0705582	7.27E-10	22.83	
32	41.00432	0.0662	2.0031	40.952833	0.1177	1.9894	41.0705582	5.12E-11	3.83	
64	41.05400	0.0166	2.0008	41.041072	0.0295	1.9973	41.0705583	9.15E-08	-10.8	
128	41.06642	0.0041	2.0002	41.063183	0.0074	1.9993	41.0705586	3.34E-07	-1.87	
256	41.06952	0.0010	2.0000	41.068714	0.0018	1.9998	41.0705603	2.08E-06	-2.64	
Exact: 41.070558		FEM analysis results - 100000 elem. (10x10x1000)						41.0672		

Table 2.5 Fundamental frequency parameter Ω_1 values for a clamped-pinned beam ($\beta=2$, exact solution 11.18278324)

N	HWM			FDM			DQM			
	Ω_1	AbsErr	RConv	Ω_1	AbsErr	RConv	Ω_1	AbsErr	RConv	
4	8.76459	2.4182		9.455451	1.7273					
8	10.64780	0.5350	2.1764	10.572089	0.6107	1.5000	11.1725812	1.02E-02		
16	11.05259	0.1302	2.0389	11.012971	0.1698	1.8465	11.1827832	1.75E-10	25.80	
32	11.15044	0.0323	2.0094	11.139111	0.0437	1.9592	11.1827832	1.53E-11	3.51	
64	11.17471	0.0081	2.0023	11.171786	0.0110	1.9896	11.1827832	2.55E-08	-10.7	
128	11.18076	0.0020	2.0006	11.180029	0.0028	1.9974	11.1827830	2.25E-07	-3.14	
256	11.18227	0.0005	2.0001	11.182094	0.0007	1.9993	11.1827828	3.94E-07	-0.81	
Exact: 11.182783		FEM analysis results - 100000 elem.(10x10x1000)						11.1901		

Table 2.6 Fundamental frequency parameter Ω_2 values for a clamped-pinned beam ($\beta=2$, exact solution 48.26066843)

N	HWM			FDM			DQM			
	Ω_2	AbsErr	RConv	Ω_2	AbsErr	RConv	Ω_2	AbsErr	RConv	
4	41.945882	6.3148		35.930268	12.330					
8	46.799191	1.4615	2.1113	43.888087	4.3726	1.4957	48.3140160	5.33E-02		
16	47.903565	0.3571	2.0330	47.016589	1.2441	1.8134	48.2606684	4.22E-08	20.27	
32	48.171942	0.0887	2.0089	47.938093	0.3226	1.9474	48.2606684	1.22E-11	11.76	
64	48.238522	0.0221	2.0023	48.179262	0.0814	1.9864	48.2606685	4.19E-08	-11.75	
128	48.255134	0.0055	2.0006	48.240268	0.0204	1.9966	48.2606685	8.33E-08	-0.99	
256	48.259285	0.0014	2.0001	48.255565	0.0051	1.9991	48.2606684	1.86E-08	2.16	
Exact: 48.260668		FEM analysis results - 100000 elem.(10x10x1000)						48.2589		

Table 2.7 Fundamental frequency parameter Ω_1 values for a pinned-clamped beam ($\beta=2$, exact solution 20.77797932)

N	HWM			FDM			DQM		
	Ω_1	AbsErr	RConv	Ω_1	AbsErr	RConv	Ω_1	AbsErr	RConv
4	18.79963	1.9783		19.770973	1.0070				
8	20.30997	0.4680	2.0797	20.506995	0.2710	1.8938	20.7785283	5.49E-04	
16	20.66246	0.1155	2.0184	20.708729	0.0693	1.9683	20.7779793	6.45E-10	19.70
32	20.74919	0.0288	2.0045	20.760567	0.0174	1.9917	20.7779793	2.67E-11	4.59

64	20.77078	0.0072	2.0011	20.773620	0.0044	1.9979	20.7779793	9.10E-09	-8.41	
128	20.77618	0.0018	2.0003	20.776889	0.0011	1.9995	20.7779792	1.13E-07	-3.63	
256	20.77753	0.0004	2.0001	20.777707	0.0003	1.9999	20.7779784	9.49E-07	-3.07	
Exact: 20.777979		FEM analysis results - 100000 elem.(10x10x1000)					20.7897			

Table 2.8 Fundamental frequency parameter Ω_2 values for a pinned-clamped beam ($\beta=2$, exact solution 56.29443858)

N	HWM			FDM			DQM			
	Ω_2	AbsErr	RConv	Ω_2	AbsErr	RConv	Ω_2	AbsErr	RConv	
8	54.96516	0.4680		52.599124	0.2710					
16	55.96900	0.1155	2.0302	55.338806	0.0693	1.9512	56.0970548	2.18E-07		
32	56.21350	0.0288	2.0075	56.053355	0.0174	1.9869	56.2944388	1.13E-11	14.23	
64	56.27423	0.0072	2.0019	56.234028	0.0044	1.9967	56.2944386	7.51E-09	-9.38	
128	56.28938	0.0018	2.0005	56.279327	0.0011	1.9992	56.2944386	9.66E-08	-3.68	
256	56.29317	0.0004	2.0001	56.290660	0.0003	1.9998	56.2944385	2.37E-06	-4.62	
Exact: 56.294439		FEM analysis results - 100000 elem.(10x10x1000)					56.2907			

Table 2.9 Fundamental frequency parameter Ω_1 values for a clamped-free beam ($\beta=-0.549306$, exact solution 4.87119849)

N	HWM			FDM			DQM			
	Ω_1	AbsErr	RConv	Ω_1	AbsErr	RConv	Ω_1	AbsErr	RConv	
4	4.92596	0.0548					4.74555243	1.26E-01		
8	4.88462	0.0134	2.0280	4.842031	0.0292		4.87118515	1.33E-05	13.20	
16	4.87454	0.0033	2.0068	4.863858	0.0073	1.9904	4.87119849	7.46E-11	17.44	
32	4.87203	0.0008	2.0017	4.869360	0.0018	1.9974	4.87119849	1.08E-10	-0.54	
64	4.87140	0.0002	2.0004	4.870739	0.0005	2.0004	4.87119860	1.16E-07	-10.1	
128	4.87125	0.0001	2.0001	4.871084	0.0001	2.0049	4.87120710	8.62E-06	-6.21	
256	4.87121	0.0000	2.0000	4.871170	0.0000	2.0069	4.86997855	1.22E-03	-7.15	
Exact: 4.871198		FEM analysis results - 100000 elem.(10x10x1000)					4.8758			

Table 2.10 Fundamental frequency parameter Ω_2 values for a clamped-free beam ($\beta=-0.549306$, exact solution 24.42645172)

N	HWM			FDM			DQM			
	Ω_2	AbsErr	RConv	Ω_2	AbsErr	RConv	Ω_2	AbsErr	RConv	
4	26.04020	1.6138								
8	24.79828	0.3718	2.1177	23.143597	1.2829		24.4170467	9.41E-03	29.46	
16	24.51767	0.0912	2.0272	24.092313	0.3341	1.9408	24.4264517	1.27E-11	-0.71	
32	24.44915	0.0227	2.0067	24.342014	0.0844	1.9845	24.4264517	2.08E-11	-11.9	
64	24.43212	0.0057	2.0017	24.405285	0.0212	1.9961	24.4264516	8.21E-08	-5.35	
128	24.42786	0.0014	2.0004	24.421156	0.0053	1.9989	24.4264484	3.35E-06	-6.40	
256	24.42680	0.0004	2.0001	24.425128	0.0013	2.0002	24.4261691	2.83E-04	29.46	
Exact: 24.426452		FEM analysis results - 100000 elem.(10x10x1000)					24.4397			

Abbreviations in Tables 2.1-2.10 AbsErr and RConv stand for the absolute error and the rate of convergence computed by formulas (1.30) and (1.33), respectively. In all Tables 2.1-2.10, the material properties are varied according to the exponential law (2.10).

It can be observed from Tables 2.1-2.10 that:

- In all 10 sample problems (5 boundary conditions and first 2 frequencies for each), the rate of the convergence of the HWM and FDM methods tends to two, but in the HWM, the final value is reached more strictly.
- In most sample problems (7 of 10), the accuracy (AbsErr) of the HWM outperforms that of FDM. However, in the pinned-clamped beam, the accuracy of the FDM is higher for both the first and the second frequency and in the pinned-pinned beam for the first frequency. Note that in the latter cases, the accuracy of the HWM and FDM are nearing to each other with a growing mesh.
- The accuracy of the HWM and FDM remains in the same range.
- The accuracy of the DQM is substantially higher than that of the HWM and FDM if the number of collocation points is in the range 8-32. With a higher mesh, the accuracy of DQM declines, but for a wide class of practical problems, the required accuracy is already achieved with 32 collocation points. However, such a mesh is not capable of covering local behaviour of the solution. Also, DQM is not applicable or gives relatively poor results for the smallest mesh considered ($N=4$, see Table 2.9).
- The numerical rate of the convergence of DQM is extremely high in a small mesh (in range 5-30) and will be negative for a larger mesh.
- The results obtained by HWM, DQM and FDM are in excellent agreement with the exact solution given in table headings and FEM results given in the last row of the tables. Since FEM analysis results were obtained using 3D analysis, 100000 elements and weak formulation based method, the direct/detailed comparison with FEM seems not reasonable.

The reason why the exponent parameter β has “normal” value 2 in Tables 2.1-2.8, but “strange” value $\beta = -0.549306$ in Tables 2.9-2.10 is as follows. The values 2 used in Tables 2.1-2.8 were taken from the literature. In Tables 2.9-2.10, it is taken into account that the left and right side materials of the beam are steel and aluminium with material properties given in Table 2.11.

Table 2.11 Material properties of the aluminium and steel

Property	Unit	Steel	Aluminium
E	GPa	210	70
ρ	kg/m ³	7800	2600

Thus, the value of the modulus of the elasticity E varies from 210 GPa to 70 GPa and the value of the density ρ varies from 7800 kg/m³ to 2600 kg/m³. The value of the β is computed based on formulas (2.10) and values of material properties given in Table 2.11. Table 2.12 shows FEM results in more detail (different mesh) for three boundary conditions.

Table 2.12 Fundamental frequency parameter values obtained by FEM analysis ($\beta=2$)

Number of elements	Clamped-Clamped		Clamped- Pinned		Pinned-Pinned		Pinned-Clamped	
	Ω_1	Ω_2	Ω_1	Ω_2	Ω_1	Ω_2	Ω_1	Ω_2
3x3x300	24.92177	65.00745	11.24135	48.48355	8.45222	41.25789	20.88545	56.55424
4x4x400	24.87612	64.88564	11.22081	48.39319	8.43663	41.18073	20.84697	56.44809
5x5x500	24.84950	64.81488	11.20887	48.34088	8.42762	41.13628	20.82465	56.38673
10x10x1000	24.80744	64.70323	11.19007	48.25888	8.41360	41.06718	20.78967	56.29065
Exact sol.	24.78955	64.70943	11.18278	48.26067	8.41048	41.07056	20.77798	56.29444

The convergence of the FEM results to the exact solution given in the last row of Table 2.12 can be observed in the case all boundary conditions and frequencies considered.

In Table 2.13 it is suggested that the bending stiffness and distributed mass per unit length of the beam are varying according to power law functions (2.11). The material properties given in Table 2.11 are considered and the value of the exponent is taken equal to 1.5. The first four values of the frequency parameter Ω computed by HWM are given for clamped-clamped and clamped-free boundary conditions.

Table 2.13 Fundamental frequency parameter values obtained by HWM (power law fun., $k = 1.5$)

N	Clamped-Clamped				Clamped-Free (Console)			
	Ω_1	Ω_2	Ω_3	Ω_4	Ω_1	Ω_2	Ω_3	Ω_4
8	22.5738	62.6483	124.8020	211.3142	4.8951	24.8537	66.4053	131.2274
16	22.5598	62.0976	122.0458	202.7884	4.8861	24.5613	64.6866	125.2330
32	22.5529	61.9585	121.3843	200.7914	4.8855	24.4863	64.2716	123.8332
64	22.5489	61.9206	121.2166	200.2947	4.8866	24.4653	64.1658	123.4860
128	22.5463	61.9089	121.1723	200.1682	4.8877	24.4584	64.1373	123.3972
256	22.5445	61.9044	121.1595	200.1348	4.8887	24.4556	64.1286	123.3733
512	22.5433	61.9022	121.1551	200.1252	4.8893	24.4541	64.1254	123.3661
1024	22.5424	61.9008	121.1531	200.1219	4.8898	24.4531	64.1238	123.3635

In the latter case, the exact solution is unknown, but the obtained results are close to those obtained by applying the exponent law at the same boundary conditions. In general, the exponential and power law functions are different and thus, the results may also differ substantially. In the current case, the parameter k in the power law function (2.11) is selected such that the material distributions are similar. The variation of the elastic modulus corresponding to the exponential and power law functions is shown in (Paper I) in Fig.3.

Tables 2.14-2.16 compare the results obtained by using the HWM based on expansion (1.7) and higher order approach (HOHWM) based on expansion (1.37).

Table 2.14 Fundamental frequency parameter Ω_1 values, absolute errors and convergence rates for a pinned-pinned FGM beam ($\beta=3$)

N	HWM (Chen and Hsiao, 1997)			HOHWM (Majak et al., 2018)			Error ratio
	Fundamental frequency Ω_1	Absolute error	Converg. rate	Fundamental frequency Ω_1	Absolute error	Converg. rate	
4	5.49612520	1.35E+00		7.81629606	9.73E-01		1.4
8	6.56237797	2.81E-01	2.2627	6.87693058	3.39E-02	4.8442	8.3
16	6.76542022	7.76E-02	1.8542	6.84538131	2.33E-03	3.8607	33.3
32	6.82322484	1.98E-02	1.9693	6.84319842	1.49E-04	3.9644	133.0
64	6.83806767	4.98E-03	1.9927	6.84305841	9.40E-06	3.9908	529.9
128	6.84180211	1.25E-03	1.9982	6.84304960	5.88E-07	3.9977	2120.6
256	6.84273719	3.12E-04	1.9995	6.84304905	3.68E-08	3.9995	8473.5
512	6.84297105	7.80E-05	1.9999	6.84304901	2.29E-09	4.0074	34044.6
Exact	6.84304901			6.84304901			

Table 2.15 Fundamental frequency parameter Ω_2 values, absolute errors and convergence rates for a pinned-pinned FGM beam ($\beta=3$)

N	HWM (Chen and Hsiao, 1997)			HOHWM (Majak et al., 2018)			Error ratio
	Frequency Ω_2	Absolute error	Converg. rate	Frequency Ω_2	Absolute error	Converg. rate	
4	34.46004357	8.95E+00		43.08502120	3.26E-01		27.5
8	41.13904609	2.27E+00	1.9781	43.43718723	2.61E-02	3.6437	87.1
16	42.85246913	5.59E-01	2.0240	43.41285000	1.75E-03	3.8961	318.8
32	43.27200957	1.39E-01	2.0059	43.41121057	1.13E-04	3.9555	1231.4
64	43.37636085	3.47E-02	2.0015	43.41110475	7.13E-06	3.9859	4872.5
128	43.40241562	8.68E-03	2.0004	43.41109806	4.47E-07	3.9960	19431.3
256	43.40892726	2.17E-03	2.0001	43.41109764	2.80E-08	3.9941	77401.5
512	43.41055504	5.43E-04	2.0000	43.41109762	3.65E-09	2.9418	148680.8
Exact	43.41109762			43.41109762			

Table 2.16 Fundamental frequency parameter Ω_3 values, absolute errors and convergence rates for a pinned-pinned FGM beam ($\beta=3$)

N	HWM (Chen and Hsiao, 1997)			HOHWM (Majak et al., 2018)			Error ratio
	Frequency Ω_3	Absolute error	Converg. rate	Frequency Ω_3	Absolute error	Converg. rate	
4	67.93869901	2.63E+01		85.92836185	8.33E+00		3.2
8	88.96819949	5.29E+00	2.3149	93.89193730	3.66E-01	4.5095	14.5
16	92.97128669	1.29E+00	2.0398	94.23719747	2.04E-02	4.1616	62.9
32	93.93811063	3.20E-01	2.0093	94.25640628	1.23E-03	4.0594	260.7
64	94.17787846	7.98E-02	2.0023	94.25755622	7.57E-05	4.0179	1054.1
128	94.23770142	1.99E-02	2.0006	94.25762716	4.71E-06	4.0048	4229.1
256	94.25264975	4.98E-03	2.0001	94.25763158	2.95E-07	3.9991	16904.5
512	94.25638638	1.25E-03	2.0000	94.25763185	2.51E-08	3.5536	49621.3
Exact	94.25763187			94.25763187			

Obviously, it can be observed from Tables 2.14-2.16 that the HOHWM outperforms HWM with the fourth order convergence and absolute error lower than that of HWM (in the case of a larger mesh several magnitudes lower). However, the accuracy and rate of convergence are not the only measures important from an engineering/practical

point of view. The complexities of the solution as well as the implementation of the method are important. In the case of the problem and boundary conditions considered, the increase of the solution, also implementation complexity are minimal (see details in Majak et al., 2018).

2.2 Nanostructures

Nanoscience is an emerging research area due to the outstanding mechanical, chemical, electrical, optical and electronic properties of nanomaterials/structures. This chapter is focused on nanomechanics. Modelling of nanomechanics is under development, but a number of approaches and models are available in (Paper II).

2.2.1 Nonlocal elasticity model

Classical continuum models neglect the scale effect in nanomaterial studies and therefore applicability of classical or local continuum models is incorrect. On a small scale, the influences of long range interatomic and intermolecular cohesive forces on the static and dynamic properties become significant and thus could not be neglected (Narendar et al., 2012).

In the analysis of nanostructures, the small-scale effect is most commonly introduced by (Elishakov, 2012):

- nonlocal continuum mechanics or
- atomic theory of lattice dynamics.

For taking into account the scale effect, various size-dependent continuum mechanics models have been developed, such as nonlocal elasticity theory (Eringen, 1983), strain gradient theory (Nix et al., 1998), modified couple stress theory (Asghari et al., 2010), and couple stress theory (Hadjesfandiari et al., 2011). In the current study, the nonlocal Eringen theory is considered (Eringen, 1983).

$$(1 - \mu \nabla^2) \sigma_{ij}^{NL} = C_{ijkl} \varepsilon_{kl}, \quad (2.14)$$

$$\mu = e_0^2 a^2, \quad (2.15)$$

where σ_{ij}^{NL} , ε_{kl} and C_{ijkl} stand for the nonlocal stress tensor, strain tensor and fourth order elasticity tensor, respectively. In (2.14) ∇^2 and μ stand for the Laplacian operator and nonlocal parameter, respectively. The parameters e_0 and a in (2.15) describe material properties and internal characteristic length. In the nonlocal elasticity theory, the stress at a point is a function of the strains at all points in the domain whereas in the classical continuum models, the stress at a point is a function of the strains at those points in the domain (Murmu et al., 2010).

2.2.2 Free Vibration analysis of nanobeams

In the following, a brief problem formulation is introduced and numerical results for three boundary conditions are presented.

Problem formulation

The governing differential equations for the free vibration analysis of the nanobeams can be derived similar to classical continuum mechanics, but the classical Hook's law should be replaced with the nonlocal model (2.14). Combining the nonlocal constitutive equation (2.14) and the moment deflection relation of the Euler-Bernoulli beam, the governing differential equation for the nonlocal Euler-Bernoulli beam in terms of displacement can be derived as in (Paper II):

$$\frac{d^4 W}{dX^4} + \frac{\mu \lambda^2}{L^2} \frac{d^2 W}{dX^2} = \lambda^2 W, \quad (2.16)$$

$$\lambda^2 = m_0 \omega^2 L^4 / EI, \quad (2.17)$$

where W is the deflection, L is external length, μ is defined by formula (2.15), ω , m_0 and EI stand for natural frequency of vibration, the moment of inertia and bending stiffness of the beam, respectively. Detailed derivation is omitted herein for conciseness sake; details can be found in (Paper II; Aydogdu, 2009; Elishakov, 2012). Obviously, in particular cases when the nonlocal parameter $\mu = 0$, equation (2.16) reduces to the classical Euler-Bernoulli beam equation. Because the governing differential equation of the nonlocal Euler-Bernoulli beam (2.16) is a fourth order ODE, the traditional and higher order wavelet expansions (1.7) and (1.37) introduced above can be applied and the solution can be reached similar that done for FGM beam in section 2.1.

Numerical results

In the following, two symmetric (pinned-pinned and clamped-clamped) conditions and one asymmetric (clamped-pinned) boundary condition are considered (see Fig. 2.5). The non-dimensional governing differential equations (2.16) are solved. The value of the nonlocal parameter μ is varied from 0 to 5 and the length of the beam is taken equal to 10 nm.

a) Pinned-pinned nanobeam

Tables 2.17-2.19 compare the results obtained by the use of HWM, FDM and DQM. The values of the fundamental frequency parameter $F = \sqrt{\lambda}$, absolute error (*AbsErr*) and rate of convergence (*RConv*) are given.

Table 2.17 Fundamental frequency parameter F values, rates of convergence and absolute errors ($\mu = 0$)

N	HWM			FDM			DQM		
	F	$AbsErr$	$RConv$	F	$AbsErr$	$RConv$	F	$AbsErr$	$RConv$
4	3.161916	2.03E-02		3.061468	8.01E-02		3.26598632	0.12439	
8	3.146649	5.06E-03	2.0069	3.121445	2.01E-02	1.9916	3.14159694	4.29E-06	14.8
16	3.142855	1.26E-03	2.0021	3.136549	5.04E-03	1.9981	3.14159265	7.48E-13	22.4
32	3.141908	3.15E-04	2.0006	3.140331	1.26E-03	1.9992	3.14159265	7.03E-12	-3.2
64	3.141672	7.89E-05	2.0001	3.141277	3.16E-04	1.9989	3.14159266	1.14E-08	-10.7
128	3.141612	1.97E-05	2.0000	3.141514	7.87E-05	2.0048	3.14159271	5.16E-08	-2.2
256	3.141598	4.93E-06	2.0000	3.141573	1.97E-05	2.0007	3.14159109	1.57E-06	-4.9
512	3.141594	1.23E-06	2.0000	3.141588	4.65E-06	2.0784	3.14159932	6.67E-06	-2.1
Exact:		3.141593							

Table 2.18 Fundamental frequency parameter F values, rates of convergence and absolute errors ($\mu = 3$)

N	HWM			FDM			DQM		
	F	$AbsErr$	$RConv$	F	$AbsErr$	$RConv$	F	$AbsErr$	$RConv$
4	2.963169	1.88E-02		2.877579	6.68E-02		3.04698895	1.03E-01	
8	2.949087	4.72E-03	1.9930	2.927620	1.67E-02	1.9960	2.94436580	3.56E-06	14.8
16	2.945544	1.18E-03	1.9988	2.940174	4.19E-03	1.9991	2.94436224	8.44E-15	28.7
32	2.944658	2.96E-04	1.9997	2.943315	1.05E-03	1.9998	2.94436224	6.62E-14	-3.0
64	2.944436	7.39E-05	1.9999	2.944100	2.62E-04	1.9976	2.94436224	4.68E-12	-6.1
128	2.944381	1.85E-05	2.0000	2.944297	6.52E-05	2.0071	2.94436224	7.01E-10	-7.2
256	2.944367	4.62E-06	2.0000	2.944346	1.62E-05	2.0063	2.94436222	1.96E-08	-4.8
512	2.944363	1.15E-06	2.0000	2.944358	4.24E-06	1.9379	2.94436204	1.96E-07	-3.3
Exact:		2.944362							

Table 2.19 Fundamental frequency parameter F values, rates of convergence and absolute errors ($\mu = 5$)

N	HWM			FDM			DQM		
	F	$AbsErr$	$RConv$	F	$AbsErr$	$RConv$	F	$AbsErr$	$RConv$
4	2.859891	1.80E-02		2.781004	6.08E-02		2.93498048	9.31E-02	
8	2.846396	4.55E-03	1.9868	2.826607	1.52E-02	1.9975	2.84184573	3.24E-06	14.8
16	2.842983	1.14E-03	1.9973	2.838032	3.81E-03	1.9994	2.84184249	2.62E-14	26.9
32	2.842128	2.85E-04	1.9993	2.840890	9.52E-04	2.0002	2.84184249	2.36E-13	-3.2
64	2.841914	7.13E-05	1.9998	2.841604	2.38E-04	1.9978	2.84184249	2.67E-12	-3.5
128	2.841860	1.78E-05	2.0000	2.841783	5.95E-05	2.0031	2.84184249	6.68E-10	-8.0
256	2.841847	4.46E-06	2.0000	2.841828	1.45E-05	2.0373	2.84184248	1.86E-08	-4.8
512	2.841844	1.11E-06	2.0000	2.841839	3.49E-06	2.0526	2.84184231	1.89E-07	-3.3
Exact:		2.841842							

In Table 2.17-2.19, the nonlocal parameter μ is varied from 0 to 5 and the results are compared against exact solution given in (Wang et al., 2007).

It can be observed from Tables 2.17-2.19 that the absolute error of the Haar wavelet method is less than that of the finite difference method, but remains in the same range. The numerical rate of convergence tends to two in both methods,

independent of the value of nonlocal parameter μ . With a growing mesh (see case $N=512$), the rate of convergence of the FDM has significant deviations from 2, which refers to the loss of accuracy. The convergence of the DQM is extremely fast in the case of a small mesh ($N=16, N=32$) and decline to negative values thereafter. Also, Tables 2.17-2.19 show that in the case of the smallest mesh considered $N=4$, the frequency computed by DQM has largest deviation from the final values to that solution converge (i.e., the DQM has the largest absolute error for $N=4$). The convergence to the same final value is obvious with all the methods utilized. Note that the small scale effect is significant. Increase of the nonlocal parameter from 0 to 5 causes a decrease of the fundamental frequency from 3.141593 to 2.841842.

b) Clamped-clamped nanobeam

The results obtained by use of HWM, FDM and DQM are presented in Table 2.17. The value of the nonlocal parameter μ is taken equal to five in order to cover the small scale effect (nonlocal behaviour).

Table 2.20 Fundamental frequency parameter F values and rates of convergence ($\mu = 5$)

N	HWM		FDM		DQM	
	F	$RConv$	F	$RConv$	F	$RConv$
4	4.252952		3.832771		4.125996322243	
8	4.207325		4.095779		4.191209634539	
16	4.195622	2.0817	4.167331	1.8781	4.191682530895	7.11
32	4.192669	2.0018	4.185572	1.9718	4.191682530902	26.14
64	4.191929	1.9993	4.190153	1.9932	4.191682530908	-0.10
128	4.191744	1.9998	4.191300	1.9983	4.191682531462	-6.34
256	4.191698	1.9999	4.191587	1.9996	4.191682527306	-2.91
512	4.191686	2.0000	4.191659	2.0006	4.191682535006	-0.89

The structure of Table 2.20 differs from that of Tables 2.17-2.19. The columns for the absolute error are omitted, since closed form exact solution not given. Also, the rate of convergence is computed by utilizing formula (1.34), i.e. without the use of exact solution. Again, the rate of convergence of the HWM and FDM tends to two, but in HWM it is more strict. The DQM has excellent convergence at 16 and 32 collocation points. High accuracy is achieved fast (10 digits after comma coincide), thereafter the rate of convergence turns to negative and the accuracy is lost due to computing errors (double precision computing used).

c) Clamped-pinned nanobeam

Table 2.21 compares the results obtained by use of HWM, FDM and DQM. The structure of Table 2.21 coincides with that of Table 2.20 and the same value of the nonlocal parameter μ is used ($\mu = 5$).

Table 2.21 Fundamental frequency parameter F values and rates of convergence ($\mu = 5$)

N	HWM		FDM		DQM	
	F	$RConv$	F	$RConv$	F	$RConv$
4	3.535756		3.320272		3.481931648438	
8	3.510894		3.455128		3.502377143331	
16	3.504564	1.9737	3.490504	1.9306	3.502443568840	8.27
32	3.502974	1.9932	3.499452	1.9831	3.502443568841	27.11
64	3.502576	1.9983	3.501695	1.9958	3.502443568833	-4.07
128	3.502477	1.9996	3.502256	1.9990	3.502443569003	-4.46
256	3.502452	1.9999	3.502397	2.0000	3.502443575002	-5.14
512	3.502446	2.0000	3.502431	2.0489	3.502443511944	-3.39

The behaviour of the solutions obtained by applying HWM, FDM and DQM is similar to that described for clamped – clamped nanobeam. The asymmetric boundary conditions do not affect this behaviour. High number of decimal places for DQM is used to show that up to 10 digits after comma coincide at $N=16$, $N=32$ and $N=64$.

Tables 2.22-2.23 compare the results obtained by the widely used HWM and HOHWM.

Table 2.22 Fundamental frequency parameter Ω_1 values, absolute errors and convergence rates for pinned-pinned nanobeam ($\mu = 3$)

N	HWM (Chen and Hsiao, 1997)			HOHWM (Majak et al., 2018)			Error ratio
	Frequency Ω_1	Absolute error	Converg. rate	Frequency Ω_1	Absolute error	Converg. rate	
4	2.9631691775	1.88E-02		2.9454323919	1.07E-03		17.6
8	2.9490867632	4.72E-03	1.9930	2.9444268262	6.46E-05	4.0504	73.1
16	2.9455443778	1.18E-03	1.9988	2.9443662390	4.00E-06	4.0129	295.5
32	2.9446578302	2.96E-04	1.9997	2.9443624877	2.49E-07	4.0032	1184.8
64	2.9444361397	7.39E-05	1.9999	2.9443622538	1.56E-08	4.0008	4742.0
128	2.9443807138	1.85E-05	2.0000	2.9443622392	9.74E-10	4.0004	18973.2
256	2.9443668571	4.62E-06	2.0000	2.9443622383	6.28E-11	3.9559	73607.9
512	2.9443633929	1.15E-06	2.0000	2.9443622382	2.84E-12	4.4650	406411.2
Exact	2.9443622382			2.9443622382			

Table 2.23 Fundamental frequency parameter Ω_1 values, absolute errors and convergence rates for pinned-pinned nanobeam ($\mu = 5$)

N	HWM (Chen and Hsiao, 1997)			HOHWM (Majak et al., 2018)			Error ratio
	Frequency Ω_1	Absolute error	Converg. rate	Frequency Ω_1	Absolute error	Converg. rate	
4	2.8598908866	1.80E-02		2.8428724147	1.03E-03	0	17.5
8	2.8463961818	4.55E-03	1.9868	2.8419047893	6.23E-05	4.0473	73.1
16	2.8429830790	1.14E-03	1.9973	2.8418463546	3.86E-06	4.0121	295.4
32	2.8421277689	2.85E-04	1.9993	2.8418427345	2.41E-07	4.0031	1184.7
64	2.8419138205	7.13E-05	1.9998	2.8418425088	1.50E-08	4.0008	4742.0
128	2.8418603259	1.78E-05	2.0000	2.8418424947	9.40E-10	4.0004	18973.1
256	2.8418469518	4.46E-06	2.0000	2.8418424938	6.06E-11	3.9559	73608.3
512	2.8418436082	1.11E-06	2.0000	2.8418424937	2.74E-12	4.4641	406162.2
Exact	2.8418424937			2.8418424937			

Similar to the FGM beam considered above, the HOHWM outperforms HWM in accuracy. The complexities of the solution and implementation have a minimal increase in the case of the considered problem and boundary conditions. However, the complexities of the solution and implementation depend on the problem considered, the boundary conditions applied, effectiveness of the implementation, etc.

3 Conclusions

According to the main goal set for the thesis research, the Chen and Hsiao wavelet expansion based on the Haar Wavelet method was applied in the analysis of functionally graded structures and nanostructures, to study the accuracy of the numerical results, simplicity of the implementation and complexity of the solution of the HWM. The numerical results from the analysis were validated against the results obtained by the finite difference and differential quadrature methods (FDM and DQM). The reference method FDM and DQM were selected as widely used strong formulation based numerical methods in engineering. These methods are known for simple implementation as well as the HWM considered. In the case of FGM structures, the general validation was performed additionally by FEM (more complex weak formulation based method). Based on the numerical analysis performed for FGM and nanostructures, the following conclusions can be made for the activities set at the early stage of the current research:

1. The results obtained by HWM are in good agreement with those obtained by FDM, DQM and FEM for all numerical samples performed for FGM and nanostructures.
2. Implementation of HWM appeared simple in all the problems considered.
3. The accuracy of the HWM is in the same range of those of FDM. The rate of convergence tends to two in both methods, but this process is stricter in HWM. For most samples considered, the accuracy of the HWM was higher, however, not for all cases.
4. The accuracy of the HWM appeared lower than that of DQM, except at high resolution where DQM has complications.
5. The improved wavelet method HOHWM tested in the current study provides an increase of the rate of convergence from two to four and a decrease of the absolute error for several orders of magnitude depending on the mesh level used.
6. HOHWM with improved accuracy is more competitive and has preliminaries for use in future for the analysis of new materials and constitutive models.

The above conclusions cover the work hypotheses posed in the introduction of the study.

The scientific novelty

The comparison of HWM with mainstream methods in engineering (FDM, DQM) in the current study leads to a principally new understanding – the accuracy of widely used HWM is substantially lower than that of DQM and in the same range with FDM.

Results of the validation of widely used HWM against FDM and DQM obtained in the current study form a reason and a base for the development of an improved HOHWM.

Testing of new HOHWM led to accuracy higher than that initially expected. Also, some tests performed provide input for design/configure HOHWM.

Future work

HOHWM presented in the current study showed good results on the basis of the analysed case studies and evaluation criteria against HWM. To acquire a clearer picture of the strengths and weaknesses of HOHWM, further studies are required. Therefore, the focus in the future work will be on the application and evaluation of HOHWM for a wider class of engineering design problems.

References

- Arbabi, S., Nazari, A., Darvishi, M.T. (2017) A two-dimensional Haar wavelets method for solving systems of PDEs. *Applied Mathematics and Computation*, 292, 33–46.
- Asghari, M., Kahrobaiyan, M. H., Ahmadian, M.T. (2010). A nonlinear Timoshenko beam formulation based on the modified couple stress theory. *International Journal of Engineering Science*, 48, 1749–1761.
- Aziz, I., Islam S. U. (2013). New algorithms for the numerical solution of nonlinear Fredholm and Volterra integral equations using Haar wavelets. *Journal of Computational and Applied Mathematics*, 239(1), 333–345.
- Aziz, I., Islam S. U., Khana F. (2014). A new method based on Haar wavelet for the numerical solution of two-dimensional nonlinear integral equations. *Journal of Computational and Applied Mathematics*, 272, 70–80.
- Aydogdu, M. (2009). A general nonlocal beam theory: Its application to nanobeam bending, buckling and vibration. *Physica E: Low-dimensional Systems and Nanostructures*, 41, 1651–1655.
- Babaaghaie, A., Maleknejad, K. (2017). Numerical solution of integro-differential equations of high order by wavelet basis, its algorithm and convergence analysis. *Journal of Computational and Applied Mathematics*, 325, 125–133.
- Bellman, R., Kashef, B. G., Casti, J. (1972). Differential quadrature: a technique for the rapid solution of non-linear partial differential equations. *Journal of Computational Physics*, 10, 40–52.
- Bhandari, M., Purohit, K. (2015). Response of Functionally Graded Material Plate under Thermomechanical Load Subjected to Various Boundary Conditions. *International Journal of Metals*, Article ID 416824.
- Castro, L. M. S., Ferreira A. J. M., Bertoluzza S., Batra R. C., Reddy J. N. (2010). A wavelet collocation method for the static analysis of sandwich plates using a layerwise theory. *Composite Structures*, 92(8), 1786–1792.
- Cattani, C. (2005). Harmonic wavelets toward the solution of nonlinear PDE. *Computers & Mathematics with Applications*, 50, 1191–1210.
- Chen, C. F., Hsiao, C. H. (1997). Haar wavelet method for solving lumped and distributed-parameter systems. *IEE Proceedings - Control Theory and Applications*, 144(1), 87–94.

- Chi, S., Chung, Y. (2006). Mechanical behavior of functionally graded material plates under transverse load—Part I: Analysis. *International Journal of Solids and Structures*, 43, 3657–3674.
- Chung, Y. L., Chi, S. H. (2001). The residual stress of functionally graded materials. *Journal of the Chinese Institute of Civil and Hydraulic Engineering*, 13, 1–9.
- Chun, Z., Zheng, Z. (2007). Three-Dimensional Analysis of Functionally Graded Plate Based on the Haar Wavelet Method. *Acta Mechanica Solida Sinica*, 20(2), 95–102.
- Ebrahimi, M. J., Najafizadeh, M. M. (2014). Free vibration analysis of two-dimensional functionally graded cylindrical shells. *Applied Mathematical Modelling*, 38, 308–324.
- Ekrem, M., Ataberk, N., Avci, A., Akdemir, A. (2016). Improving electrical and mechanical properties of a conductive nano adhesive. *Journal of Adhesion Science and Technology*, 31 (7), 699–712.
- Elishakoff, I., Dujat, K., Muscolino, G., Bucas, S., Natsuki, T., Wang, C. M., et al. (2012). *Carbon Nanotubes and Nanosensors: Vibration, Buckling and Ballistic Impact*. ISTE/Wiley, Portland.
- Eringen, A. C. (1983). On differential equations of nonlocal elasticity and solutions of screw dislocation and surface waves. *Journal of Applied Physics*, 54, 4703–4710.
- Feklistova, L., Hein, H. (2015). Stability Determination in Vibrating Non-homogeneous Functionally Graded Timoshenko Beams. *International Conference on Mechanics and Control Engineering (MCE)*, Nanjing, Destech Publicat Inc, 618–623.
- Gupta, A., Talha, M. (2015). Recent development in modeling and analysis of functionally graded materials and structures. *Progress in Aerospace Sciences*, 79, 1–14.
- Hadjefandiari, A. R., Dargush, G. F. (2011). Couple stress theory for solids. *International Journal of Solids and Structures*, 48, 2496–2510.
- Hariharan, G., Kannan K. (2014). Review of wavelet methods for the solution of reaction-diffusion problems in science and Engineering. *Applied Mathematical Modelling*, 38(3), 799–813.
- Hein, H., Feklistova L. (2011). Computationally efficient delamination detection in composite beams using Haar wavelets. *Mechanical Systems and Signal Processing*, 25(6), 2257–2270.

- Hsiao, C. H. (1997). State analysis of the linear time delayed systems via Haar wavelets. *Mathematics and Computers in Simulations*, 44(5), 457–470.
- Islam, S. U., Aziz I., Al-Fhaid, A. S., Shah, A. (2013). A numerical assessment of parabolic partial differential equations using Haar and Legendre wavelets. *Applied Mathematical Modelling*, 37, 9455–9481.
- Islam S. U., Aziz I., Fayyaz, M. (2013). A new approach for numerical solution of integro-differential equations via Haar wavelets. *International Journal of Computer Mathematics*, 90 (9), 1971–1989.
- Islam, S. U., Aziz, I., Al-Fhaid, A. S. (2014). An improved method based on Haar wavelets for numerical solution of nonlinear integral and integro-differential equations of first and higher orders. *Journal of Computational and Applied Mathematics*, 260, 449–469.
- Jin, G., Xie X., Liu Z. (2013). Free vibration analysis of cylindrical shells using the Haar wavelet method. *International Journal of Mechanical Sciences*, 77, 47–56.
- Jin, G., Xie X., Liu Z. (2014). The Haar wavelet method for free vibration analysis of functionally graded cylindrical shells based on the shear deformation theory. *Composite Structures*, 108, 435–448.
- Jiwari, R. (2012). A Haar wavelet quasilinearization approach for numerical simulation of Burgers' equation. *Computer Physics Communications*, 183 (11), 2413–2423.
- Ke, L., Wang, Y., Yang, J., Kitipornchai, S. (2012). Nonlinear free vibration of size-dependent functionally graded microbeams. *International Journal of Engineering Science*, 50(1), 256–267.
- Kumar, K. H., Vijesh, V. A. (2018). Wavelet based iterative methods for a class of 2D-partial integro-differential equations. *Computers and Mathematics with Applications*, 75, 187–198.
- Lepik, Ü. (2005). Numerical solution of differential equations using Haar wavelets. *Mathematics and Computers in Simulations*, 68, 127–143.
- Lepik, Ü. (2006). Haar wavelet method for nonlinear integro-differential equations. *Applied Mathematics and Computation*, 176, 324–333.
- Lepik, Ü. (2007a). Numerical solution of evolution equations by the Haar wavelet method. *Applied Mathematics and Computation*, 185, 695–704.

- Lepik, Ü. (2007b). Application of the Haar wavelet transform to solving integral and differential Equations. *Proceedings of the Estonian Academy of Sciences, Physics and Mathematics*, 56(1), 28–46.
- Lepik, Ü. (2008). Solving integral and differential equations by the aid of non-uniform Haar wavelets. *Applied Mathematics and Computation*, 198, 326–332.
- Lepik, Ü. (2009). Solving fractional integral equations by the Haar wavelet method. *Applied Mathematics and Computation*, 214(2), 468–478.
- Lepik, Ü. (2011). Solving PDEs with the aid of two dimensional Haar wavelets. *Computers & Mathematics with Applications*, 61, 1873– 1879.
- Lepik, Ü., Hein, H. (2014). *Haar Wavelets: With Applications*. New York, Springer.
- LeVeque, R. J. (2005). *Finite Difference Methods for Differential Equations*. University of Washington.
- Li, X. F., Kang, Y. A., Wu, J. X. (2013). Exact frequency equations of free vibration of exponentially functionally graded beams. *Applied Acoustics*, 74, 413–420.
- Li, Y., Zhao, W. (2010). Haar wavelet operational matrix of fractional order integration and its applications in solving the fractional order differential equations. *Applied Mathematics and Computation*, 216(8), 2276–2285.
- Li, Y., Sun, N., Zheng, B., Wang, Q., Zhang, Y. (2014). Wavelet operational matrix method for solving the Riccati differential equation. *Communications in Nonlinear Science and Numerical Simulation*, 19(3), 483–493.
- Lu, Z. R., Lin, X. X., Chen, Y. M., Huang, M. (2017). Hybrid sensitivity matrix for damage identification in axially functionally graded beams. *Applied Mathematical Modelling*, 41, 604–617.
- Mahamood, R. M., Akinlabi, E. T. (2017). *Functionally Graded Materials*. Springer International Publishing AG.
- Majak, J., Pohlak M., Eerme M. (2009a). Application of the Haar wavelet-based discretization technique to problems of orthotropic plates and shells. *Mechanics of Composite Materials*, 45(6), 631–642.
- Majak, J., Pohlak M., Eerme M., Lepikult T. (2009b). Weak formulation based Haar wavelet method for solving differential equations. *Applied Mathematics and Computation*, 211(2), 488–494.

- Majak, J., Kirs, M., Mikola, M., Heero, M., Herranen, H. (2013). Nanoscale vibration analysis of graphene sheets using nonlocal elasticity theory. *ICCE 21 Proceedings*. (Ed. D. Hui). University of New Orleans, USA.
- Majak, J., Shvartsman, B., Pohlak, M., Karjust, K., Eerme, M., Tungel, E. (2016). Solution of fractional order differential equation by the Haar wavelet method. Numerical convergence analysis for most commonly used approach. *AIP Conference Proceedings*, 1738.
- Majak, J., Pohlak, M., Karjust, K., Eerme, M., Kurnitski, J., Shvartsman, B.S. (2018). New higher order Haar wavelet method: Application to FGM structures. *Composite Structures*, 201, 72-78.
- Miyamoto, Y., Kaysser, W. A., Rabin, B. H., Kawasaki, A., Ford, R. G. (1999). *Functionally Graded Materials: Design, Processing and Applications*. US, Springer.
- Moaveni, S. (2007). *Finite Element Analysis: Theory and Applications with ANSYS. Third Edition*. Prentice Hall.
- Mohsen, M. F. N. (1982). Some details of the Galerkin finite element method. *Applied Mathematical Modelling*, 6, 165–170.
- Moita, J. S., Araujo, A. L., Mota Soares, C. M., Mota Soares, C. A., Herskovits, J. (2016). Material and Geometric Nonlinear Analysis of Functionally Graded Plate-Shell Type Structures. *Applied Composite Materials*, 23, 537–554.
- Mori, T., Tanaka, K. (1973). Average stress in matrix and average elastic energy of materials with misfitting inclusions. *Acta Metallurgica*, 21(5), 571–574.
- Murmu, T., Adhikari, S. (2010). Nonlocal effects in the longitudinal vibration of double-nanorod systems. *Physica E: Low-dimensional Systems and Nanostructures*, 43(1), 415–422.
- Narendar, S., Gopalakrishnan, S. (2012). Nonlocal continuum mechanics formulation for axial, flexural, shear and contraction coupled wave propagation in single walled carbon nanotubes. *Latin American Journal of Solids and Structures*, 9(4), 497–514.
- Nix, W. D., Gao, H. (1998). Indentation size effects in crystalline materials: A law for strain gradient plasticity. *Journal of the Mechanics and Physics of Solids*, 46(3), 411–425.
- Podlubny, I., (1999). *Fractional Differential Equations*. San Diego, California, Academic Press.

- Ray, S. S. (2012). On Haar wavelet operational matrix of general order and its application for the numerical solution of fractional Bagley Torvik equation. *Applied Mathematics and Computation*, 218, 5239–5248.
- Ray, S. S., Patra A. (2014). Numerical simulation for fractional order stationary neutron transport equation using Haar wavelet collocation method. *Nuclear Engineering and Design*, 278, 71–85.
- Saeed, U., Rehman M. (2013). Haar wavelet–quasilinearization technique for fractional nonlinear differential equations. *Applied Mathematics and Computation*, 220(1), 630–648.
- Saeed, U., Rehman, M. (2014). Assessment of Haar wavelet-quasilinearization technique in heat convection-radiation equations. *Applied Computational Intelligence and Soft Computing*, 2014, 1–5.
- Saeed, U., Rehman, M. (2015). Haar wavelet Picard method for fractional nonlinear partial differential equations. *Applied Mathematics and Computation*, 264(1), 310–322.
- Sayyad, A. S., Ghugal, Y. M. (2018). Modeling and analysis of functionally graded sandwich beams: A review. *Mechanics of Advanced Materials and Structures*, <https://doi.org/10.1080/15376494.2018.1447178>.
- Shu, C., Richards, B. E. (1990). High resolution of natural convection in a square cavity by generalized differential quadrature. *Proceedings of 3rd International Conference on Advanced in numerical Methods in Engineering: Theory and Applications*, Swansea, U.K 2: 978–985.
- Shu, C., Richards, B. E. (1992). Parallel simulation of incompressible viscous flows by generalized differential quadrature. *Computing Systems in Engineering*, 3 (1–4), 271–281.
- Shu, C. (1991). *Generalized Differential-Integral Quadrature and Application to the Simulation of Incompressible Viscous Flows Including Parallel Computation*. PhD thesis, University of Glasgow.
- Shu, C. (2000). *Differential Quadrature and its Application in Engineering*. Berlin, Springer.
- Singh, I., Kumar, S. (2016). Haar wavelet method for some nonlinear Volterra integral equations of the first kind. *Journal of Computational and Applied Mathematics*, 292, 541–552.

- Xie, X., Jin, G., Li, W., Liu, Z. (2013). Free vibration analysis of cylindrical shells using the Haar wavelet method. *International Journal of Mechanics Sciences*, 77, 47–56.
- Xie, X., Jin, G., Li, W., Liu, Z. (2014a). A numerical solution for vibration analysis of composite laminated conical, cylindrical shell and annular plate structures. *Composite Structures*, 111, 20–30.
- Xie, X., Jin, G., Yan, Y., Shi, S. X., Liu, Z. (2014b). Free vibration analysis of composite laminated cylindrical shells using the Haar wavelet method. *Composite Structures*, 109, 169–177.
- Xie, X., Jin, G., Ye, T., Liu, Z. (2014c). Free vibration analysis of functionally graded conical shells and annular plates using the Haar wavelet method. *Applied Acoustics*, 85, 130–142.
- Yi, M., Huang, J. (2014). Wavelet operational matrix method for solving fractional differential equations with variable coefficients. *Applied Mathematics and Computation*, 230(1) 383–394.
- Zienkiewicz, O. C. (1977). *The Finite Element Method. (3rd editon)*. London, McGraw-Hill.
- Wang, C. M., Zhang, Y.Y., He, X.Q. (2007). Vibration of nonlocal Timoshenko beams. *Nanotechnology*, 18, 1–9.
- Wang, L., Ma, Y., Meng, Z. (2014). Haar wavelet method for solving fractional partial differential equations numerically. *Applied Mathematics and Computation*, 227, 66–76.

Acknowledgements

The research was supported by the Estonian Research Council (grant PUT1300); Estonian Centre of Excellence in Zero Energy and Resource Efficient Smart Buildings and Districts, ZEBE, TK146 funded by the European Regional Development Fund (grant 2014-2020.4.01.15-0016); Innovative Manufacturing Engineering Systems Competence Centre IMECC (supported by Enterprise Estonia and co-financed by the European Union Regional Development Fund, project EU48685).

I would like to thank my supervisors leading researcher Jüri Majak and Associate Professor Kristo Karjust for their guidance, advice and encouragement. This dissertation would not be like it is without their systematic supervising and guidance.

Abstract

Evaluation of Haar wavelet method for analysis of functionally graded and nanostructures

Advanced materials, like functionally graded materials and nanomaterials, are increasingly used in various structures and products, but the numerical techniques available for the analysis of FG structures and nanostructures are limited in comparison with traditional solid mechanics. Based on the literature, the most popular methods for the analysis of FG structures and nanostructures are FDM, DQM and FEM that may be classified as the most widely used methods in engineering design. From recent methods, the Haar wavelet method has been reported as a simple and an effective method; however, most commonly, HWM has been evaluated based on its simplicity of implementation and reasonable absolute error against other simple and strong formulation based methods. Thus, comparisons of the method with mainstream methods in engineering design appear insufficient.

The main objective of the current study was to evaluate HWM for the analysis of FG and nanostructures based on the comparison with FDM, DQM and FEM. This thesis research is based on the published articles.

Chapter 1 introduces the widely used Chen and Hsiao approach based Haar wavelet method and reference methods FDM, DQM and FEM. Next, the evaluation criteria are described. The absolute error and the rate of convergence, also simplicity of the implementation of the method, are considered as evaluation criteria. At the end of Chapter 1, the basics of the higher order Haar wavelet method (HOHWM) are given.

Chapter 2 presents two case studies for evaluating the Haar wavelet method for the analysis of FG and nanostructures. The problem of case study 1 was the free vibration analysis of the FGM beam; the following steps were taken:

- FG materials and FG structures were reviewed with their advantages pointed out.
- Four widely used gradient functions were described.
- Free vibration analysis of an axially graded FG Euler-Bernoulli beam was made by applying HWM, FDM and DQM. Five different boundary conditions and two gradient functions (exponential law and power law) were examined.
- User code was developed for modelling an axially graded 3D FG beam in ANSYS APDL and the FEM analysis was performed.
- HOHWM was compared with the widely used Chen and Hsiao approach based HWM.
- The results were compared according to the evaluation criteria and the conclusions were made.

The problem of case study 2 was the free vibration analysis of the nanobeam and the following steps were performed:

- The nonlocal elasticity theory considering the small scale effect was introduced.
- Free vibration analysis of the nonlocal Bernoulli – Euler nanobeam was performed at three different boundary conditions.
- The HOHWM was compared with the widely used Chen and Hsiao approach based HWM.
- The results were compared according to the evaluation criteria and the conclusions were made.

The main goal of the study was achieved. The comparison of HWM with mainstream methods in engineering design leads to a principally new understanding about the accuracy of HWM in relation to FDM and DQM. The obtained results form a basis for the development of an improved Haar wavelet method.

Lühikokkuvõte

Haar'i lainikute meetodi hindamine funktsionaalgradient- ja nanostruktuuride analüüsiks

Uued materjalid, nagu funktsionaalse gradiendiga materjalid ja nanomaterjalid, leiavad üha enam kasutamist erinevates konstruktsioonides ja toodetes, kuid numbrilised meetodid, mis võimaldaks funktsionaalgradient- ja nanostruktuure analüüsida, on piiratud võrreldes sarnaste meetoditega traditsioonilise tahke keha mehaanika jaoks. Lähtuvalt kirjandusest on kõige populaarsemad meetodid funktsionaalgradientstruktuuride ja nanostruktuuride analüüsimiseks lõplike vahede meetod (LVM), diferentsiaalkvadratuuride meetod (DKM) ja (lõplike elementide meetod (LEM), mida võib klassifitseerida kõige levinumateks meetoditeks insenerirakendustes. Uuematest meetoditest on esile tõstetud Haari lainikute meetodit (HLM), kui lihtsat ja efektiivset meetodit lähtudes meetodi rakendatavuse lihtsusest ja mõõdukast absoluutsest veast, võrreldes teiste lihtsate tugeval formulatsioonil põhinevate meetoditega. HLM võrdlust insenerirakendustes laialdaselt kasutatavate numbriliste meetoditega (LVM, DKM) leiab kirjandusest vähe.

Käesoleva uurimustöö peamine eesmärk on hinnata Haari lainikute meetodit funktsionaalgradient- ja nanostruktuuride analüüsimiseks lähtudes võrdlusest insenerirakendustes laialdaselt kasutatavate tugeval formulatsioonil põhinevate meetoditega (LVM,DKM). Käesolev töö põhineb avaldatud artiklil.

Esimeses peatükis tutvustatakse Chen ja Hsiao aproksimatsioonil baseeruvat Haari lainikute meetodit ning referentsmeetodeid FDM, DQM ja LEM (see viimane on keerukam nõrgal formulatsioonil põhinev meetod ning seda kasutatakse üldiseks evalveerimiseks). Seejärel on antud ülevaade hindamiskriteeriumidest, milleks kasutatakse absoluutset viga ja koonduvuskiirust aga ka meetodi rakendamise keerukust. Esimese peatüki lõpus tutvustatakse kõrgemat järku Haari lainikute meetodi (KJHLM) üldist tööpõhimõtet.

Teises peatükis on toodud kaks rakendusnäidet Haari lainikute meetodi hindamiseks funktsionaalgradient- ja nanostruktuuride analüüsiks. Esimese rakendusnäite probleemiks oli funktsionaalse gradiendiga materjalist tala vabavõnkumise analüüs, mille realiseerimiseks teostati järgmised sammud:

- Anti lühike ülevaade funktsionaalse gradiendiga materjalidest ja struktuuridest ning nende eelistest;
- Kirjeldati nelja peamist gradiendi funktsiooni;
- Kasutades HLM, LVM ja DKM meetodeid teostati vabavõnkumise analüüs pikitelje sihis gradueeritud funktsionaalse gradiendiga materialist Euler-Bernoulli talale viiel erinevatel rajatingimustel ning kahe erineva gradiendifunktsiooni korral;

- Koostati programmikood modelleerimaks ANSYS APDL tarkvaras ruumiline pikitelje sihiliselt gradueeritud funktsionaalse gradiendiga materjalist tala ning teostati arvutused lõplike elementide meetodil;
- Võrreldi KJHLM-i ja Chen ja Hsiao aproksimatsioonil põhinevat meetodit;
- Rakendusnäite tulemusi võrreldi vastavalt hindamiskriteeriumitele ja toodi välja järeldused.

Teise rakendusnäite probleemiks oli nanotala vabavõnkumise analüüs, mille realiseerimiseks teostati järgmised sammud:

- Tutvustati mastaabiefekti arvessevõtvat mittelokaalset elastsusteooriat;
- Teostati mittelokaalse Bernoulli – Euler tala vabavõnkumise analüüs kolme rajatingimuse jaoks;
- Võrreldi KJHLM-dit ja Chen ja Hsiao aproksimatsioonil baseeruvat Haari lainikute meetodit;
- Rakendusnäite tulemusi võrreldi vastavalt hindamiskriteeriumitele ja toodi välja järeldused.

Käesoleva töö peamine eesmärk on saavutatud. Haari lainikute meetodi evalveerimine andis uue arusaamise HLM-i täpsuse osas võrreldes peamiste insenerirakendustes kasutatavate meetoditega (LVM ja DKM). Saadud tulemused loovad baasi Haari lainikute meetodi edasiarendamiseks.

Appendix

PUBLICATION I

Kirs, M., Karjust, K., Aziz, I., Õunapuu, E., Tungel, E. (2018). Free vibration analysis of a functionally graded material beam: evaluation of the Haar wavelet method. *Proceedings of the Estonian Academy of Sciences*, 67 (1), 1–9.



Free vibration analysis of a functionally graded material beam: evaluation of the Haar wavelet method

Maarjus Kirs^{a*}, Kristo Karjust^a, Imran Aziz^b, Erko Õunapuu^a, and Ernst Tungel^a

^a Department of Mechanical and Industrial Engineering, School of Engineering, Tallinn University of Technology, Ehitajate tee 5, 19086 Tallinn, Estonia

^b Department of Mathematics, University of Peshawar, Peshawar, Pakistan

Received 1 December 2016, revised 14 March 2017, accepted 10 May 2017, available online 17 August 2017

© 2018 Authors. This is an Open Access article distributed under the terms and conditions of the Creative Commons Attribution-NonCommercial 4.0 International License (<http://creativecommons.org/licenses/by-nc/4.0/>).

Abstract. The current study focuses on the evaluation of the Haar wavelet method, i.e. its comparison with widely used strong formulation based methods (FDM-finite difference method and DQM-differential quadrature method). A solid element 3D finite element model is developed and the numerical results obtained by using simplified approaches are confirmed.

Key words: Haar wavelet method, convergence, accuracy evaluation.

1. INTRODUCTION

Accuracy and complexity are two key factors characterizing any numerical method. The Haar wavelet method (HWM) considered in the current study was introduced by Chen and Hsiao in [1,2] almost 20 years ago and up to now it has been applied for solving a wide class of differential and integral equations covering engineering, economic, etc. problems [3–7]. An overview of the applications of the HWM is given in [8]. The wavelet techniques based on the use of an operational matrix of integration are developed for solving ordinal and partial differential equations in [1–10] and for integral equations in [11–13]. All these studies implement the strong formulation based approach of the HWM. The weak formulation based approach of the HWM was introduced in [14].

Most of the authors characterize the HWM as a simple and effective method [3–9]. These estimates cover mainly implementation of the HWM, less its

accuracy and convergence results, which are still under development. It is shown in [15] that in the case of function approximation with direct expansion into the Haar wavelet the convergence is of order one. However, according to the HWM approach considered, the highest order derivative included in the differential equation is expanded into a series of Haar functions. Thus, the estimate given in [15] holds good for estimating the accuracy of the highest order derivative, but not the solution of the differential equation. Recently, the convergence theorem of the HWM was proved in [16] for the n th order ordinal differential equations (ODEs) ($n \geq 2$). It was stated that the order of convergence of the HWM is equal to two. In [17] the accuracy estimates for the extrapolated results in the case of the fourth order ODE are derived, and it is shown that the order of convergence of the extrapolated results is equal to four (Richardson extrapolation is applied).

The application area of new simple methods often includes problems with advanced material models, constitutive laws, etc., which are not yet (well) covered by commercial software.

* Corresponding author, Maarjus.Kirs@ttu.ee

A new trend in the development of wavelet methods can be outlined as solution of fractional differential and integral equations [15,18–24], which is an area not yet well covered by commercial software (finite element method (FEM), etc.). It is observed in [21] that in the case of fractional ODE the order of convergence of the HWM is equal to two if higher order derivative α in the fractional differential equation exceeds one ($\alpha > 1$). However, in the case of $0 < \alpha < 1$ the order of convergence of the HWM tends to the value $1 + \alpha$.

In [25,26] the HWM was adapted for the analysis of structures of functionally graded material (FGM). In the current study the vibration analysis of the FGM beams is performed and the results obtained by the HWM are compared with the corresponding results obtained by using the finite difference method (FDM) and the differential quadrature method (DQM). Selection of FDM and DQM for comparison of results was motivated by the fact that these methods are widely used numerical methods in engineering and are based on strong formulation (the complexity of implementation is similar). The methods considered are implemented by the authors in the MATLAB code.

In order to verify the obtained results and prepare solution procedures for structures with complex geometry and loading cases, the solid element 3D finite element model was developed.

2. BASICS OF HAAR WAVELETS

The Haar function is defined in [8,9] as

$$h_i(x) = \begin{cases} 1 & \text{for } x \in [\xi_1(i), \xi_2(i)] \\ -1 & \text{for } x \in [\xi_2(i), \xi_3(i)] \\ 0 & \text{elsewhere} \end{cases} \quad (1)$$

In (1) $i = m + k + 1$, $m = 2^j$ is the maximum number of square waves that can be sequentially deployed in interval $[A, B]$ and the parameter k indicates the location of the particular square wave,

$$\begin{aligned} \xi_1(i) &= A + 2k\mu\Delta x, \\ \xi_2(i) &= A + (2k+1)\mu\Delta x, \\ \xi_3(i) &= A + 2(k+1)\mu\Delta x, \\ \mu &= M/m, \Delta x = (B-A)/(2M), M = 2^j. \end{aligned} \quad (2)$$

The Haar functions are orthogonal to one another and form a good transform basis

$$\int_0^1 h_i(x)h_l(x)dx = \begin{cases} 2^{-j} & i = l = 2^j + k \\ 0 & i \neq l \end{cases} \quad (3)$$

Any function $f(x)$ that is square integrable and finite in the interval $[A, B]$ can be expanded into Haar wavelets as

$$f(x) = \sum_{i=1}^m a_i h_i(x). \quad (4)$$

The integrals of the Haar functions (1) of order n can be calculated analytically as [9]

$$p_n(x) = \begin{cases} 0 & x \in [A, \xi_1(i)] \\ \frac{(x - \xi_1(i))^n}{n!} & x \in [\xi_1(i), \xi_2(i)] \\ \frac{(x - \xi_1(i))^n - 2(x - \xi_2(i))^n}{n!} & x \in [\xi_2(i), \xi_3(i)] \\ \frac{(x - \xi_1(i))^n - 2(x - \xi_2(i))^n + (x - \xi_3(i))^n}{n!} & x \in [\xi_3(i), B] \end{cases} \quad (5)$$

The integrals of the Haar functions determined by (5) are continuous functions in the interval $[A, B]$.

3. FREE VIBRATION ANALYSIS OF THE FGM BEAM

In the following the free vibration analysis of the FGM beam is considered [27–29]. It is assumed that the material properties of the beam of length L vary axially. The governing differential equation of the beam can be written as

$$\frac{\partial^2}{\partial x^2} \left(EI(x) \frac{\partial^2 w(x,t)}{\partial x^2} \right) + \rho A(x) \frac{\partial^2 w(x,t)}{\partial t^2} = 0, \quad 0 < x < L. \quad (6)$$

The varying properties of the bending stiffness $EI(x)$ and the distributed mass per unit length $\rho A(x)$ are described by exponential functions as

$$EI(x) = EI(0)e^{2\beta x/L}, \quad \rho A(x) = \rho A(0)e^{2\beta x/L}. \quad (7)$$

The reference values of the bending stiffness and distributed mass per unit length at $x = 0$ are denoted by $EI(0)$ and $\rho A(0)$, respectively. Relation (7) is used in a number of papers [27–29]. The volume fractions of the material corresponding to relation (7) can be derived as

$$V_1 = \frac{e^{2\beta} - e^{2\beta x}}{e^{2\beta} - 1}, \quad V_2 = \frac{e^{2\beta x} - 1}{e^{2\beta} - 1}. \quad (8)$$

The wavelet method approach considered can be applied for a wide range of functions describing

properties of FGM. In the following a more general power law relation for describing FG materials is considered:

$$E = (E_L - E_R) \left(1 - \frac{x}{L}\right)^k + E_R, \quad (9)$$

$$\rho = (\rho_L - \rho_R) \left(1 - \frac{x}{L}\right)^k + \rho_R. \quad (10)$$

Here k is the non-negative power-law exponent describing the material variation profile along the length of the beam and the indexes L and R stand for the values of the material properties on the left and right support of the beam, respectively. Relations (9)–(10) seem to be the most widely used relations for describing FGM properties found in the literature [30].

In the following the solution of the partial differential equation (6) is assumed in the form

$$w(x, t) = W(x) \sin(\omega t). \quad (11)$$

Considering Eqs (7) and (11), the governing differential equation (6) can be rewritten in a non-dimensional form as

$$\frac{d^2}{dx^2} \left(e^{2\beta x} \frac{d^2 W}{dx^2} \right) - \Omega^2 e^{2\beta x} W = 0, \quad (12)$$

where

$$X = \frac{x}{L}, \Omega = 2\pi f L^2 \sqrt{\frac{\rho_A(0)}{EI(0)}}. \quad (13)$$

As a result, the vibration analysis problem of the FGM beam considered above is converted to solving the ordinal differential equation (12). The particular boundary conditions are introduced in Section 7.

4. THE HAAR WAVELET DISCRETIZATION METHOD

Herein the most commonly used approach of the HWM is employed. According to this method, the highest order derivative existing in a differential equation is expanded into Haar wavelets. Thus, Eq. (12) implies that the fourth order derivative should be expanded into Haar wavelets as

$$\frac{d^4 W}{dX^4} = \sum_{i=1}^N a_i h_i(X), \quad (14)$$

where $N = 2M$ is the resolution used.

The solution of the differential governing equation (12) $W(X)$ can be obtained by integrating the expansion (14) four times with respect to X as

$$W(X) = a^T P^{(4)} + c_3 \frac{X^3}{6} + c_2 \frac{X^2}{2} + c_1 X + c_0. \quad (15)$$

In (15) the operational matrix of integration $P^{(4)}$ is defined by formulas (5) and a^T is a vector of coefficients. The integration constants c_0, \dots, c_3 can be determined for each particular boundary condition separately. Corresponding expressions of the integration constants are omitted for conciseness sake.

Inserting the solution of (15) in the differential equation (12) and assuming uniform grid points in the form

$$t_l = (2l-1)/(2N), \quad l = 1, \dots, N, \quad (16)$$

one obtains a linear system of algebraic equations, which can be solved with respect to coefficient vector a^T . Finally, substituting the values of a^T in (15) gives the solution of the posed problem in an analytical form.

5. CONVERGENCE AND ACCURACY ESTIMATES

The convergence theorem for the HWM is given in [16] for the n th order ODE ($n \geq 2$) as

THEOREM: Let us assume that $f(x) = \frac{d^n u(x)}{dx^n} \in L^2(R)$

is a continuous function on $[0, 1]$ and its first derivative is bounded

$$\forall x \in [0, 1] \exists \eta: \left| \frac{df(x)}{dx} \right| \leq \eta. \quad (17)$$

Then the HWM, based on the approach in [1, 2], will be convergent, i.e. $|E_M|$ will vanish as the number of collocation points approaches N infinity. The convergence is of the order two

$$\|E_M\|_2 = O\left[\left(\frac{1}{N}\right)^2\right]. \quad (18)$$

The proof of the theorem is given in [16]. Furthermore, the quadrate of the L^2 -norm of the error function can be estimated as

$$\|E_M\|_2 \leq \frac{4}{9} \frac{\eta}{(\text{floor}(n/2)!)^2} \left(\frac{1}{N}\right)^2. \quad (19)$$

In the case of the considered problem the highest order derivative in differential equation equals four ($n = 4$) and formula (19) reduces to

$$\|E_M\|_2 \leq \frac{\eta}{9} \left(\frac{1}{N}\right)^2. \quad (20)$$

Furthermore, it is proved in [17] that in the case of the general fourth-order ODE the accuracy of the results of the HWM can be improved from two to four by applying Richardson's extrapolation method. The theoretical estimates pointed out above are validated numerically in the following section.

6. FEM SIMULATION MODEL

Commercial analysis software Mechanical APDL 16.0 was used to develop a 3D finite element simulation model for free vibration analysis of an axially functionally graded beam. The FGM beam was partitioned through its length into a number of strips with constant material properties inside the strip (see Fig. 1).

Figure 1 shows the mesh of the zoomed right-hand side of the beam corresponding to the third row of Table 1 (5 elements in the thickness and width directions and 500 elements in the length direction). The elements considered were cubical 3D 8-Node Homogeneous Structural Elements SOLID185. The detailed mesh values used are given in column 1 of Table 1.

The geometrical parameters of the beam considered are width (b), height (h), and length (L). The material properties of the steel and aluminium used in the FEM analysis are given in Table 2. The boundary conditions considered correspond to a cantilever beam. The results obtained from FEM analysis were originally in the

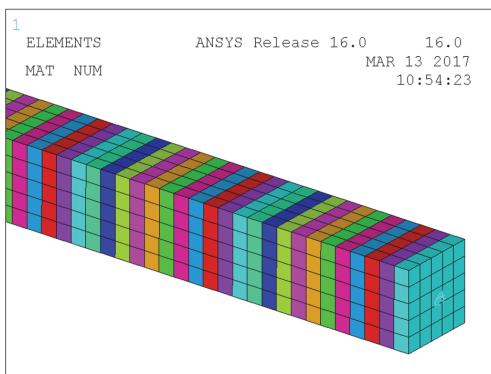


Fig. 1. FGM beam. Mesh, zoomed right end of the beam.

Table 1. FEM model. First three values of frequency parameter, pinned–pinned beam

N	Ω_1	Ω_2	Ω_3
2700 ($3 \times 3 \times 300$)	8.4522	41.2579	91.5302
6400 ($4 \times 4 \times 400$)	8.4366	41.1807	91.3549
12500 ($5 \times 5 \times 500$)	8.4276	41.1363	91.2543
100000 ($10 \times 10 \times 1000$)	8.4136	41.0672	91.0984

Table 2. Material properties of FG steel/aluminium material

Property	Unit	Steel	Aluminium
E	GPa	210	70
ρ	Kg/m ³	7800	2600

dimensional form, i.e. computed for a particular beam with the given geometry, rigidity, and mass per unit length values. In order to compare these results with the results of the FDM, DQM, and HWM, the frequency parameter was converted into the non-dimensional form using the following formula:

$$\Omega = 2\pi fL^2 \sqrt{\frac{\rho A(0)}{EI(0)}}, \quad (21)$$

where f stands for natural/dimensional frequency parameter value (in Hz). The FEM results are discussed in detail in the following section.

7. NUMERICAL RESULTS

In the following five different boundary conditions of the FGM beam are considered (see Fig. 2) and the results obtained by applying HWM, FDM, and DQM are compared (two symmetric and three non-symmetric conditions).

The first two values of the fundamental frequency parameter Ω are presented in Tables 3 and 4 for a pinned–pinned beam, in Tables 5 and 6 for a clamped–clamped beam, in Tables 7 and 8 for a clamped–pinned beam, in Tables 9 and 10 for a pinned–clamped beam, and in Tables 11 and 12 for a clamped–free beam).

Note that in the FE model all supports with pinned boundary conditions (a, c, and d) have the ability to move in the horizontal direction ($u_y = u_z = 0, u_x \neq 0$).

In Tables 1–10 the properties of the beam are considered to vary according to formula (7), i.e. by exponential functions.

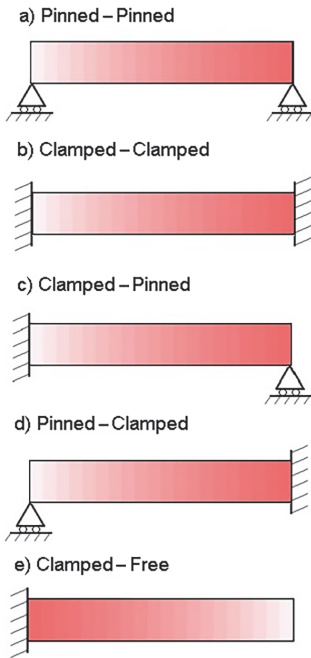


Fig. 2. Boundary conditions of the FGM beam.

Table 3. Fundamental frequency parameter Ω_1 ($\beta = 2$, exact solution 8.41047573)

N	HWM	FDM	DQM
4	7.235577	8.157141	
8	8.118951	8.332735	8.40822662
16	8.337942	8.390010	8.41047574
32	8.392365	8.405292	8.41047574
64	8.405950	8.409176	8.41047568
128	8.409344	8.410150	8.41047711
256	8.410193	8.410394	8.41047514
FEM results ($10 \times 10 \times 1000$ el.)			8.4136

Table 4. Second natural frequency parameter Ω_2 ($\beta = 2$, exact solution 41.07055822)

N	HWM	FDM	DQM
4	36.595239	34.453858	
8	39.999094	39.252370	41.07596761
16	40.805039	40.603112	41.07055821
32	41.004320	40.952833	41.07055821
64	41.054008	41.041072	41.07055830
128	41.066421	41.063183	41.07055855
256	41.069524	41.068714	41.07056029
FEM results ($10 \times 10 \times 1000$ el.)			41.0672

Table 5. Fundamental frequency parameter Ω_1 ($\beta = 2$, exact solution 24.78955023)

N	HWM	FDM	DQM
4	21.242723	21.212781	
8	24.016796	23.517337	24.24277247
16	24.602325	24.432036	24.78954915
32	24.743104	24.697286	24.78955023
64	24.777961	24.766296	24.78955023
128	24.786654	24.783725	24.78955013
256	24.788826	24.788093	24.78955092
FEM results ($10 \times 10 \times 1000$ el.)			24.8074

Table 6. Second natural frequency parameter Ω_2 ($\beta = 2$, exact solution 64.70943426)

N	HWM	FDM	DQM
4	57.202697		
8	62.966887	57.405312	65.21032574
16	64.287324	62.612504	64.70946202
32	64.604874	64.163748	64.70943427
64	64.683357	64.571582	64.70943427
128	64.702919	64.674880	64.70943434
256	64.707806	64.700790	64.70943804
FEM results ($10 \times 10 \times 1000$ el.)			64.7032

Table 7. Fundamental frequency parameter Ω_1 ($\beta = 2$, exact solution 11.18278324)

N	HWM	FDM	DQM
4	8.764599	9.455451	
8	10.647800	10.572089	11.17258124
16	11.052596	11.012971	11.18278324
32	11.150448	11.139111	11.18278324
64	11.174712	11.171786	11.18278327
128	11.180766	11.180029	11.18278302
256	11.182279	11.182094	11.18278285
FEM results ($10 \times 10 \times 1000$ el.)			11.1901

Table 8. Second natural frequency parameter Ω_2 ($\beta = 2$, exact solution 48.26066843)

N	HWM	FDM	DQM
4	41.945882	35.930268	
8	46.799191	43.888087	48.31401606
16	47.903565	47.016589	48.26066840
32	48.171942	47.938093	48.26066844
64	48.238522	48.179262	48.26066848
128	48.255134	48.240268	48.26066852
256	48.259285	48.255565	48.26066842
FEM results ($10 \times 10 \times 1000$ el.)			48.2589

Table 9. Fundamental frequency parameter Ω_1 ($\beta = 2$, exact solution 20.777978)

N	HWM	FDM	DQM
4	18.799637	19.770973	
8	20.309972	20.506995	20.77852832
16	20.662461	20.708729	20.77797932
32	20.749190	20.760567	20.77797932
64	20.770788	20.773620	20.77797931
128	20.776182	20.776889	20.77797921
256	20.777530	20.777707	20.77797837
FEM results ($10 \times 10 \times 1000$ el.)			20.7897

Table 10. Second natural frequency parameter Ω_2 ($\beta = 2$, exact solution 56.294438)

N	HWM	FDM	DQM
8	54.965168	52.599124	
16	55.969009	55.338806	56.09705480
32	56.213501	56.053355	56.29443879
64	56.274230	56.234028	56.29443858
128	56.289388	56.279327	56.29443857
256	56.293176	56.290660	56.29443848
FEM results ($10 \times 10 \times 1000$ el.)			56.2907

Table 11. Fundamental frequency parameter Ω_1 ($\beta = -0.549306$)

N	HWM	FDM	DQM
8	4.884627	4.842031	4.87118515
16	4.874540	4.863858	4.87119849
32	4.872033	4.869360	4.87119848
64	4.871407	4.870739	4.87119797
128	4.871251	4.871084	4.87120621
256	4.871212	4.871170	4.87220829
FEM results ($10 \times 10 \times 1000$ el.)			4.8758

Table 12. Second natural frequency parameter Ω_2 ($\beta = -0.549306$)

N	HWM	FDM	DQM
8	24.798280	23.143597	24.41704668
16	24.517676	24.092313	24.42645172
32	24.449153	24.342014	24.42645172
64	24.432120	24.405285	24.42645167
128	24.427868	24.421156	24.42645138
256	24.426806	24.425128	24.42665633
FEM results ($10 \times 10 \times 1000$ el.)			24.4397

In Tables 3–10 the value of the parameter β is taken equal to 2. The exact solutions computed based on transcendental algebraic equations derived in [27] are given in the headings of Tables 3–10. Obviously, the convergence of the HWM (also of the FDM and DQM) to the exact solution can be observed in all these tables.

The numerical rates of the convergence, computed for the solutions presented in Table 3, are presented in Table 13.

In Table 13 the values of N start from 16 because each rate of convergence was computed on the basis of three consecutive values of the solution [16]. The rate of the convergence of the HWM and FDM obviously tends to two, but the DQM has an ultrafast rate for $N \leq 32$ and a negative rate for $N > 32$ (loss of accuracy).

In Table 14, the convergence rates of the extrapolated results of the HWM are given for four different boundary conditions considered above. The Richardson extrapolation method was applied, and it can be seen from Table 14 that the order of the convergence of extrapolated results tends to four in the case of all boundary conditions considered.

Based on results given in Tables 3–12, it can be concluded that in the case of the posed problem the highest accuracy was achieved by applying the DQM, also in most cases the accuracy of the results obtained by the HWM is higher than that obtained by the FDM (there fundamental frequencies in Tables 3 and 7 are exceptions). Detailed analysis of DQM results shows that the maximum accuracy was achieved extremely quickly with $N = 16$ or $N = 32$; thereafter the accuracy of the solution decreased with increasing resolution. These results are in agreement with the theoretical concept of the DQM (it is based on the use of high order polynomials whose denominator vanishes for large N) and results found in the literature.

It can be seen from Fig. 3 that in the case of the parameter value $k = 1.5$ the functions of the elasticity modulus corresponding to the exponential and power law functions (7) and (9) are close (here a steel/aluminium cantilever beam with $\beta = -0.549306$ is considered).

Table 13. Rates of convergence corresponding to results given in Table 3

N	HWM	FDM	QDM
16	2.0122	1.6163	–
32	2.0086	1.9060	23.8789
64	2.0023	1.9766	–8.6258
128	2.0006	1.9942	–4.6331
256	2.0001	1.9985	–0.4590

Table 14. Fundamental frequency parameter Ω_1 , convergence rates of extrapolated results

N	Pinned–pinned	Clamped–clamped	Clamped–pinned	Pinned–clamped
32	2.514821	4.2685	4.3015	4.1711
64	3.916921	4.0516	4.0774	4.0425
128	3.984539	4.0120	4.0191	4.0105
256	3.996411	4.0029	4.0047	4.0026

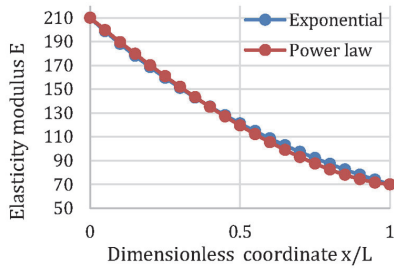


Fig. 3. Variation of elastic modulus.

In Tables 11 and 12 the FG material properties corresponding to steel/aluminium are considered with steel in the left and aluminium in the right support. The particular values of the material used are presented in Table 2.

The exponential model (7) does not include directly material properties at the right end of the beam. The required values of the material are obtained by determining the value of the parameter β ($\beta = -0.549306$).

The first four mode shapes for the above-considered FG steel/aluminium cantilever beam are depicted in Fig. 4. The corresponding mode shapes obtained by a FEM are shown in Figs 5–8.

The results given in Table 15 were obtained by applying the HWM with the general power law function (9)–(10).

The steel/aluminium FGM with properties given in Table 2 is considered and the value of the exponent is taken equal to 1.5 ($k = 1.5$). The boundary conditions for a clamped–clamped beam are applied.

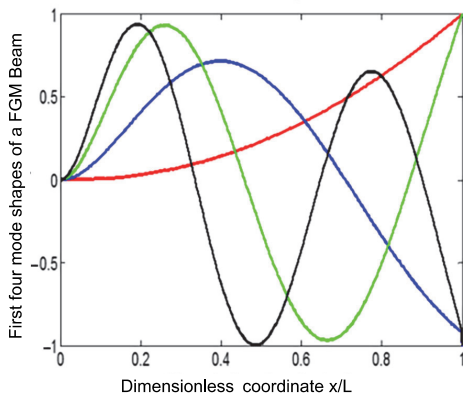


Fig. 4. First four mode shapes of a cantilever FGM beam.

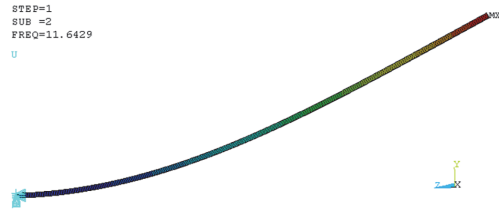


Fig. 5. First mode shape of a cantilever FGM beam in FEM.



Fig. 6. Second mode shape of a cantilever FGM beam in FEM.

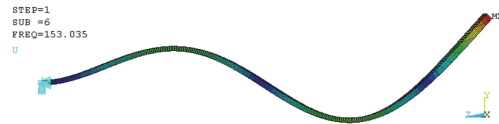


Fig. 7. Third mode shape of a cantilever FGM beam in FEM.

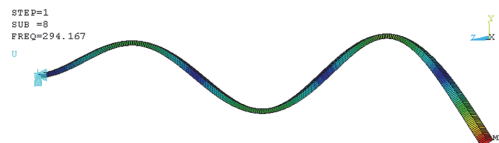


Fig. 8. Fourth mode shape of a cantilever FGM beam in FEM.

Table 15. First three values of fundamental frequency parameter ($k = 1.5$, power law)

N	Ω_1	Ω_2	Ω_3
8	22.573818	62.648322	124.802042
16	22.559805	62.097576	122.045771
32	22.552926	61.958469	121.384345
64	22.548905	61.920592	121.216644
128	22.546296	61.908898	121.172322
256	22.544517	61.904408	121.159519

The FEM results computed for all boundary conditions considered above are given in the last row of each table. The number of elements used is $10 \times 10 \times 1000$.

Obviously, the values of the frequency parameters computed using 3D FEM analysis are in excellent agreement with those given in Tables 3–12, obtained by applying the HWM, DQM, and FDM.

An example of the results of more detailed FEM analysis is given in Table 15. In this table the first free frequencies for a pinned–pinned beam are presented. The convergence of the solution with increasing mesh can be observed. The results are in agreement with corresponding results obtained by applying the HWM, FDM, and DQM given in Tables 3 and 4.

8. CONCLUSIONS

Three strong formulation based numerical methods (HWM, FDM, and DQM) were applied for the analysis of the FGM beam and the obtained results were compared. The algorithms for all methods were coded by the authors in MATLAB. Good performance was observed in the case of all three methods used.

It can be concluded that in the case of the considered problem the accuracy of the solutions obtained by applying the HWM and FDM was in the same range. However, in most cases the accuracy of the results of the HWM outperformed that of the FDM. The accuracy of the DQM appears to be higher than that of the HWM and FDM. The convergence results presented in Table 13 confirm the accuracy of the HWM, FDM, and DQM. Similar accuracy was observed also for cylindrical shells in [16].

The obtained numerical results were validated with the solid element 3D finite element model developed for analysing more complex FGM structures. The results obtained with applying the 3D FEM and HWM were found to be in good (rather excellent) agreement.

Our future studies will focus on the application of the HWM for the analysis of nanostructures and solving fractional differential equations, which are not yet well covered by commercial software solutions. An interesting subtopic, whose research is underway, is adaption of global optimization methods and techniques, developed by the workgroup of design composite structures [31–36] to design nano- and graphene structures.

ACKNOWLEDGEMENTS

The research was supported by the Estonian Research Council (grant PUT1300); Estonian Centre of Excellence in Zero Energy and Resource Efficient Smart Buildings and Districts, ZEBE, TK146 funded by the European Regional Development Fund (grant 2014-2020.4.01.15-0016); Innovative Manufacturing Engineering Systems

Competence Centre IMECC (supported by Enterprise Estonia and co-financed by the European Union Regional Development Fund, project EU48685). The publication costs of this article were covered by Tallinn University of Technology and the Estonian Academy of Sciences.

REFERENCES

1. Chen, C. F. and Hsiao, C. H. Haar wavelet method for solving lumped and distributed-parameter systems. *IEE Proc. Contr. Theor. Appl.*, 1997, **144**(1), 87–94.
2. Hsiao, C. H. State analysis of the linear time delayed systems via Haar wavelets. *Math. Comp. Simulat.*, 1997, **44**(5), 457–470.
3. Majak, J., Pohlak, M., and Eerme, M. Application of the Haar wavelet problems of orthotropic plates and shells. *Mechanic of Composite Materials*, 2009, **45**(6), 631–642.
4. Kirs, M., Mikola, M., Haavajõe, A., Õunapuu, E., Shvartsman, B., and Majak, J. Haar wavelet method for vibration analysis of nanobeams. *Waves, Wavelets and Fractals – Advanced Analysis*, 2016, **2**, 20–28.
5. Lepik, Ü. Solving PDEs with the aid of two dimensional Haar wavelets. *Comput. Math. Appl.*, 2011, **61**, 1873–1879.
6. Lepik, Ü. Solving fractional integral equations by the Haar wavelet method. *Appl. Math. Comput.*, 2009, **214**(2), 468–478.
7. Xie, X., Jin, G., Yan, Y., Shi, S. X., and Liu, Z. Free vibration analysis of composite laminated cylindrical shells using the Haar wavelet method. *Compos. Struct.*, 2014, **109**, 169–177.
8. Lepik, Ü. Numerical solution of differential equations using Haar wavelets. *Math. Comput. Simulat.*, 2005, **68**, 127–143.
9. Lepik, Ü. and Hein, H. *Haar Wavelets: With Applications*. Springer, New York, 2014.
10. Ray, S. S. and Patra, A. Numerical simulation based on Haar wavelet operational method to solve neutron point kinetics equation involving sinusoidal and pulse reactivity. *Ann. Nucl. Energy*, 2014, **73**, 408–412.
11. Islam, S. U., Aziz, I., and Al-Fhaid, A. S. An improved method based on Haar wavelets for numerical solution of nonlinear integral and integro-differential equations of first and higher orders. *J. Comput. Appl. Math.*, 2014, **260**, 449–469.
12. Aziz, I., Islam, S. U., and Khana, F. A new method based on Haar wavelet for the numerical solution of two-dimensional nonlinear integral equations. *J. Comput. Appl. Math.*, 2014, **272**, 70–80.
13. Aziz, I. and Islam, S. U. New algorithms for the numerical solution of nonlinear Fredholm and Volterra integral equations using Haar wavelets. *J. Comput. Appl. Math.*, 2013, **239**, 333–345.
14. Majak, J., Pohlak, M., Eerme, M., and Lepikult, T. Weak formulation based Haar wavelet method for solving differential equations. *Appl. Math. Comput.*, 2009, **211**(2), 488–494.
15. Saeedi, H., Mollahasani, N., Moghadam, M., and Chuev, G. An operational Haar wavelet method for solving fractional Volterra integral equations. *Int. J. Appl. Math. Comput. Sci.*, 2011, **21**(3), 535–547.

16. Majak, J., Shvartsman, B. S., Kirs, M., Pohlak, M., and Herranen, H. Convergence theorem for the Haar wavelet based discretization method. *Compos. Struct.*, 2015, **126**, 227–232.
17. Majak, J., Shvartsman, B. S., Karjust, K., Mikola, M., Haavajõe, A., and Pohlak, M. *Composites. Part B: Engineering*, 2015, **80**, 321–327.
18. Heydari, M. H., Hooshmandasl, M. R., and Mohammadi, F. Legendre wavelets method for solving fractional partial differential equations with Dirichlet boundary conditions. *Appl. Math. Comput.*, 2014, **234**, 267–276.
19. Heydari, M. H., Hooshmandasl, M. R., and Mohammadi, F. Two-dimensional Legendre wavelets for solving time-fractional telegraph equation. *Adv. Appl. Math. Mech.*, 2014, **6**(2), 247–260.
20. Heydari, M. H., Hooshmandasl, M. R., and Ghaini, F. M. M. A new approach of the Chebyshev wavelets method for partial differential equations with boundary conditions of the telegraph type. *Appl. Math. Model.*, 2014, **38**(5–6), 1597–1606.
21. Majak, J., Shvartsman, B., Pohlak, M., Karjust, K., Eerme, M., and Tungel, E. 2016. Solution of fractional order differential equation by the Haar wavelet method. Numerical convergence analysis for most commonly used approach. In *AIP Conference Proceedings*, **1738** (Simos, T., ed.), 480110. <http://dx.doi.org/10.1063/1.4952346> (accessed 2016-11-30).
22. Rehman, M. U. and Khan, R. A. Numerical solutions to initial and boundary value problems for linear fractional partial differential equations. *Appl. Math. Model.*, 2013, **37**, 5233–5244.
23. Ray, S. S. and Patra, A. Haar wavelet operational methods for the numerical solutions of fractional order nonlinear oscillatory Van der Pol system. *Appl. Math. Comput.*, 2013, **220**, 659–667.
24. Saeed, U., Rejman, M., and Iqbal, M. A. Haar wavelet-Picard technique for fractional order nonlinear initial and boundary value problems. *Sci. Res. Essays*, 2014, **9**(12), 571–580.
25. Hein, H. and Feklistova, L. Computationally efficient delamination detection in composite beams using Haar wavelets. *Mech. Syst. Signal Pr.*, 2011, **25**, 2257–2270.
26. Jin, G., Xie, X., and Liu, Z. The Haar wavelet method for free vibration analysis of functionally graded cylindrical shells based on the shear deformation theory. *Compos. Struct.*, 2014, **108**, 435–448.
27. Li, X. F., Kang, Y. A., and Wu, J. X. Exact frequency equations of free vibration of exponentially functionally graded beams. *Appl. Acoust.*, 2013, **74**, 413–420.
28. Lu, Z. R., Lin, X. X., Chen, Y. M., and Huang, M. Hybrid sensitivity matrix for damage identification in axially functionally graded beams. *Appl. Math. Model.*, 2017, **41**, 604–617.
29. Shvartsman, B. and Majak, J. Numerical method for stability analysis of functionally graded beams on elastic foundation. *Appl. Math. Model.*, 2016, **40**, 3713–3719.
30. Alshorbagy, A. E., Eltahir, M. A., and Mahmoud, F. F. Free vibration characteristics of a functionally graded beam by finite element method. *Appl. Math. Model.*, 2011, **35**, 412–425.
31. Aruniit, A., Kers, J., Goljandin, D., Saarna, M., Tall, K., Majak, J., and Herranen, H. Particulate filled composite plastic materials from recycled glass fibre reinforced plastics. *Materials Science (Medžiagotyra)*, 2011, **17**(3), 276–281.
32. Lellep, J. and Majak, J. On optimal orientation of nonlinear elastic orthotropic materials. *Struct. Optimization*, 1997, **14**, 116–120.
33. Majak, J. and Hannus, S. Orientational design of anisotropic materials using the Hill and Tsai-Wu strength criteria. *Mech. Compos. Mater.*, 2003, **39**(6), 509–520.
34. Aruniit, A., Kers, J., Majak, J., Krumme, A., and Tall, K. Influence of hollow glass microspheres on the mechanical and physical properties and cost of particle reinforced polymer composites. *Proc. Estonian Acad. Sci.*, 2012, **61**, 160–165.
35. Herranen, H., Allikas, G., Eerme, M., Vene, K., Otto, T., Gregor, A., et al. Visualization of strain distribution around the edges of a rectangular foreign object inside the woven carbon fibre specimen. *Estonian J. Eng.*, 2012, **18**, 279–287.
36. Pohlak, M., Majak, J., and Eerme, M. 2008. Optimization of car frontal protection systems. In *Proceedings of the 6th international conference of DAAAM Baltic Industrial Engineering, 24–26th April 2008* (Küttner, R. ed.), 123–128.

Funktsionaalgradientmaterjalist tala vabavõnkumised: Haari lainikute meetodi evalveerimine

Maarjus Kirs, Kristo Karjust, Imran Aziz, Erko Õunapuu ja Ernst Tungel

Uurimistöö on keskendunud Haari lainikute meetodi evalveerimisele. Haari lainikute meetodi abil saadud tulemusi on võrreldud insenerirakendustes laialdaselt kasutatavate tugeval formulatsioonil põhinevate meetodite, nagu lõplike vahede meetodi ja diferentsiaalkvadratuuride meetodi tulemustega. Vaadeldava ülesande korral on Haari lainikute meetod lõplike vahede meetodist täpsem. Diferentsiaalkvadratuuride meetod osutus väiksema kollokatsioonipunktide arvu korral Haari lainikute meetodist täpsemaks, kuid selle rakendamine suurema kollokatsioonipunktide arvu korral on komplitseeritud. Samuti on loodud 3D lõplike elementide meetodil põhinev mudel ja selle rakendamisel saadud tulemused on eeltoodud meetodite tulemustega kooskõlas. Haari lainikute meetodi abil saadud lahendi ja ekstraoleeritud tulemuste koordinaatide kiirus on kooskõlas vastavate koordinaatidega tõiostatud teoreetiliste tulemustega.

PUBLICATION II

Kirs, M., Mikola, M., Haavajõe, A., Õunapuu, E., Shvartsman, B., Majak, J. (2016). Haar wavelet method for vibration analysis of nanobeams. *Waves Wavelets and Fractals Advanced Analysis*, 2, 20–28.

Research Article

Open Access

M. Kirs, M. Mikola, A. Haavajõe, E. Õunapuu, B. Shvartsman, and J. Majak

Haar wavelet method for vibration analysis of nanobeams

DOI 10.1515/wwfaa-2016-0003

Received Jan 29, 2016; accepted Feb 29, 2016

Abstract: In the current study the Haar wavelet method is adopted for free vibration analysis of nanobeams. The size-dependent behavior of the nanobeams, occurring in nanostructures, is described by Eringen nonlocal elasticity model. The accuracy of the solution is explored. The obtained results are compared with ones computed by finite difference method. The numerical convergence rates determined are found to be in agreement with corresponding convergence theorems.

Keywords: Haar wavelet method; nonlocal elasticity; nanobeams; Richardson extrapolation

AMS: 74S30, 74B99, 65L10

1 Introduction

The Haar wavelet method considered herein has been introduced by Chen and Hsiao for solving lumped and distributed parameter systems [12]. According to approach proposed in [12] the highest order derivative included in the differential equation is expanded into the series of Haar functions. Such an approach allows to overcome shortcomings caused by discontinuities of the Haar functions. An alternate approach has been proposed by Cattani [10], Castro *et al.* [9], according to which the quadratic waves are “smoothed” with interpolating splines.

The Haar wavelet method introduced in [12] has been adjusted for solving wide class of differential and integral equations covering solid and fluid mechanics [15, 16, 19–22, 29, 46–48], mathematical physics [18, 36, 38–40], evolutionary equations [23, 30], etc. In [22] the Haar wavelet method for solving PDE is developed. In [16, 19, 20, 29, 46–48] the Haar wavelet method is adopted for analysis of composite structures. In [18] the Haar wavelets method is applied for solving differential equations characterizing the dynamics of a current collection system for an electric locomotive. The nuclear reactor dynamics equations are considered in [36, 38–40].

Recent treatments in the area of Haar wavelet method development cover solution of integral and integro-differential equations [6, 7, 17, 25], fractional partial differential equations [26, 41, 43, 44]. The accuracy issues of the Haar wavelet method are studied in [31, 32]. It has been proved in [31] that the order of convergence of the Haar wavelet method is equal to two. In [32] the Richardson extrapolation method is applied and it has been shown that the order of convergence of the extrapolated results is equal to four.

Some review papers covering development of the Haar wavelet method and its application can be referred as [27, 28].

The vibration analysis of nanostructures, based on nonlocal elasticity theory, is performed commonly by applying finite difference (FD) or differential quadrature (DQ) methods [8, 33, 34, 37], also finite element method [13, 42], Rayleigh-Ritz method [11], etc. A number of analytical or semi-analytical solutions are derived

M. Kirs, M. Mikola, A. Haavajõe, E. Õunapuu: Tallinn University of Technology, Ehitajate tee 5, Tallinn, Estonia 19086

B. Shvartsman: Estonian Entrepreneurship University of Applied Sciences, Suur-Sõjamäe 10, Tallinn, Estonia, 11415

J. Majak: Tallinn University of Technology, Ehitajate tee 5, Tallinn, Estonia 19086; Email: juri.majak@ttu.ee



© 2016 M. Kirs *et al.*, published by De Gruyter Open.

This work is licensed under the Creative Commons Attribution-NonCommercial-NoDerivs 3.0 License.

for particular problems [2, 5]. These solutions can be employed for estimating the accuracy of numerical methods.

In the current study the Haar wavelet method is adopted for free vibration analysis of nanobeams. The obtained numerical results are compared with the results achieved by applying FD method (the study is focused on strong formulation based method). The numerical order of convergence of the results is computed and validated.

2 Basics of Haar wavelets

The Haar function $h_i(x)$ is defined as [12, 21]

$$h_i(x) = \begin{cases} 1 & \text{for } x \in [\xi_1(i), \xi_2(i)] \\ -1 & \text{for } x \in [\xi_2(i), \xi_3(i)] \\ 0 & \text{elsewhere} \end{cases} \quad (1)$$

In (1) $i = m + k + 1$, $m = 2^j$ ($M = 2^J$) stands for a maximum number of square waves that can be sequentially deployed in interval $[A, B]$ and the parameter k indicates the location of the particular square wave

$$\xi_1(i) = A + 2k\mu\Delta x, \quad \xi_2(i) = A + (2k + 1)\mu\Delta x, \quad \xi_3(i) = A + 2(k + 1)\mu\Delta x, \quad \mu = M/m, \quad \Delta x = (B - A)/(2M). \quad (2)$$

The components of the operational matrix of integration can be obtained as n -th order integrals of Haar function (1)

$$p_{n,i}(x) = \frac{1}{n!} \begin{cases} 0 & \text{for } x \in [A, \xi_1(i)] \\ (x - \xi_1(i))^n & \text{for } x \in [\xi_1(i), \xi_2(i)] \\ (x - \xi_1(i))^n - 2(x - \xi_2(i))^n & \text{for } x \in [\xi_2(i), \xi_3(i)] \\ (x - \xi_1(i))^n - 2(x - \xi_2(i))^n + (x - \xi_3(i))^n & \text{for } x \in [\xi_3(i), B] \end{cases} \quad (3)$$

An integrable and finite function in the interval $[A, B]$ can be expanded into Haar wavelets as

$$f(x) = \sum_{i=1}^{\infty} a_i h_i(x) = a^T H \quad (4)$$

In the following sections an approach of the Haar wavelet method proposed in [1] is employed.

3 Governing differential equations for nonlocal Euler-Bernoulli beam

The governing differential equations for Euler-Bernoulli beam are derived in a number of papers [3, 8]. Thus, herein the detailed derivation of governing equations is omitted for conciseness sake. In the following, a short description of the basic concepts, assumptions and principles used is given.

Classical *e.g.* Euler-Bernoulli beam theory is founded on the following two key assumptions:

- Cross sections of the beam do not deform in a significant manner under the application of transverse or axial loads and can be assumed as rigid,
- During deformation, the cross section of the beam is assumed to remain planar and normal to the deformed axis of the beam.

Based on above assumptions the classical Euler-Bernoulli beam model describing free harmonic vibrations read

$$EI \frac{d^4 W}{dx^4} - m_0 \Omega^2 W = 0, \quad (5)$$

According to free harmonic motion, the deflection is assumed in form $w(x, t) = W(x) \sin(\omega t)$, where ω stand for natural frequency of vibration. In (5) m_0 is mass moment of inertia, E and I stand for the Young's modulus and the second moment of area, respectively.

However, the classical beam governing equation (5) does not cover nonlocal behavior of the structure *i.e.* "small scale effect". In order to consider small scale effect the nonlocal elasticity theory should be introduced instead of Hooke's law. Herein we considered continuum mechanics based on nonlocal elasticity theory and most widely used Eringen model [46] as

$$(1 - \alpha^2 L^2 \nabla^2) \sigma = C \epsilon, \quad (6)$$

In (6) C stands for the fourth-order elasticity tensor, σ and ϵ are the second order stress and strain tensors, respectively. The operator ∇^2 is a Laplace operator and $\alpha = (e_0 a)/L$. The parameter e_0 describes material properties. The parameters L and a stand for external and internal characteristic lengths, respectively.

The nonlocal constitutive equation (6) can be rewritten in terms of moments and deflection as (multiplying (6) by z and integrating through the cross sectional area)

$$M - \mu \frac{d^2 M}{dx^2} = -EI \frac{d^2 W}{dx^2}. \quad (7)$$

In (7) μ stands for nonlocal parameter. Combining the nonlocal constitutive equation (7) and the moment and deflection relation of Euler-Bernoulli beam

$$\frac{d^2 M}{dx^2} = -m_0 \omega^2 W, \quad (8)$$

one obtains the governing differential equation for nonlocal Euler-Bernoulli beam in terms of displacement as

$$EI \frac{d^4 W}{dx^4} + \mu m_0 \omega^2 \frac{d^2 W}{dx^2} = m_0 \omega^2 W. \quad (9)$$

In non-dimensional variables the governing differential equation for nonlocal Euler-Bernoulli beam reads

$$\frac{d^4 W}{dX^4} + \frac{\mu \lambda^2}{L^2} \frac{d^2 W}{dX^2} = \lambda^2 W, \quad (10)$$

where $X = x/L$, $\lambda^2 = m_0 \omega^2 L^4 / EI$.

In the following section the governing differential equation (10) will be discretized by applying Haar wavelet method.

4 Application of the Haar wavelet method

According to the HWDM considered, the highest order derivative existing in differential equation is expanded into Haar wavelets. In the case of considered problem the fourth order derivative can be expanded into Haar wavelets as

$$\frac{d^4 W}{dX^4} = a^T H. \quad (11)$$

By integrating (11) four times with respect to x , one obtains the solution $W(x)$ as

$$W(X) = a^T P^{(4)} + c_3 \frac{X^3}{6} + c_2 \frac{X^2}{2} + c_1 X + c_0, \quad (12)$$

where $P^{(4)}$ is a fourth order operational matrix defined by formula (4) and c_0, \dots, c_3 stand for integration constants determined for each particular boundary conditions separately.

Inserting (10), (11) in governing differential equation (9) one obtains

$$a^T H + \mu \frac{\lambda^2}{L^2} (a^T P^{(2)} + c_3 X + c_2) = \lambda^2 \left(a^T P^{(4)} + c_3 \frac{X^3}{6} + c_2 \frac{X^2}{2} + c_1 X + c_0 \right). \quad (13)$$

The following boundary conditions are considered:

a) Pinned-pinned nanobeam

$$W(0) = 0, W(1) = 0, W'(0) = 0, W'(1) = 0. \quad (14)$$

b) Clamped-clamped nanobeam

$$W(0) = 0, W(1) = 0, W'(0) = 0, W'(1) = 0. \quad (15)$$

c) Clamped-pinned nanobeam

$$W(0) = 0, W(1) = 0, W'(0) = 0, W'(1) = 0. \quad (16)$$

In the current study, firstly the integrations constants c_0, \dots, c_3 are determined from particular boundary conditions and then the system (13) is solved with respect to frequency parameter λ as an eigenvalue problem.

5 Numerical results and convergence analysis

In the following, the three types of boundary conditions are considered (pinned-pinned, clamped-clamped and clamped-pinned) for numerical analysis of nanobeam. It is assumed that the external characteristic length parameter L is equal to 10 nm and the nonlocal parameter varies in range $[0; 5]$.

Let us denote two numerical solutions found on nested grids $h_{i-1}, h_i = h_{i-1}/2$ by F_{i-1}, F_i . According to Richardson extrapolation formulas, the extrapolated values of the solution can be computed as [35, 45]

$$R_i = F_i + \frac{F_i - F_{i-1}}{2^k - 1}, \quad (17)$$

where k stands for the theoretical order of convergence. However, the theoretical order of convergence of the numerical method may be not preliminarily known. In latter case using the Eq. (16) and three solutions on a sequence of grids $F_{i-2}, F_{i-1}, F_i, h_{i-2}/h_{i-1} = h_{i-1}/h_i = 2$ one can obtain the estimate on the theoretical order of convergence k as [48]

$$k \approx k_i = \log \left(\frac{F_{i-2} - F_{i-1}}{F_{i-1} - F_i} \right) / \log(2). \quad (18)$$

In (17) k_i is the value of the observed order of convergence.

a) Pinned-pinned nanobeam (PP)

The values of the fundamental frequency parameter $F = \sqrt{\lambda}$ (square root is taken in order to compare with results found in literature), the numerical rates of convergence and absolute errors for different grid levels are presented in Table 1.

It can be seen from Table 1, that the error of the Haar wavelet method is less than that of finite difference method, but remains in the same range. The numerical rate of convergence tends to two in the case of both methods (see columns 4 and 5), but this process is faster in the case of Haar wavelet method. In Table 1 the scaling parameter μ is equal to zero and the results are compared with exact solution given in [8] (nanoscale effect is not considered). In Tables 2–3 the value of the scaling parameter μ is varied ($\mu = 3$ and $\mu = 5$) and instead of absolute error the values of the extrapolated results and their convergence rates are given.

Obviously, the fundamental frequency parameters F_j corresponding to HWDM and FDM are close and converge to the same value (columns 2–3 in Tables 2–3), but in the case of lower grid ($N = 4; 8; 16$) the error of the+ HWDM is significantly smaller than that of the FDM. Here the error is computed as difference from final value achieved with $N = 1024$. The numerically estimated rates of convergence k_j tend to two in the case of both methods HWDM and FDM (columns 4 and 5). The numerical rates of convergence of the extrapolated results tend to four for both methods (some deviation can be observed in the case of FDM for larger grid, which may be caused by too close values of the frequencies). These results are in agreement with convergence

Table 1: The values of the fundamental frequencies F_j , rates of convergence k_j and errors ($\mu = 0$).

Grid N	Fundamental frequency F_j		Rate of convergence k_j		Error	
	HWM	FDM	HWM	FDM	HWM	FDM
4	3.161916	3.061468			0.0203	0.0801
8	3.146649	3.121445			0.0051	0.0202
16	3.142855	3.136549	2.0085	1.9896	0.0013	0.0050
32	3.141908	3.140331	2.0027	1.9974	0.0003	0.0013
64	3.141672	3.141277	2.0007	1.9993	7.8855E-05	0.0003
128	3.141612	3.141514	2.0002	1.9998	1.9713E-05	7.8854E-05
256	3.141598	3.141573	2.0000	2.0001	4.9283E-06	1.9754E-05
512	3.141594	3.141588	2.0000	2.0009	1.2321E-06	4.9536E-06
1024	3.141593	3.141592	2.0000	1.9053	3.0800E-07	9.5359E-07
Exact	3.14159265					

Table 2: The values of the fundamental frequencies F_j , rates of convergence k_j , extrapolated results and their rates of convergence ($\mu = 3$).

Grid N	Fundamental frequency F_j		Rate of convergence k_j		Extrapolated results R_i		Rate of convergence of extr. results	
	HWM	FDM	HWM	FDM	HWM	FDM	HWM	FDM
4	2.963169	2.877579						
8	2.949087	2.927620			2.944393	2.944300		
16	2.945544	2.940174	1.9911	1.9949	2.944364	2.944358		
32	2.944658	2.943315	1.9985	1.9987	2.944362	2.944362	4.5171	4.0137
64	2.944436	2.944100	1.9997	1.9997	2.944362	2.944362	4.1501	4.0029
128	2.944381	2.944297	1.9999	1.9999	2.944362	2.944362	4.0393	4.0608
256	2.944367	2.944346	2.0000	1.9996	2.944362	2.944362	4.0098	
512	2.944363	2.944358	2.0000	1.9983	2.944362	2.944362	3.9942	
1024	2.944363	2.944359	2.0000	4.0219	2.944362	2.944359	4.2251	

Table 3: The values of the fundamental frequencies F_j , rates of convergence k_j , extrapolated results and their rates of convergence ($\mu = 5$).

Grid N	Fundamental frequency F_j		Rate of convergence k_j		Extrapolated results R_i		Rate of convergence of extr. results	
	HWM	FDM	HWM	FDM	HWM	FDM	HWM	FDM
4	2.859891	2.781004						
8	2.846396	2.826607			2.841898	2.841809		
16	2.842983	2.838032	1.9832	1.9970	2.841845	2.841840		
32	2.842128	2.840890	1.9966	1.9993	2.841843	2.841842	4.2765	4.0265
64	2.841914	2.841604	1.9992	1.9998	2.841843	2.841843	4.0725	4.0063
128	2.841860	2.841783	1.9998	2.0000	2.841842	2.841843	4.0184	3.9482
256	2.841847	2.841828	1.9999	1.9997	2.841842	2.841843	4.0044	
512	2.841844	2.841839	2.0000	1.9937	2.841842	2.841843	4.0045	
1024	2.841843	2.841844	2.0000	1.1015	2.841842	2.841846	4.0066	

Table 4: The values of the fundamental frequencies F_j , rates of convergence k_j , extrapolated results and their rates of convergence ($\mu = 5$).

Grid N	Fundamental frequency F_j		Rate of convergence k_j		Extrapolated results R_i		Rate of convergence of extr. results	
	HWM	FDM	HWM	FDM	HWM	FDM	HWM	FDM
4	3.535756	3.320272						
8	3.510894	3.455128			3.502607	3.500080		
16	3.504564	3.490504	1.9737	1.9306	3.502454	3.502296		
32	3.502974	3.499452	1.9932	1.9831	3.502444	3.502434	3.9299	3.9965
64	3.502576	3.501695	1.9983	1.9958	3.502444	3.502443	3.9874	4.0018
128	3.502477	3.502256	1.9996	1.9990	3.502444	3.502444	3.9971	3.9999
256	3.502452	3.502397	1.9999	2.0000	3.502444	3.502444	3.9999	
512	3.502446	3.502431	2.0000	2.0489	3.502444	3.502442	3.9959	
1024	3.502444	3.502441	2.0000	1.6797	3.502444	3.502445	3.9069	

theorems proved in [31, 32]. Interesting is the small scale effect of the beam or dependency of the solution on scaling parameter μ . Figure 1 shows the relation between non-dimensional frequency parameter and scaling parameter μ .

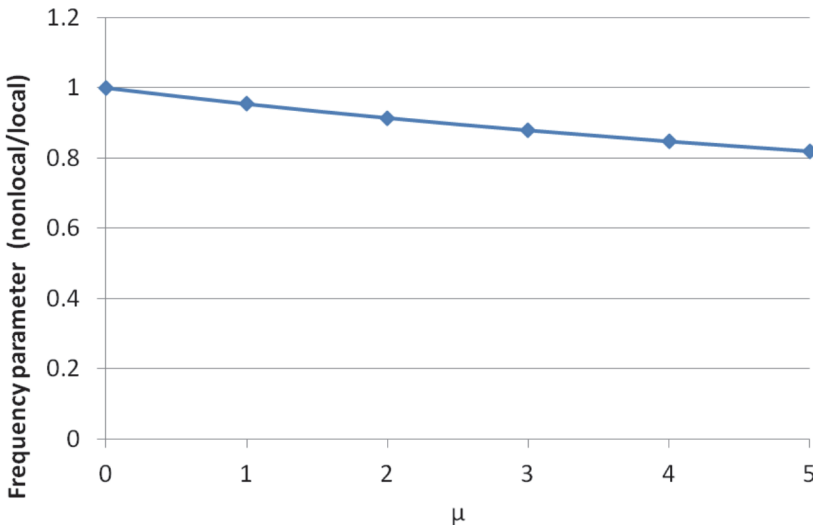


Figure 1: Effect of scaling parameter μ on fundamental frequency.

Increasing the value of the scaling parameter μ from 0 to 5 causes remarkable reduction of the value of fundamental frequency parameter λ (18.2%). Thus, it is reasonable to consider small scale effect for analysis of nanobeams.

b) Pinned-clamped nanobeam

The structure of the Table 4 is the same as Tables 2–3. It can be seen from columns 2 and 3 of Table 4 that the fundamental frequency parameters corresponding to HWDM and FDM are close and converge to the same value. The numerical rates of convergence k_j tend to two in the case of both methods and the rates of convergence of extrapolated results tend to four in the case of both methods (certain deviations appears in the case of larger grid, which may be caused by too close values of the frequencies). Again, in the case of small grid size ($N = 4; 8; 16$) the error of the HWDM is substantially smaller than that of FDM.

c) Clamped-clamped nanobeam

The structure of the Table 5 coincides with that of Table 4. In can be seen from Table 5 that in the case of clamped-clamped nanobeam the behavior of the solutions is similar with the previous two boundary conditions considered above.

Table 5: The values of the fundamental frequencies F_j , rates of convergence k_j , extrapolated results and their rates of convergence ($\mu = 5$).

Grid N	Fundamental frequency F_j		Rate of convergence k_j		Extrapolated results R_i		Rate of conv. of extr. results	
	HWM	FDM	HWM	FDM	HWM	FDM	HWM	FDM
4	4.252952	3.832771						
8	4.207325	4.095779			4.192116	4.183449		
16	4.195622	4.167331	1.9629	1.8781	4.191720	4.191182		
32	4.192669	4.185572	1.9870	1.9718	4.191685	4.191652	3.4847	4.0397
64	4.191929	4.190153	1.9966	1.9932	4.191683	4.191681	3.9239	4.0225
128	4.191744	4.191300	1.9991	1.9983	4.191683	4.191682	3.9832	4.0068
256	4.191698	4.191587	1.9998	1.9996	4.191683	4.191683	3.9959	3.9994
512	4.191686	4.191659	1.9999	2.0006	4.191683	4.191683	4.0009	
1024	4.191683	4.191677	2.0000	1.9645	4.191683	4.191683	3.9621	

Similarly to pinned-pinned beam, the influence of the scaling parameter μ on fundamental frequency parameter λ is significant (21.5%).

6 Conclusions

The Haar wavelet method has been treated for free vibration analysis of nanobeams. The reference solution is realized by FD method (also strong formulation based method). The results obtained by applying HWDM and FDM were similar. The accuracy of the solutions obtained by applying HWDM appears higher in the case of all three boundary conditions considered, especially in the case of small grid size ($N = 4; 8; 16$). The numerical rate of convergence has been observed to be equal to two for HWDM and equal to four for extrapolated results. These results are in agreement with convergence theorems proved recently for HWDM in [31, 32]. The obtained results coincide also with the results given in [8] achieved by applying the differential quadrature method (DQM).

Acknowledgement: The research was supported by the Estonian Centre of Excellence in Zero Energy and Resource Efficient Smart Buildings and Districts, ZEBE, grant TK146 funded by the European Regional De-

velopment Fund; Innovative Manufacturing Engineering Systems Competence Centre IMECC and Enterprise Estonia (EAS) and co-financed by European Union Regional Development Fund (project EU48685); Estonian Research Council grant PUT1300.

References

- [1] Aksencer T., Aydogdu M., [Forced transverse vibration of nanoplates using nonlocal elasticity](#), *Physica E* 2012, 44, 1752–1759
- [2] Ansari R., Pourashraf T., Gholam R., An exact solution for the nonlinear forced vibration of functionally graded nanobeams in thermal environment based on surface elasticity theory, *Thin-Walled Struct.*, 2015, 93, 169–176
- [3] Aydogdu M., A general nonlocal beam theory: Its application to nanobeam bending, buckling and vibration, *Physica E* 2009, 41, 1651–1655
- [4] Aydogdu M., Elishakoff I., On the vibration of nanorods restrained by a linear spring in-span, *Mech. Res. Com.*, 2014, 57, 90–96.
- [5] Aydogdu M., Axial vibration analysis of nanorods (carbon nanotubes) embedded in an elastic medium using nonlocal elasticity, *Mech. Res. Com.* 2012, 43, 34–40
- [6] Aziz I., Islam S.U., Khana F., A new method based on Haar wavelet for the numerical solution of two-dimensional nonlinear integral equations, *J. Comput. Appl. Math.*, 2014, 272, 70–80
- [7] Aziz I., Islam S.U., New algorithms for the numerical solution of nonlinear Fredholm and Volterra integral equations using Haar wavelets, *J. Comput. Appl. Math.*, 2013, 239(1), 333–345
- [8] Behera L., Chakraverty S., Application of Differential Quadrature method in free vibration analysis of nanobeams based on various nonlocal theories, *Comput. Math. App.*, 2015, 69, 1444–1462.
- [9] Castro LMS., Ferreira AJM., Bertoluzza S., Batra RC., Reddy JN., A wavelet collocation method for the static analysis of sandwich plates using a layerwise theory, *Compos. Struct.*, 2010, 92(8), 1786–1792
- [10] Cattani C., Harmonic wavelets toward the solution of nonlinear PDE, *Comput. Math. Appl.*, 2005, 50, 1191–1210
- [11] Chakraverty S., Behera L., Free vibration of rectangular nanoplates using Rayleigh-Ritz method, *Physica E*, 2014, 56, 357–363
- [12] Chen CF., Hsiao CH., Haar wavelet method for solving lumped and distributed-parameter systems, *IEE Proc. Contr. Theor. Appl.*, 1997, 144(1), 87–94
- [13] Eltahir MA., Emam S.A., Mahmoud FF., Static and stability analysis of nonlocal functionally graded nanobeams, *Compos. Struct.*, 2013, 96, 82–88
- [14] Eringen A.C., On differential equations of nonlocal elasticity and solutions of screw dislocation and surface waves, *J. App. Phys.*, 1983, 54, 4703–4710
- [15] Hariharan G., Kannan K., [Review of wavelet methods for the solution of reaction-diffusion problems in science and Engineering](#), *Appl. Math. Model.* 2014, 38(3), 799–813
- [16] Hein H., Feklistova L., [Computationally efficient delamination detection in composite beams using Haar wavelets](#), *Mech. Syst. Signal. Pr.*, 2011, 25(6), 2257–2270
- [17] Heydari MH., Hooshmandasl MR., Mohammadi F., Cattani, C., Wavelets method for solving systems of nonlinear singular fractional Volterra integro-differential equations, *Communications in Nonlinear Science and Numerical Simulation*, 2014, 19(1), 37–48
- [18] Hsiao CH., A Haar wavelets method of solving differential equations characterizing the dynamics of a current collection system for an electric locomotive, *Appl. Math. Comp.*, 2015, 265, 928–935
- [19] Jin G., Xie X., Liu Z., [The Haar wavelet method for free vibration analysis of functionally graded cylindrical shells based on the shear deformation theory](#), *Compos. Struct.* 2014, 108, 435–448
- [20] Jin G., Xie X., Liu Z., Free vibration analysis of cylindrical shells using the Haar wavelet method, *Int. J. Mech. Sci.* 2013, 77, 47–56
- [21] Lepik Ü., Numerical solution of differential equations using Haar wavelets, *Math. Comput. Simulat.*, 2005, 68, 127–143
- [22] Lepik Ü., [Solving PDEs with the aid of two dimensional Haar wavelets](#), *Comput. Math. Appl.*, 2011, 61, 1873–1879
- [23] Lepik Ü., [Numerical solution of evolution equations by the Haar wavelet method](#), *Appl. Math. Comput.*, 2007, 185, 695–704
- [24] Lepik Ü., Application of the Haar wavelet transform to solving integral and differential Equations, *Proc. Est. Acad. Sci. Phys. Math.*, 2007, 56(1), 28–46
- [25] Lepik Ü., Haar wavelet method for nonlinear integro-differential equations, *Appl. Math. Comput.*, 2006, 176, 324–333
- [26] Lepik Ü., [Solving fractional integral equations by the Haar wavelet method](#), *Appl. Math. Comput.*, 2009, 214(2), 468–478
- [27] Lepik Ü., Hein H., Application of the Haar wavelet method for solution the problems of mathematical calculus, *Waves Wavelets Fractals, Adv. Anal.*, 2015, 1, 1–16
- [28] Lepik Ü., Hein H., Haar wavelets: with applications, New York, Springer, 2014
- [29] Majak J., Pohlak M., Eerme M., Application of the Haar Wavelet-based discretization technique to problems of orthotropic plates and shells, *Mech. Compos. Mater.*, 2009, 45(6), 631–642

- [30] Majak J., Pohlak M., Eerme M., Lepikult T., Weak formulation based Haar wavelet method for solving differential equations, *Appl. Math. Comput.* 2009, 211(2), 488–494
- [31] Majak J., Shvartsman BS., Kirs M., Pohlak M., Herranen H., *Compos. Struct.*, 2015, 126, 227–232
- [32] Majak J., Shvartsman BS., Karjust K., Mikola M., Haavajõe A., Pohlak M., *Composites Part B: Engineering*, 2015, 80, 321–327
- [33] Malekzadeh P., Shojaee M., Free vibration of nanoplates based on a nonlocal two-variable refined plate theory, *Compos. Struct.*, 2013, 95, 443–452
- [34] Malekzadeh P., Setoodeh AR., Beni AA., Small scale effect on the free vibration of orthotropic arbitrary straight sided quadrilateral nanoplates, *Compos., Struct.*, 2011, 93(7), 1631–1639
- [35] Marchuk GI., Shaidurov VV., *Difference Methods and Their Extrapolations*, Springer, Berlin, 1983
- [36] Patra A., Ray SS., A numerical approach based on Haar wavelet operational method to solve neutron point kinetics equation involving imposed reactivity insertions, *Ann. Nucl. Energy*, 2014, 68, 112–117
- [37] Ravari MRK., Shahidi AR., Axisymmetric buckling of the circular annular nanoplates using finite difference method, *Meccanica*, 2013, 48(1), 135–144
- [38] Ray SS., Patra A., Numerical simulation based on Haar wavelet operational method to solve neutron point kinetics equation involving sinusoidal and pulse reactivity, *Ann. Nucl. Energy*, 2014, 73, 408–412
- [39] Ray SS., Patra A., Numerical simulation for fractional order stationary neutron transport equation using Haar wavelet collocation method, *Nucl. Eng. Des.*, 2014, 278, 71–85
- [40] Ray SS., Patra A., Two-dimensional Haar wavelet Collocation Method for the solution of Stationary Neutron Transport Equation in a homogeneous isotropic medium, *Ann. Nucl. Energy*, 2014, 70, 30–35
- [41] Ray SS., Patra A., Haar wavelet operational methods for the numerical solutions of fractional order nonlinear oscillatory Van der Pol system, *Appl. Math. Comput.*, 2013, 220, 659–667
- [42] Reddy JN., El-Borgi S., Romanoff J., Non-linear analysis of functionally graded microbeams using Eringen's non-local differential model, *Int. J. Non-Lin. Mech.*, 2014, 67, 308–318
- [43] Saeed U., Rejman M., Iqbal MA., Haar wavelet-Picard technique for fractional order nonlinear initial and boundary value problems, *Sci. Res. Essays*. 2014, 9(12), 571–580
- [44] Saeedi H., Mollahasani N., Moghadam M., Chuev G., An operational Haar wavelet method for solving fractional Volterra integral equations, *Int. J. Appl. Math. Comput. Sci.* 2011, 21(3), 535–547
- [45] Shvartsman BS., Majak J., Numerical method for stability analysis of functionally graded beams on elastic foundation, *Appl. Math. Mod.*, 40 (4–5), 3713–3719
- [46] Xie X., Jin G., Li W., Liu Z., A numerical solution for vibration analysis of composite laminated conical, cylindrical shell and annular plate structures, *Compos. Struct.*, 2014, 111, 20–30
- [47] Xie X., Jin G., Yan Y., Shi SX., Liu Z., Free vibration analysis of composite laminated cylindrical shells using the Haar wavelet method, *Compos. Struct.*, 2014, 109, 169–177
- [48] Xie X., Jin G., Ye T., Liu Z., Free vibration analysis of functionally graded conical shells and annular plates using the Haar wavelet method, *Appl. Acoust.*, 2014, 85, 130–142

PUBLICATION III

Majak, J., Shvartsman, B., Kirs, M., Pohlak, M., Herranen, H. (2015). Convergence theorem for the Haar wavelet based discretization method. *Composite Structures*, 126, 227–232.



Convergence theorem for the Haar wavelet based discretization method



J. Majak^{a,*}, B.S. Shvartsman^b, M. Kirs^a, M. Pohlak^a, H. Herranen^a

^a Dept. of Machinery, Tallinn University of Technology, 19086 Tallinn, Estonia

^b Estonian Entrepreneurship University of Applied Sciences, 11415 Tallinn, Estonia

ARTICLE INFO

Article history:

Available online 25 February 2015

Keywords:

Haar wavelet method
Accuracy issues
Convergence theorem
Numerical evaluation of the order of convergence
Extrapolation

ABSTRACT

The accuracy issues of Haar wavelet method are studied. The order of convergence as well as error bound of the Haar wavelet method is derived for general n th order ODE. The Richardson extrapolation method is utilized for improving the accuracy of the solution. A number of model problems are examined. The numerically estimated order of convergence has been found in agreement with convergence theorem results in the case of all model problems considered.

© 2015 Elsevier Ltd. All rights reserved.

1. Introduction

Nowadays, the Haar wavelets are most widely used wavelets for solving differential and integro-differential equations, outperforming Legendre, Daubechie, etc. wavelets (Elsevier scientific publication statistics). Prevalent attention on Haar wavelet discretization methods (HWDM) can be explained by their simplicity. The Haar wavelets are generated from pairs of piecewise constant functions and can be simply integrated. Furthermore, the Haar functions are orthogonal and form a good transform basis.

Obviously, the Haar functions are not differentiable due to discontinuities in breaking points. As pointed out in [1] there are two main possibilities to overcome latter shortcomings. First, the quadratic waves can be regularized (“smoofted”) with interpolating splines, etc. [2,3]. Secondly, an approach proposed by Chen and Hsiao in [4,5], according to which the highest order derivative included in the differential equation is expanded into the series of Haar functions, can be applied. Latter approach is applied successfully for solving differential and integro-differential equations in most research papers covering HWDM [1,4–28]. Following the pioneering works Chen and Hsiao in [4,5] Lepik developed the HWDM for solving wide class of differential, fractional differential and integro-differential equations covering problems from elastostatics, mathematical physics, nonlinear oscillations, evolution equations [1,6–10]. The results are summarized in monograph [11]. It is pointed out by Lepik in [1,11] that the HWDM is convenient for solving boundary value problems, since the boundary

conditions can be satisfied automatically (simple analytical approach).

Composite structures are examined by use of wavelets first in [12,2]. In [12] the free vibration analysis of the multilayer composite plate is performed by adapting HWDM. The static analysis of sandwich plates using a layerwise theory and Daubechie's wavelets is presented in [2]. The delamination of the composite beam is studied in [13]. During last year Xiang et al. adapted HWDM for free vibration analysis of functionally graded composite structures [14–18]. In [14–18] a general approach for handling boundary conditions has been proposed. In all above listed studies the Haar wavelet direct method is applied. The weak form based HWDM has been developed in [19], where the complexity analysis of the HWDM has been performed. Recent studies in area of wavelet based discretization methods cover solving fractional partial differential equations by use of Haar, Legendre and Chebyshev wavelets [20–25]. In [26–28] the Haar wavelets are utilized for solving nuclear reactor dynamics equations. The neutron point kinetics equation with sinusoidal and pulse reactivity is studied in [26]. In [27,28] are solved neutron particle transport equations. In [29–31] the HWDM is employed with success for solving nonlinear integral and integro-differential equations.

Most of papers overviewed above found that the implementation of the HWDM is simple. Also, the HWDM is characterized most commonly with terms „simple”, “easy” and “effective” (see [1,14–18,25–28] and others). The review paper [32] concludes that the HWDM is efficient and powerful in solving wide class of linear and nonlinear reaction–diffusion equations.

However, no convergence rate proof found in literature for this method. It is shown in several papers [33–35] that in the case of

* Corresponding author.

E-mail address: juri.majak@ttu.ee (J. Majak).

function approximation with direct expansion into Haar wavelets, the convergence rate is one. This result hold good for function approximation in integral equations, but does not hold good for HWDM developed for differential equations above, since in these methods instead of the solution its higher order derivative is expanded into wavelets.

The aim of the current study is to clarify the accuracy issues of the HWDM, based on approach introduced by Chen and Hsiao in [4,5], and featured for solving general n th order ordinal differential equations (ODE). This question is open from 1997 up to now. Answer to this question allows to give scientifically founded estimate to HWDM, also to make comparisons with other methods.

2. Haar wavelet family

In the following the Haar wavelet family is defined by using notation introduced by Lepik [1]. Let us assume that the integration domain $[A, B]$ is divided into $2M$ equal subintervals each of length $\Delta x = (B - A)/(2M)$. The maximal level of resolution J is defined as $M = 2^J$. The Haar wavelet family $h_i(x)$ is defined as a group of square waves with magnitude ± 1 in some intervals and zero elsewhere

$$h_i(x) = \begin{cases} 1 & \text{for } x \in [\xi_1(i), \xi_2(i)], \\ -1 & \text{for } x \in [\xi_2(i), \xi_3(i)], \\ 0 & \text{elsewhere,} \end{cases} \tag{1}$$

where

$$\begin{aligned} \xi_1(i) &= A + 2k\mu\Delta x, & \xi_2(i) &= A + (2k + 1)\mu\Delta x, \\ \xi_3(i) &= A + 2(k + 1)\mu\Delta x, & \mu &= M/m, \quad \Delta x = (B - A)/(2M). \end{aligned} \tag{2}$$

In Eqs. (1) and (2) $j = 0, 1, \dots, J$ and $k = 0, 1, \dots, m - 1$ stand for dilatation and translations parameters, respectively. The index i is calculated as $i = m + k + 1$. Each Haar function contains one square wave, except scaling function $h_1(x) \equiv 1$. The parameter $m = 2^j$ ($M = 2^J$) corresponds to a maximum number of square waves can be sequentially deployed in interval $[A, B]$ and the parameter k indicates the location of the particular square wave. Since the scaling function $h_1(x) \equiv 1$ does not include any waves here $m = 0, \xi_1 = A, \xi_2 = \xi_3 = B$. The Haar functions are orthogonal to each other and form a good transform basis

$$\int_0^1 h_l(x)h_i(x)dt = \begin{cases} 2^{-j} & i = l = 2^j + k, \\ 0 & i \neq l. \end{cases} \tag{3}$$

Any function $f(x)$ that is square integrable and finite in the interval $[A, B]$ can be expanded into a Haar wavelets as

$$f(x) = \sum_{i=1}^{\infty} a_i h_i(x). \tag{4}$$

The Haar coefficients

$$a_i = 2^j \int_A^B f(x)h_i(x)dx, \quad i = 1, \dots, 2^j + k + 1 \tag{5}$$

can be determined from minimum condition of integral square error as

$$\int_A^B E_M^2 dx \rightarrow \min, \quad |E_M| = |f(x) - f_M(x)|, \quad f_M(x) = \sum_{i=0}^{2M} a_i h_i(x). \tag{6}$$

In Eq. (5) $f(x)$ and $f_M(x)$ stand for the exact and approximate solutions, respectively. The integrals of the Haar functions (1) of order n can be calculated analytically as [1]

$$p_{n,i}(x) = \begin{cases} 0 & \text{for } x \in [A, \xi_1(i)], \\ \frac{(x - \xi_1(i))^n}{n!} & \text{for } x \in [\xi_1(i), \xi_2(i)], \\ \frac{(x - \xi_1(i))^n - 2(x - \xi_2(i))^n}{n!} & \text{for } x \in [\xi_2(i), \xi_3(i)], \\ \frac{(x - \xi_1(i))^n - 2(x - \xi_2(i))^n + (x - \xi_3(i))^n}{n!} & \text{for } x \in [\xi_3(i), B]. \end{cases} \tag{7}$$

Note that the integrals of the Haar functions are continuous functions in interval $[A, B]$. Also, the first integrals of the Haar functions are triangular functions ($\alpha = 1$).

3. Convergence analysis of Haar wavelet discretization method

Let us consider n th order ordinal differential equation (ODE) in general form

$$G(x, u, u', u'', \dots, u^{(n-1)}, u^{(n)}) = 0, \tag{8}$$

where prime stand for derivative with respect to x . According to most commonly used approach introduced in [4,5] instead of solution of the differential equation its higher order derivative is expanded into Haar wavelets

$$f(x) = \frac{d^n u(x)}{dx^n} = \sum_{i=1}^{\infty} a_i h_i(x). \tag{9}$$

Using notation introduced in previous section, the sum in Eq. (9) can be rewritten as

$$f(x) = a_1 h_1 + \sum_{j=0}^{\infty} \sum_{k=0}^{2^j-1} a_{2^j+k+1} h_{2^j+k+1}(x). \tag{10}$$

In Eqs. (9) and (10) $i = m + k + 1, j = 0, 1, \dots, J, k = 0, 1, \dots, m - 1, m = 2^j$ ($M = 2^J$). By integrating relation (9) n times one obtains the solution of the differential equation (8) as

$$u(x) = \frac{a_1(B - A)^n}{n!} + \sum_{j=0}^{\infty} \sum_{k=0}^{2^j-1} a_{2^j+k+1} p_{n,2^j+k+1}(x) + B_T(x). \tag{11}$$

In Eq. (11) $B_T(x)$ and $p_{n,2^j+k+1}(x)$ stand for boundary term and n th order integrals of the Haar functions are determined by formula (7), respectively.

Without loss of generality it can be assumed in the following that $A = 0, B = 1$ since the differential equations can be converted into non-dimensional form by use of transform $\tau = (x - A)/(B - A)$ i.e. $x = A + (B - A)\tau$ (see [19]).

Theorem 1. *Let us assume that $f(x) = \frac{d^n u(x)}{dx^n} \in L^2(R)$ is a continuous function on $[0, 1]$ and its first derivative is bounded*

$$\forall x \in [0, 1] \quad \exists \eta : \left| \frac{df(x)}{dx} \right| \leq \eta, \quad n \geq 2 \text{ (boundary value problems)}. \tag{12}$$

Then the Haar wavelet method, based on approach proposed in [4,5], will be convergent i.e. $|E_M|$ vanishes as J goes to infinity. the convergence is of order two

$$\|E_M\|_2 = O\left[\left(\frac{1}{2^{J+1}}\right)^2\right]. \tag{13}$$

Proof. It implies from Eqs. (5), (6) and (10) The error at the J th level resolution can be written as

$$|E_M| = |u(x) - u_M(x)| = \left| \sum_{j=J+1}^{\infty} \sum_{k=0}^{2^j-1} a_{2^j+k+1} p_{n,2^j+k+1}(x) \right|. \tag{14}$$

Expanding quadrate of the L^2 -norm of error function, one obtains

$$\begin{aligned} \|E_M\|_2^2 &= \int_0^1 \left(\sum_{j=1}^{\infty} \sum_{k=0}^{2^j-1} a_{2^j+k+1} p_{n,2^j+k+1}(x) \right)^2 dx \\ &= \sum_{j=1}^{\infty} \sum_{k=0}^{2^j-1} \sum_{r=j+1}^{\infty} \sum_{s=0}^{2^r-1} a_{2^j+k+1} a_{2^r+s+1} \int_0^1 p_{n,2^j+k+1}(x) p_{n,2^r+s+1}(x) dx. \end{aligned} \tag{15}$$

In order to estimate complex expression (15) it is reasonable first to derive estimates for its components: the coefficients a_i and the integrals of the Haar wavelets $p_{n,i}(x)$. By use of and formulas (5) and (1) the coefficients a_i ($i = 2^j + k + 1$) can be evaluated as

$$\begin{aligned} a_i &= 2^j \int_0^1 f(x) h_i(x) dx = 2^j \left[\int_{\xi_1}^{\xi_2} f(x) dx - \int_{\xi_2}^{\xi_3} f(x) dx \right] \\ &= 2^j [(\xi_2 - \xi_1) f(\xi_1) - (\xi_3 - \xi_2) f(\xi_2)]. \end{aligned} \tag{16}$$

In Eq. (16) $\xi_1 \in (\xi_1, \xi_2)$ and $\xi_2 \in (\xi_2, \xi_3)$. It follows from Eq. (2) that $\xi_2 - \xi_1 = \xi_3 - \xi_2 = 1/(2m) = 1/(2^{j+1})$ and the expression for coefficients a_i in Eq. (16) can be reduced to

$$a_i = \frac{1}{2} [f(\xi_1) - f(\xi_2)] = \frac{1}{2} (\xi_1 - \xi_2) \frac{df}{dx}(\xi), \quad \xi \in (\xi_1, \xi_2). \tag{17}$$

It implies from Eq. (17) and assumption (12) of the theorem that

$$a_i \leq \eta \frac{1}{2^{j+1}}. \tag{18}$$

Note that there are no significant differences in estimation of coefficients in cases where function itself of its n th order derivative is expanded into Haar wavelets. The formula (18) is in accordance with the results obtained in [36].

However, the function estimation is principally different, since the integrals of the Haar wavelets $p_{n,i}(x)$ are not orthogonal i.e. all terms in Eq. (15) should be considered. Before direct estimation of the integral $\int_0^1 p_{n,2^j+k+1}(x) p_{n,2^r+s+1}(x) dx$ it is reasonable to derive estimates on the integrals of the Haar wavelets $p_{n,i}(x)$. It is assumed in the following that $n \geq 2$ (boundary value problems). Particular case $n = 1$ needs little different approach but leads to the same order of convergence (studied by authors in [38]). Let us proceed from formula (7) and derive upper bound of the function $p_{n,i}(x)$ in each subinterval. First note that the function $p_{n,i}(x) \equiv 0$ for $x \in [0, \xi_1(i)]$.

In the interval $x \in [\xi_1(i), \xi_2(i)]$ the function $p_{n,i}(x)$ is monotonically increasing (power law). Thus, the upper bound value of the function $p_{n,i}(x)$ is reached at $x = \xi_2(i)$ as follows (see Eqs. (2) and (7))

$$\begin{aligned} p_{n,i}(x) = p_{n,2^j+k+1} &\leq \frac{[\xi_2(i) - \xi_1(i)]^n}{n!} = \frac{1}{n!} \left(\frac{1}{2^{j+1}} \right)^n, \quad x \\ &\in [\xi_1(i), \xi_2(i)]. \end{aligned} \tag{19}$$

In the interval $x \in [\xi_2(i), \xi_3(i)]$ the function $p_{n,i}(x)$ is monotonically increasing if

$$x \leq \xi_2 + (\xi_3 - \xi_2) \left[\frac{1}{2^{1/m-1}} - 1 \right]. \tag{20}$$

The inequality (20) can be derived from formulas (2) and (7) and condition $\frac{dp_{n,i}(x)}{dx} > 0$. Since the right hand size of the inequality (20) is greater or equal to ξ_3 for considered values of parameter $n(n \geq 2)$ it can be stated that the function $p_{n,i}(x)$ has a maximum at $x = \xi_3(i)$ in the interval $x \in [\xi_2(i), \xi_3(i)]$. The maximum value of

the function $p_{n,i}(x)$ can be obtained by substituting $x = \xi_3(i)$ in Eq. (7) as

$$p_{n,i}(x) = p_{n,2^j+k+1} \leq \frac{2^n - 2}{n!} \left(\frac{1}{2^{j+1}} \right)^n, \quad x \in [\xi_2(i), \xi_3(i)]. \tag{21}$$

In the interval $x \in [\xi_3(i), 1]$ the function $p_{n,i}(x)$ can be expanded as (see formula (7))

$$p_{n,i}(x) = \frac{1}{n!} \sum_{k=2}^n \binom{n}{k} (x - \xi_2)^{n-k} \left[\left(\frac{1}{2^{j+1}} \right)^k + \left(\frac{-1}{2^{j+1}} \right)^k \right]. \tag{22}$$

Obviously, all terms in sum (22) corresponding to the odd values of the parameter k are equal to zero and the function $p_{n,i}(x)$ has a maximum at $x = 1$. Thus, denoting $n_1 = \text{floor}(n/2)$, considering that $k!(n-k)! \geq (n_1!)^2$ and applying geometric progression formulas one obtains estimate on $p_{n,i}(x)$ as

$$p_{n,i}(x) = p_{n,2^j+k+1} \leq \frac{8}{3} \frac{1}{(n_1!)^2} \left(\frac{1}{2^{j+1}} \right)^2, \quad x \in [\xi_3(i), 1]. \tag{23}$$

The function $p_{n,i}(x)$ is monotonically increasing in interval $[0, 1]$, since it is monotonically increasing in each subinterval of $[0, 1]$ as shown above. Furthermore, the upper bound of the function $p_{n,i}(x)$ in interval $[0, 1]$ is determined by inequality equation (23).

Next the quadrate of the L^2 -norm of error function can be estimated. Inserting Eq. (18) in Eq. (15) one obtains

$$\|E_M\|_2^2 \leq \eta^2 \sum_{j=1}^{\infty} \sum_{k=0}^{2^j-1} \sum_{r=j+1}^{\infty} \sum_{s=0}^{2^r-1} \frac{1}{2^{j+1}} \frac{1}{2^{r+1}} \int_{\xi_1}^1 p_{n,2^j+k+1}(x) p_{n,2^r+s+1}(x) dx. \tag{24}$$

Introducing the following notation

$$C_n = \frac{8}{3} \frac{1}{(n_1!)^2}, \tag{25}$$

one can express the estimates on upper bounds of the integrals of Haar wavelets $p_{n,2^j+k+1}(x)$ and $p_{n,2^r+s+1}(x)$ as

$$p_{n,2^j+k+1}(x) \leq C_n \left(\frac{1}{2^{j+1}} \right)^2, \quad p_{n,2^r+s+1}(x) \leq C_n \left(\frac{1}{2^{r+1}} \right)^2. \tag{26}$$

The coefficient C_n depends on order of the differential equation only, not on level of the resolution.

Inserting Eq. (26) in Eq. (24) yields

$$\begin{aligned} \|E_M\|_2^2 \Big|_{j=s} &\leq \eta^2 C_n^2 \sum_{j=1}^{\infty} \sum_{r=j+1}^{\infty} \left(\frac{1}{2^{j+1}} \right)^3 \left(\frac{1}{2^{r+1}} \right)^3 2^{2r} (1 - \xi_1) \\ &\leq \frac{1}{36} \eta^2 C_n^2 \left(\frac{1}{2^{j+1}} \right)^4. \end{aligned} \tag{27}$$

Based on Eq. (27) it can be stated that the convergence of the Haar wavelet method considered is of order two, since the integration domain is divided into $2M = 2^{j+1}$ equal subintervals i.e.

$$\|E_M\|_2 = O \left[\left(\frac{1}{2^{j+1}} \right)^2 \right], \tag{28}$$

The error bound can be expressed as

$$\|E_M\|_2 \leq \frac{\eta C_n}{6} \left(\frac{1}{2^{j+1}} \right)^2 = \frac{4}{9} \frac{\eta}{(\text{floor}(n/2))^2} \left(\frac{1}{2^{j+1}} \right)^2. \tag{29}$$

The theorem is proved. \square

4. Numerical validation of the rate of convergence and extrapolation of results

In the following the analytical formulas are provided for numerical estimation of the order of convergence and extrapolation of the results.

4.1. Theoretical background

Let us consider the asymptotic error expansion in powers of the step size h as

$$F(h) - F(0) = \alpha h^k + O(h^l), \quad 0 < k < l. \tag{30}$$

Here $F(h)$ denote the value obtained by any numerical method with step size h , $F(0)$ is an unknown exact value, α is unknown constant independent on h and k is theoretical order of accuracy of the numerical method. Such expansions have been proven for a wide range of finite difference and finite element solutions [36].

Denote two numerical solutions found on nested grids h_{i-1} , $h_i = h_{i-1}/2$ as follows $F_{i-1} = F(h_{i-1})$, $F_i = F(h_i)$. Applying (30) for these solutions one can write the following equality

$$\begin{aligned} F_{i-1} - F(0) &= \alpha h_{i-1}^k + O(h_{i-1}^l), \\ F_i - F(0) &= \alpha h_i^k + O(h_i^l). \end{aligned} \tag{31}$$

By taking a linear combination of these two solutions, one can obtain the error estimate as

$$F(0) - F_i = \frac{F_i - F_{i-1}}{2^k - 1} + O(h_i^l) \tag{32}$$

or another approximation of the value $F(0)$ as

$$R_i = F_i + \frac{F_i - F_{i-1}}{2^k - 1} = F(0) + O(h_i^l). \tag{33}$$

This formula is simple Richardson extrapolation formula [36,37]. In other words, the approximate solutions R_i have error with higher order in relation to h than F_i . Therefore, if numerical solutions of the problem for two grids and the theoretical order of accuracy k of the numerical method are known, a simple linear extrapolation formula (33) eliminates the leading term from error expansion equation (30) and leads to reasonably accurate results [36,37]. The Richardson extrapolation is an efficient method for error estimation and increase the accuracy of finite difference and finite element solutions of different problems of mathematical physics.

On the other hand, if exact solution $F(0)$ is known, Eq. (31) give simple method for estimating the order of convergence of numerical method as

$$\begin{aligned} \frac{F_{i-1} - F(0)}{F_i - F(0)} &= 2^k + O(h_i^{l-k}), \quad k \approx k_i^E \\ &= \log \left(\frac{F_{i-1} - F(0)}{F_i - F(0)} \right) / \log(2). \end{aligned} \tag{34}$$

In practice, the order of convergence of numerical method can be estimated even when the exact solution $F(0)$ is unknown. In latter case, the theoretical order of accuracy can be estimated using three solutions on a sequence of nested grids F_{i-2} , F_{i-1} , F_i , $h_{i-2}/h_{i-1} = h_{i-1}/h_i = 2$. The following ratio can be obtained from three equations similar to Eq. (34):

$$\lambda_i = \frac{F_{i-2} - F_{i-1}}{F_{i-1} - F_i} = 2^k + O(h_i^{l-k}). \tag{35}$$

Further, from Eq. (35) the theoretical order of accuracy k can be easily estimated [37]:

$$k \approx k_i = \log(\lambda_i) / \log(2). \tag{36}$$

Here k_i is a value of observed order of accuracy and Eq. (36) gives experimental method for determining or verifying the value of theoretical order of accuracy k of the numerical method. Obviously, Eq. (36) can be used only for $\lambda_i > 0$, i.e. three successive values F_{i-2} , F_{i-1} , F_i must be monotonic. The proximity of obtained values of the ratio λ_i or observed order of accuracy k_i respectively to theoretical values 2^k or k is a confirmation of asymptotic error expansion (30) with leading term αh^k .

Moreover, the following formula can be used to estimate the order of convergence of the improved values R_i :

$$l \approx l_i = \log \left(\frac{R_{i-2} - R_{i-1}}{R_{i-1} - R_i} \right) / \log(2). \tag{37}$$

This formula follows from Eq. (33) and can be obtained similarly to Eq. (36). In the next sections the order of convergence of the HWDM is evaluated numerically in the case of three model problems.

4.2. Free transverse vibrations of the orthotropic rectangular plates of variable thickness

In the current section the order of convergence of the HWDM treated by author in [12] is examined. Assuming that the principal directions of orthotropy coincide with natural co-ordinate system one can represent the equation of motion governing natural vibration of a thin orthotropic rectangular plate as

$$\begin{aligned} D_x \frac{\partial^4 w}{\partial x^4} + D_y \frac{\partial^4 w}{\partial y^4} + 2T \frac{\partial^4 w}{\partial x^2 \partial y^2} + 2 \frac{\partial T}{\partial x} \frac{\partial^3 w}{\partial x \partial y^2} + 2 \frac{\partial T}{\partial y} \frac{\partial^3 w}{\partial y \partial x^2} \\ + 2 \frac{\partial D_x}{\partial x} \frac{\partial^3 w}{\partial x^3} + 2 \frac{\partial D_y}{\partial y} \frac{\partial^3 w}{\partial y^3} + 2 \frac{\partial^2 D_x}{\partial x^2} \frac{\partial^2 w}{\partial x^2} + 2 \frac{\partial^2 D_y}{\partial y^2} \frac{\partial^2 w}{\partial y^2} \\ + \frac{\partial^2 D}{\partial y^2} \frac{\partial^2 w}{\partial x^2} + \frac{\partial^2 D}{\partial x^2} \frac{\partial^2 w}{\partial y^2} + 4 \frac{\partial^2 D_{xy}}{\partial x \partial y} \frac{\partial^2 w}{\partial y \partial x} = -\rho \gamma \frac{\partial^2 w}{\partial t^2} - kw, \end{aligned} \tag{38}$$

where

$$\begin{aligned} D_x = E_x^* \gamma^3 / 12, \quad D_y = E_y^* \gamma^3 / 12, \quad D_{xy} = G_{xy} \gamma^3 / 12, \quad D = E^* \gamma^3 / 12, \\ T = D + 2D_{xy}, \quad E_x^* = \frac{E_x}{1 - \nu_x \nu_y}, \quad E_y^* = \frac{E_y}{1 - \nu_x \nu_y}, \quad E^* = \nu_y E_x^* = \nu_x E_y^*. \end{aligned} \tag{39}$$

In Eqs. (38) and (39) ν is a Poisson's ratio, D and E stand for flexural rigidity and modulus of elasticity, respectively. The transverse deflection of the plate and variable plate thickness are denoted by $w = w(t, x, y)$ and $\gamma = \gamma(x)$, respectively. The variables ρ and k stand for the mass density and the modulus of a Winkler type foundation, respectively. It is assumed that the edges of the plate are simply supported along $y = 0$, $y = b$ and the other two edges ($x = 0$, $x = a$) are clamped or simply supported. According to the Lévi approach the time-harmonic-dependent solution can be expanded as

$$w(t, x, y) = w_n(x) \sin(n\pi y/b) e^{i\omega t}. \tag{40}$$

In Eq. (40) ω is the harmonic frequency, n - positive number and $i = \sqrt{-1}$. The system (38)–(40) can be written in terms of non-dimensional variables as

$$\begin{aligned} W_n^{IV} + \frac{6\bar{\gamma}^2 \bar{\gamma}'}{\bar{\gamma}^3} W_n''' + \left[\frac{3(\bar{\gamma} \bar{\gamma}'' + 2\bar{\gamma}'^2)}{\bar{\gamma}^2} - 2\alpha \lambda^2 \right] W_n'' - \eta \alpha^2 \frac{6\bar{\gamma}^2 \bar{\gamma}'}{\bar{\gamma}^3} W_n' \\ + \frac{E_y^*}{E_x^*} \left[\alpha^4 - \frac{3(\bar{\gamma} \bar{\gamma}'' + 2\bar{\gamma}'^2)}{\bar{\gamma}^2} \alpha^2 \nu_x - \Omega^2 \frac{\gamma_0^2}{\bar{\gamma}^2} + 12K/\bar{\gamma}^3 \right] W_n = 0, \end{aligned} \tag{41}$$

where prime denotes derivative with respect to τ and

Table 1
Numerical results for Ω . Simply supported plate (all sides).

j	Fund. freq.	Extrap_res	k_i	k_i^E	l_i
3	48.655448				
4	48.651658	48.650394		2.007	
5	48.650716	48.650402	2.009	2.002	
6	48.650481	48.650402	2.002	2.000	4.001
7	48.650422	48.650402	2.001	2.000	4.000
8	48.650407	48.650402	2.000	2.000	4.000

$$\tau = \frac{x}{a}, \quad W_n = \frac{w_n}{\gamma}, \quad \bar{\gamma} = \frac{\gamma}{a}, \quad \lambda = \frac{n\pi a}{b}, \quad \eta = \frac{E^* + 2G_{xy}}{E_x^*},$$

$$K = \frac{ka}{E_y}, \quad \Omega^2 = \frac{12\rho a^2 \omega^2}{E_y \gamma_0^2}. \quad (42)$$

In Eqs. (41) and (42) γ_0 stands for the thickness of the plate at $\tau = 0$. According to the HWDM considered the higher order derivative included in ODE (41) is expanded into Haar wavelets as

$$\frac{d^4 W_n}{d\tau^4} = a^T H, \quad (43)$$

where a^T is unknown coefficient vector. The numerical results for fundamental frequency of the orthotropic rectangular plates of variable thickness are given in Table 1 (all sides simply supported) and Table 2 (simply supported along $y = 0, y = b$, clamped along $x = 0, x = a$).

In Tables 1 and 2 the j is the value of resolution (see section 2, $m = 2^j$). The second and third columns contain the values of the fundamental frequency and its extrapolation performed by formula (33), respectively. The orders of convergence k_i and k_i^E given in columns four and five of Tables 1 and 2 are computed by formulas (36) and (34), respectively. Obviously, both orders of the convergence have limit value two. Latter results are in accordance with convergence theorem proved above. It can be seen from Tables 1 and 2 that the order of convergence computed with use of the exact solution converges faster to two (column five) in the case of both boundary conditions considered. The order of convergence of the extrapolated results given in last column of the Tables 1 and 2 is equal to four (see Eq. (37)). Thus, the fundamental frequencies with improved accuracy have higher order of convergence equal to four.

4.3. Second, fourth and sixth order eigenvalue problems considered by Shi and Cao [38]

In the current section the order of convergence of the HWDM introduced by Shi and Cao in [38] is examined. Let us consider first the following second-order eigenvalue problem

$$-y'' + (\cos(x) + 2\cos(2x) + 3\cos(3x))y = \lambda y, \quad y(0, \lambda) = y(\pi, \lambda) = 0. \quad (44)$$

The orders of convergence calculated on results given in [38] are presented in Table 3.

The structure of Table 3 coincide with that of Tables 1 and 2 i.e. the columns contain the same parameters. In can be seen from Table 3 that the computed rates of convergence have values near

Table 2
Numerical results for Ω . Simply supported-clamped plate.

j	Fund. freq.	Extrap.res.	k_i	k_i^E	l_i
3	61.172805				
4	61.172392	61.172254		1.557	
5	61.172236	61.172184	1.407	1.903	
6	61.172194	61.172180	1.877	1.976	3.920
7	61.172183	61.172179	1.970	1.994	3.980
8	61.172180	61.172179	1.993	1.999	3.995

Table 3
Numerical results for second order eigenvalue problem considered in [38].

j	Fund. freq.	Extrap.res.	k_i	k_i^E	l_i
4	12.5950				
5	12.4172	12.3579		1.960	
6	12.3711	12.3557	1.947	1.998	
7	12.3595	12.3556	1.991	2.019	4.459
8	12.3566	12.3556	2.000	2.078	-

Table 4
Numerical results for fourth order eigenvalue problem considered in [38].

j	Fund. freq.	Extrap.res.	k_i	k_i^E	l_i
4	16.6666				
5	16.5364	16.4930		2.010	
6	16.5041	16.4933	2.011	2.007	
7	16.4960	16.4933	1.996	2.041	3.322

two. In [38] the results are given with four decimal places. Latter fact has obviously impact on improved solution (column three) and on its rate of convergence (column six). In this reason the only value in column six differ from theoretically expected value four. The last value in column six is not present due to division by zero (the last two values obtained by extrapolation formula (33) coincide in column four).

Next the following fourth order eigenvalue problem is considered

$$y^{(IV)} = \lambda y, \quad 0 \leq x \leq 1, \quad y(0) = y'(0) = y(1) = y'(1) = 0. \quad (45)$$

The orders of convergence calculated on results given in [38] (see Table 4 in [38]) are presented in Table 4.

Similarly to second order eigenvalue problem (Table 3) it can be confirmed that the computed orders of convergence have values near two in both cases with and without use of the exact solution (columns 4 and 5, respectively). The extrapolated solution and its order of convergence are more affected by low number (four) of decimal placed considered in [38].

Finally, the following sixth order eigenvalue problem is considered

$$y^{(VI)} = \lambda y, \quad 0 \leq x \leq 1, \quad y(0) = y'(0) = y(1) = y'(1) = 0. \quad (46)$$

The orders of convergence calculated on results given in [38] (see Table 1 in [38]) are presented in Table 5.

The results in Table 5 are similar to ones given in Tables 3 and 4 and confirm that the order of convergence of the HWDM is equal to two. In Table 5 the rate of convergence of the extrapolated results coincide unexpectedly well with theoretical value four despite to low number of decimal places presented in solution [38].

4.4. Free vibration analysis of functionally graded (FG) cylindrical shells based on the shear deformation theory [17]

In the current section the order of convergence of the HWDM treated in [17] is examined. The governing equations and boundary conditions are omitted herein for conciseness sake (see formulas

Table 5
Numerical results for sixth order eigenvalue problem considered in [38].

j	Fund. freq.	Extrap.res.	k_i	k_i^E	l_i
4	2.8068				
5	2.8272	2.8340		2.083	
6	2.8319	2.8335	2.118	1.977	
7	2.8331	2.8335	1.970	2.000	4.000

Table 6
Numerical results for FG cylindrical shells considered in [17].

j	Fund. freq.	Extrap.res.	k_i	k_i^E	l_i
2	12.308				
3	8.763	7.581			
4	7.637	7.262		1.655	
5	7.33	7.228	1.655	1.875	3.233
6	7.251	7.225	1.875	1.958	3.503
7	7.231	7.224	1.958	1.982	3.170
8	7.226	7.224	1.982	2.000	

(22) and (24) in [17]). The orders of convergence computed based on results given in [17] (see Table 2 in [17]) are presented in Table 6.

Again, the order of convergence two of the HWDm can be confirmed based on results given in Table 6. Obviously, the low number decimal places for initial solution given in Table 6 has considerable impact on columns three and six (extrapolated results and their order of convergence).

5. Conclusion

The accuracy issues of the HWDm, open from year 1997, are clarified. The convergence theorem is proved for general n th order ODE (assuming $n \geq 2$, boundary value problems). As result it is shown that the order of convergence is two and the error bound has been derived. The numerical validation of the results of convergence theorem has been performed by utilizing a number of case studies. The accuracy of the HWDm considered can be improved by adopting Richardson extrapolation method [37]. The particular case where the order of differential equation is equal to one correspond to initial value problem, which are less actual for composite structures and are omitted herein for conciseness sake. Latter problem is studied by authors and the same order of convergence is obtained.

In the case of all model problems considered the theoretical value equal to two of the order of convergence has been confirmed. The theoretical value equal to four of the order of convergence of the extrapolated results has been observed in the case of first model problem. In the case of second and third model problem, where the initial solution has less number of decimal places (these results are taken from literature) the order of convergence of the extrapolated results differ from four as it can be expected.

The convergence theorem proved for ODE obviously hold good also for integro-differential equations. However, the integral equations where the derivatives are not present need future investigation. Extension of the results for partial differential equations has been also foreseen in future study.

Acknowledgment

This research was supported by the EU structural funds project, "Smart Composites – Design and Manufacturing" 3.2.1101.12-0012, targeted financing project SF0140035s12.

References

- Lepik Ü. Solving PDEs with the aid of two dimensional Haar wavelets. *Comput Math Appl* 2011;61:1873–9.
- Castro LMS, Ferreira AJM, Bertoluzza S, Batra RC, Reddy JN. A wavelet collocation method for the static analysis of sandwich plates using a layerwise theory. *Compos Struct* 2010;92(8):1786–92.
- Cattani C. Harmonic wavelets toward the solution of nonlinear PDE. *Comput Math Appl* 2005;50:1191–210.
- Chen CF, Hsiao CH. Haar wavelet method for solving lumped and distributed-parameter systems. *IEE Proc Contr Theor Appl* 1997;144(1):87–94.
- Hsiao CH. State analysis of the linear time delayed systems via Haar wavelets. *Math Comput Simul* 1997;44(5):457–70.
- Lepik Ü. Numerical solution of differential equations using Haar wavelets. *Math Comput Simul* 2005;68:127–43.

- Lepik Ü. Haar wavelet method for nonlinear integro-differential equations. *Appl Math Comput* 2006;176:324–33.
- Lepik Ü. Application of the Haar wavelet transform to solving integral and differential equations. *Proc Estonian Acad Sci Phys Math* 2007;56(1):28–46.
- Lepik Ü. Numerical solution of evolution equations by the Haar wavelet method. *Appl Math Comput* 2007;185:695–704.
- Lepik Ü. Solving fractional integral equations by the Haar wavelet method. *Appl Math Comput* 2009;214(2):468–78.
- Lepik Ü, Hein H. Haar wavelets: with applications. New York: Springer; 2014.
- Majak J, Pohlak M, Eerme M. Application of the Haar wavelet-based discretization technique to problems of orthotropic plates and shells. *Mech Compos Mater* 2009;45(6):631–42.
- Hein H, Feklistova L. Computationally efficient delamination detection in composite beams using Haar wavelets. *Mech Syst Signal Process* 2011;25(6):2257–70.
- Xie X, Jin G, Ye T, Liu Z. Free vibration analysis of functionally graded conical shells and annular plates using the Haar wavelet method. *Appl Acoust* 2014;85:130–42.
- Xie X, Jin G, Li W, Liu Z. A numerical solution for vibration analysis of composite laminated conical, cylindrical shell and annular plate structures. *Compos Struct* 2014;111:20–30.
- Xie X, Jin G, Yan Y, Shi SX, Liu Z. Free vibration analysis of composite laminated cylindrical shells using the Haar wavelet method. *Compos Struct* 2014;109:169–77.
- Jin G, Xie X, Liu Z. The Haar wavelet method for free vibration analysis of functionally graded cylindrical shells based on the shear deformation theory. *Compos Struct* 2014;108:435–48.
- Jin G, Xie X, Liu Z. Free vibration analysis of cylindrical shells using the Haar wavelet method. *Int J Mech Sci* 2013;77:47–56.
- Majak J, Pohlak M, Eerme M, Lepikult T. Weak formulation based Haar wavelet method for solving differential equations. *Appl Math Comput* 2009;211(2):488–94.
- Heydari MH, Hooshmandasl MR, Mohammadi F. Legendre wavelets method for solving fractional partial differential equations with Dirichlet boundary conditions. *Appl Math Comput* 2014;234:267–76.
- Heydari MH, Hooshmandasl MR, Mohammadi F. Two-dimensional Legendre wavelets for solving time-fractional telegraph equation. *Adv Appl Math Mech* 2014;6(2):247–60.
- Heydari MH, Hooshmandasl MR, Ghaini FMM. A new approach of the Chebyshev wavelets method for partial differential equations with boundary conditions of the telegraph type. *Appl Math Model* 2014;38(5–6):1597–606.
- Heydari MH, Hooshmandasl MR, Ghaini FMM. Two-dimensional Legendre wavelets for solving fractional Poisson equation with Dirichlet boundary conditions. *Eng Anal Bound Elem* 2013;37(11):1331–8.
- Rehman MU, Khan RA. Numerical solutions to initial and boundary value problems for linear fractional partial differential equations. *Appl Math Modell* 2013;37(7):5233–44.
- Ray SS, Patra A. Haar wavelet operational methods for the numerical solutions of fractional order nonlinear oscillatory Van der Pol system. *Appl Math Comput* 2013;220:659–67.
- Ray SS, Patra A. Numerical simulation based on Haar wavelet operational method to solve neutron point kinetics equation involving sinusoidal and pulse reactivity. *Ann Nucl Energy* 2014;73:408–12.
- Ray SS, Patra A. Numerical simulation for fractional order stationary neutrontransport equation using Haar wavelet collocation method. *Nucl Eng Des* 2014;278:71–85.
- Ray SS, Patra A. Two-dimensional Haar wavelet collocation method for the solution of stationary neutron transport equation in a homogeneous isotropic medium. *Ann Nucl Energy* 2014;70:30–5.
- Islam SU, Aziz I, Al-Fhaid AS. An improved method based on Haar wavelets for numerical solution of nonlinear integral and integro-differential equations of first and higher orders. *J Comput Appl Math* 2014;260:449–69.
- Aziz I, Islam SU, Khana F. A new method based on Haar wavelet for the numerical solution of two-dimensional nonlinear integral equations. *J Comput Appl Math* 2014;272:70–80.
- Aziz I, Islam SU. New algorithms for the numerical solution of nonlinear Fredholm and Volterra integral equations using Haar wavelets. *J Comput Appl Math* 2013;239(1):333–45.
- Hariharan G, Kannan K. Review of wavelet methods for the solution of reaction-diffusion problems in science and engineering. *Appl Math Modell* 2014;38(3):799–813.
- Saeedi H, Mollahasani N, Moghadam M, Chuev G. An operational Haar wavelet method for solving fractional Volterra integral equations. *Int J Appl Math Comput Sci* 2011;21(3):535–47.
- Saeed U, Rejman M, Iqbal MA. Haar wavelet-Picard technique for fractional order nonlinear initial and boundary value problems. *Sci Res Essays* 2014;9(12):571–80.
- Patra A, Ray SS. A numerical approach based on Haar wavelet operational method to solve neutron point kinetics equation involving imposed reactivity insertions. *Ann Nucl Energy* 2014;68:112–7.
- Marchuk GI, Shaidurov VV. Difference methods and their extrapolations. New York: Springer; 1983.
- Atkinson KE. An introduction to numerical analysis. John Wiley & Sons; 1978.
- Shi Z, Cao Y. Application of Haar wavelet method to eigenvalue problems of high order differential equations. *Appl Math Modell* 2012;36(9):4020–6.

PUBLICATION IV

Kirs, M., Tungal, E. (2018). Evaluation of Haar wavelet method in engineering applications. *International Conference of Numerical Analysis and Applied Mathematics (ICNAAM 2018), Greece, AIP Conference Proceedings.*

Evaluation of Haar Wavelet Method in Engineering Applications

Maarjus Kirs^{1, a)} and Ernst Tungel^{2, b)}

¹ Department of Mechanical and Industrial Engineering, Tallinn University of Technology

² Faculty of Engineering, Tartu College, Tallinn University of Technology

^{a)}Corresponding author: Maarjus.Kirs@ttu.ee

^{b)}Ernst.Tungel@ttu.ee

Abstract. The results obtained by utilizing widely used Haar wavelet method (HWM) approach are compared with those obtained by finite difference method (FDM) and differential quadrature method (DQM). Latter methods (FDM and DQM) are considered as mainstream strong formulation based methods used in engineering design. The comparison and analysis of results allow to get better understanding on capabilities of most commonly used HWM. The higher order Haar wavelet method (HOHWM) introduced recently by work group is implemented and discussed.

INTRODUCTION

For solving differential equations, the HWM was introduced in [1]. In [2] an overview of the applications of the HWM is given. The operational matrix of integration is developed for solving ordinary and partial differential equations in [1-8] and integral and integro-differential equations in [9-13]. In above studies the strong formulation based approach, Chen&Hsiao wavelet extension [1] is applied and most commonly, the implementation of the HWM is estimated to simple. The accuracy and convergence issues of the Chen&Hsiao approach based HWM are studied in [14-15]. Non-uniform Haar wavelet techniques are developed in [1,16]. In [17] HOHWM was proposed.

TWO APPROACHES OF THE HAAR WAVELET METHOD

This section is organized as follows: first the Haar wavelet family is introduced, next the widely used HWM and higher order HWM introduced in [1] and [16] are described.

Haar wavelet Family

The Haar wavelet family is defined as [2]

$$h_i(x) = \begin{cases} 1 & \text{for } x \in [\xi_1(i), \xi_2(i)) \\ -1 & \text{for } x \in [\xi_2(i), \xi_3(i)) \\ 0 & \text{elsewhere} \end{cases} \quad (1)$$

where $i = m + k + 1$, $m = 2^j$ is a maximum number of square waves deployed in interval $[A, B]$ and the parameter k indicates the location of the particular square wave,

$$\begin{aligned} \xi_1(i) &= A + 2k\mu\Delta x, & \xi_2(i) &= A + (2k+1)\mu\Delta x, & \xi_3(i) &= A + 2(k+1)\mu\Delta x, \\ \mu &= M/m, & \Delta x &= (B-A)/(2M), & M &= 2^J. \end{aligned} \quad (2)$$

Widely Used Haar Wavelet Method

Let us consider n-th order ordinary differential equation (ODE) in the following form

$$G(x, u, u', u'', \dots, u^{(n-1)}, u^{(n)}) = 0, \quad (3)$$

According to the approach proposed by Chen and Hsiao the highest order derivative involved in differential equation will expanded into Haar wavelets i.e. in the case of differential equation (3) the wavelet expansion reads

$$f(x) = \frac{d^n u(x)}{dx^n} = \sum_{i=1}^{\infty} a_i h_i(x). \quad (4)$$

The solution of the differential equation (3) $u(x)$ can be obtained by integrating the relation (4) n times with respect x and determining the integration constants from boundary/initial conditions.

Higher Order Haar Wavelet Method (HOHWM)

The HOHWM introduced in [16] include higher order wavelet expansion given as

$$f(x) = \frac{d^{n+2s} u(x)}{dx^{n+2s}} = \sum_{i=1}^{\infty} a_i h_i(x), \quad s = 1, 2, \dots \quad (5)$$

and algorithm for determining $2s$ complementary boundary conditions. In [17] two different algorithms were proposed using selected uniform grid points and selected Chebyshev-Gauss-Lobatto grid points, respectively. In the case of both algorithms the point is selected nearest to the boundary, but changing boundary after each new selection.

NUMERICAL RESULTS

In the following the numerical results are given for differential governing equation of the axially graded beam introduced in [17]. In Table 1 the values of the fundamental frequency, absolute error and convergence rate obtained by applying widely used HWM, FDM and DQM are compared. In Table 2 similar results are given for second frequency. All solutions given in Tables 1-4 (HWM, FDM, DQM) are computed by workgroup.

TABLE 1. Fundamental frequency parameter Ω_1 values, HWM, FDM, DQM ($\beta = 3$, exact solution 6.8430490105)

N	HWM		FDM		DQM	
	Fundamental frequency Ω_1	Absolute error	Fundamental frequency Ω_1	Absolute error	Fundamental frequency Ω_1	Absolute error
4	5.49612520	1.35E+00	6.82589986	1.71E-02		
8	6.56237797	2.81E-01	6.80779305	3.53E-02	6.72141095	1.22E-01
16	6.76542022	7.76E-02	6.83190078	1.11E-02	6.84304901	3.43E-09
32	6.82322484	1.98E-02	6.84010804	2.94E-03	6.84304901	9.94E-11
64	6.83806767	4.98E-03	6.84230401	7.45E-04	6.84304866	3.48E-07
128	6.84180211	1.25E-03	6.84286215	1.87E-04	6.84303605	1.30E-05
256	6.84273719	3.12E-04	6.84300225	4.68E-05	6.84302115	2.79E-05

TABLE 2. Fundamental frequency parameter Ω_2 values, HWM, FDM, DQM ($\beta = 3$, exact solution 43.4110976168).

N	HWM		FDM		DQM	
	Fundamental frequency Ω_2	Absolute error	Fundamental frequency Ω_2	Absolute error	Fundamental frequency Ω_2	Absolute error
4	34.46004357	8.95E+00	37.99657810	5.41E+00		
8	41.13904609	2.27E+00	41.83587029	1.58E+00	43.43060017	1.95E-02
16	42.85246913	5.59E-01	42.99734834	4.14E-01	43.41109768	6.45E-08
32	43.27200957	1.39E-01	43.30627067	1.05E-01	43.41109762	3.97E-11
64	43.37636085	3.47E-02	43.38480149	2.63E-02	43.41109772	1.05E-07
128	43.40241562	8.68E-03	43.40451796	6.58E-03	43.41110484	7.22E-06
256	43.40892726	2.17E-03	43.40945235	1.65E-03	43.41111652	1.89E-05

In Tables 3-4 the values of the frequency parameter, absolute error and convergence rate obtained by applying widely used HWM and HOHWM are compared.

TABLE 3. Fundamental frequency parameter Ω_1 values HWM, HOHWM ($\beta = 3$, exact solution 6.8430490105).

N	HWM approach by Chen&Hsiao			HOHWM (I17)			
	Fundamental frequency Ω_1	Absolute error	Converg. rate	Fundamental frequency Ω_1	Absolute error	Converg. rate	Error ratio
4	5.49612520	1.35E+00		7.81629606	9.73E-01		1.38
8	6.56237797	2.81E-01	2.2627	6.87693058	3.39E-02	4.8442	8.28
16	6.76542022	7.76E-02	1.8542	6.84538131	2.33E-03	3.8607	33.28
32	6.82322484	1.98E-02	1.9693	6.84319842	1.49E-04	3.9644	132.68
64	6.83806767	4.98E-03	1.9927	6.84305841	9.40E-06	3.9908	530.04
128	6.84180211	1.25E-03	1.9982	6.84304960	5.88E-07	3.9977	2119.39
256	6.84273719	3.12E-04	1.9995	6.84304905	3.68E-08	3.9995	8477.23

TABLE 4. Fundamental frequency parameter Ω_2 values HWM, HOHWM ($\beta = 3$, exact solution 6.8430490105).

N	HWM approach by Chen&Hsiao			HOHWM (I17)			
	Fundamental frequency Ω_2	Absolute error	Converg. rate	Fundamental frequency Ω_2	Absolute error	Converg. rate	Error ratio
4	34.46004357	8.95E+00		43.08502120	3.26E-01		27.45
8	41.13904609	2.27E+00	2.2627	43.43718723	2.61E-02	3.6437	87.09
16	42.85246913	5.59E-01	1.8542	43.41285000	1.75E-03	3.8961	318.78
32	43.27200957	1.39E-01	1.9693	43.41121057	1.13E-04	3.9555	1231.38
64	43.37636085	3.47E-02	1.9927	43.41110475	7.13E-06	3.9859	4872.52
128	43.40241562	8.68E-03	1.9982	43.41109806	4.47E-07	3.9960	19431.27
256	43.40892726	2.17E-03	1.9995	43.41109764	2.80E-08	3.9941	77401.77

The exact solutions used in Tables 1-4 are computed according to formulas given in [18].

CONCLUSIONS AND FUTURE WORK

Based on results given in Tables 1-2 it can be concluded that the results obtained by HWM are in good agreement with those obtained by FDM and DQM, also the implementation of the HWM was simple. However, accuracy of the HWM is in the same range of those of FDM and is significantly lower than that of DQM. Obviously the widely used HWM based on Chen and Hsiao approach need improvement to be competitive with mainstream methods in engineering design. In can be seen from Tables 3-4 that HOHWM outperform HWM, the absolute error is smaller up to thousands times (depending on mesh). Future study is related with application of HOHWM for wide class of engineering problems like acoustic analysis of structures [19-22], structural analysis and design optimization of composites [23-29] and modelling monitoring systems [30-32].

ACKNOWLEDGMENTS

The study was supported by Estonian Centre of Excellence in Zero Energy and Resource Efficient Smart Buildings and Districts, ZEBE, TK146 funded by the European Regional Development Fund (grant 2014-2020.4.01.15-0016); Estonian Research Council grant PUT1300.

REFERENCES

- [1] C. F. Chen, C.H. Hsiao, IEE Proc Contr Theor Appl, **144**(1), 87-94 (1997).
- [2] Ü. Lepik, H. Hein, *Haar wavelets: with applications* (Springer, New York, 2014).
- [3] Ü. Lepik, Math. Comput. Simulat. **68**, 127-43 (2005).
- [4] L. Feklistova, H. Hein, Comp. Assisted Meth. in Eng. and Sci., **19** (4), 351–360 (2012).
- [5] L. Jaanuska, H. Hein, Int. J. of Mechanics, **10**, 281–287 (2016).
- [6] S. U. Islam, I. Aziz, M.Ahmad, Comp. and Math. with Appl., **69**(3), 180-205 (2015).
- [7] J. Majak, Pohlak M., Eerme M. Mechanic of Composite Materials, **45**(6), 631-42 (2009).
- [8] H. Hein, L. Feklistova, Mech. Syst. Signal. Pr., **25**(6), 2257-70 (2011).
- [9] Ü. Lepik, Appl. Math. and Comp., **176**, 324-333(2006).
- [10] I. Aziz, S. U. Islam, F. Khana, J. Comput. Appl. Math., **272**,70-80, (2014).
- [11] I. Aziz, S. U. Islam, J. Comput. Appl. Math., **239**(1), 333-45 (2013).
- [12] S. U. Islam, I. Aziz, A.S. Al-Fhaid, J. Comput. Appl. Math., **260**, 449–69(2014).
- [13] S. U. Islam, I. Aziz, B. Šarler, Mathematical and Computer Modelling, **52**, 1577-1590 (2010).
- [14] J. Majak, B. S. Shvartsman, M. Kirs, M. Pohlak, H. Herranen, Composite Structures, **126**, 227-232 (2015).
- [15] J. Majak, B.S. Shvartsman, K. Karjust, M. Mikola, A. Haavajõe, M. Pohlak, Composites Part B: Engineering, **80**, 321-327 (2015).
- [16] F.I. Haq, S.U. Islam, I. Aziz, Int. J. of Comp. Meth. in Eng. Sci. and Mech., **12**, 4, 168-175 (2011).
- [17] J. Majak, M. Pohlak, K. Karjust, M. Eerme, J.Kurnitski, B. S. Shvartsman, Composite Struct., **201**, 72-78, (2018).
- [18] X. F. Li, Y.A. Kang, J.X.Wu, Applied Acoustics, **74**, 413-420 (2013).
- [19] F. Auriemma, Applied Acoustics, **122**, 128-137 (2017).
- [20] F. Auriemma, Acoustics Australia, **45**(2), 411-419 (2017).
- [21] F. Auriemma, H. Rammal, J. Lavrentjev, SAE Int. J. of Materials and Manufacturing, **6**, 3, 599-610 (2013).
- [22] R. Kabral, H. Rämmal, J. Lavrentjev, F. Auriemma, SAE Technical Papers, 10.4271/2011-32-0514 (2011).
- [23] A. Aruniit, J. Kers, D. Goljandin, M. Saarna, K. Tall, J. Majak, H. Herranen Materials Science (Medžiagotyra), **17** (3), 276-281 (2011).
- [24] A. Aruniit, J. Kers, J. Majak, A. Krumme, K. Tall, Proc. of Estonian Acad. of Sci., **61**(3), 160-165 (2012).
- [25] J. Šliseris, K. Rocens, J. of Civil Engineering and Management, **19**(5), 696-704 (2013).
- [26] J. Šliseris, G. Frolovs, K. Rocens, V. Goremikins, Procedia Engineering, **57**, 1060-1069 (2013).
- [27] J. Lellep, J. Majak, Structural Optimization, **14**, 116-120 (1997).
- [28] U. Gul, M. Aydogdu, G., Gaygusuzoglu, Journal of Engineering Mathematics, **109**(1), 85-111 (2018).
- [29] B. Shvartsman, J. Majak, Applied Mathematical Modelling, **40** (4-5), 3713–3719 (2016).
- [30] T. Aruvaeli, R. Serg, K. Kaare, T. Otto, in Annals of DAAAM for 2012 & Proc. of the 23rd Int. DAAAM Symp., Zadar, 2012-10-21/28. Ed. Katalinic, B. Vienna, Austria: DAAAM Int. Vienna, 661–667 (2012).
- [31] T. Aruväli, W. Maass, T. Otto, Procedia Engineering, **69**, 449-458 (2014).
- [32] K. Lõun, J. Lavin, J. Riives, T. Otto, Estonian J. of Engineering, **19**, 1, 47-61 (2013).

Curriculum vitae

Personal data

Name: Maarjus Kirs

Date of birth: 04.03.1982

Place of birth: Kuressaare

Citizenship: Estonia

Contact data

E-mail: maarjus.kirs@ttu.ee

Education

2012–2018 Tallinn University of Technology, PhD

2000–2006 Tallinn University of Technology, BSc

1997–2000 High school

Language competence

English – Fluent

Russian – Average

German – Average

Professional employment

2013– Tallinn University of Technology, Faculty of Mechanical Engineering, Department of Mechanical and Industrial Engineering, Chair of Product Development, Junior Researcher (1.00)

2011–2013 Tallinn University of Technology, Faculty of Mechanical Engineering, Department of Mechanical and Industrial Engineering, Engineer (1.00)

2006–2011 Sami AS, design engineer

2005–2010 Commuun OÜ, technical advisor

Elulookirjeldus

Isikuandmed

Nimi: Maarjus Kirs

Sünniaeg: 04.03.1982

Sünnikoht: Kuressaare

Kodakondsus: Eesti

Kontaktandmed

E-post: maarjus.kirs@ttu.ee

Hariduskäik

2012–2018 Tallinna Tehnikaülikool, PhD

2000–2006 Tallinna Tehnikaülikool, BSc

1997–2000 Keskhariidus

Keelteoskus

Inglise keel – kõrgtase

Saksa keel – kesktase

Vene keel – kesktase

Teenistuskäik

2013– Tallinna Tehnikaülikool, Mehaanikateaduskond, Mehaanika ja tööstustehnika instituut, Tootearenduse õppetool, nooremteadur (1,0)

2011–2013 Tallinna Tehnikaülikool, Mehaanikateaduskond, Mehaanika ja tööstustehnika instituut, insener (1,0)

2006–2011 Sami AS, konstruktor

2005–2010 Commuun OÜ, tehniline konsultant

